Thesis for the Degree of Doctor of Philosophy

Towards Haptic Texture Content Library: Texture Synthesis Through Automatic Model Assignment And Texture Authoring in Haptic Attribute Space

Waseem Hassan

Department of Computer Science & Engineering

Graduate School

Kyung Hee University

South Korea

Feb 2022

Towards Haptic Texture Content Library: Texture Synthesis Through Automatic Model Assignment And Texture Authoring in Haptic Attribute Space

Waseem Hassan

Department of Computer Science & Engineering

Graduate School

Kyung Hee University

South Korea

Feb 2022

TOWARDS HAPTIC TEXTURE CONTENT LIBRARY: TEXTURE SYNTHESIS THROUGH AUTOMATIC MODEL ASSIGNMENT AND TEXTURE AUTHORING IN HAPTIC ATTRIBUTE SPACE

by

Waseem Hassan

Supervised by

Prof. Seokhee Jeon, Ph.D.

Submitted to the Department of Computer Engineering and the Faculty of Graduate School of Kyung Hee University in partial fulfillment of the requirements of the degree of Doctor of Philosophy

Dissertation Committee:

Prof. Seungkyu Lee, Ph.D. (Chairman)..…………..…………..….……....

Prof. Hyeongyeop Kang, Ph.D. ….…………………..…………………….

Prof. Tack Woo, Ph.D. ……………...…………………………..….…........

Prof. Gunhyuk Park, Ph.D. ……………………………………………..

Prof. Seokhee Jeon, Ph.D. …………………………………..……..

Abstract

In the contemporary era, one of the biggest challenges faced by haptics technology is the availability of digital haptic contents. Haptic interaction with an object in virtual, augmented, or mixed reality requires a haptic model that governs the interaction responses from the object. The haptic models can be fashioned after an object from real life or built up from scratch by a designer. This process of generating a haptic model is non-trivial and can take a significant amount of time and effort. The rapid progress of haptics technology and widespread industrial interest signifies that haptics will soon proliferate myriad aspects of our life. In an effort to make haptics technology available to the masses and scalable for personal use, there lies a need to automate and speed up the process of haptic modeling.

In this thesis, we pursue the goal of automating haptic content modeling and availability with an emphasis on haptic texture. We achieve this goal by automating the current practices of haptic texture content creation and introducing novel techniques of generating, manipulating, and authoring haptic texture. This thesis proposes a "Universal Haptic Texture Contents Library" comprising of three independent modules: 1) haptic texture model assignment, 2) haptic attribute space, and 3) haptic texture authoring. The three modules are facilitated by a dataset of 100 (or a subset of 100) real texture surfaces.

Each one of these modules facilitates the availability of haptic texture content in a unique way. The automatic assignment module can assign data-driven haptic texture models to any real texture surface based on its image features, without the need to model it. The haptic attribute space accomplishes a two-fold purpose. First, it provides a standard attribute rating space for all haptic textures to be labeled in terms of their haptic attributes. Second, it facilitates the process of extracting haptic attributes of textures based on their images instead of carrying perceptual experiments

with every texture. The haptic texture authoring module provides the tools for mixing and manipulating attributes of real textures and rendering virtual textures that inherit specific attributes of (data-driven modeled) real textures. All three sub-modules work towards automation in providing application-ready and haptic-enabled environment models without extensive modeling.
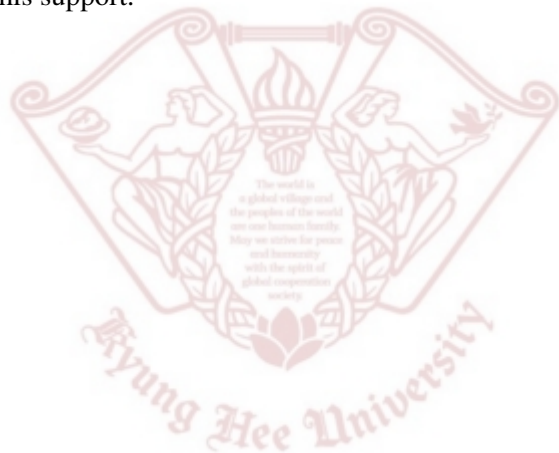
Acknowledgement

I would like to thank my supervisor Dr. Seokhee Jeon for guiding me through out my tenure as a master's student. His invaluable advice, suggestions, and guidance has helped me in improving my knowledge and skill set. He has put in a lot of effort in shaping me into a better researcher. I am truly grateful for all his support.

<div align="right">

Waseem Hassan

Feb, 2022

</div>

Table of Contents

List of Figures

List of Tables

List of Algorithms

Chapter 1

Introduction

1.1 Motivation

The initial medium that humans use for attaining information about textures is the visual sense. The appearance of a texture can provide us with enough information to be able to successfully identify its physical attributes in most cases. In order to gain in depth information about the said texture, humans rely on the sense of touch. Interaction with a texture, to reveal its haptic attributes is a trait intrinsic to human beings. In daily life interactions, human beings use these two senses to identify haptic attributes of textures all around us. Recently, researchers have pointed out that interaction sounds can play a role in haptic identification [1], however, it only stands for certain haptic attributes and as such can not be held true for holistic haptic information.

The sense of vision has been thoroughly studied throughout the years. Different dimensions of visual attributes of a texture are objectively describable and accurately capturable. For instance, colors are readily describable by the RGB model (or CMYK in case of pigments). Surface topography can be accurately described using parametric or non-parametric descriptors [2]. Similarly, capturing an image in terms of its constituent colors is easily achievable, and a large number of techniques are available to capture visual surface topography of a texture [3–5]. In essence, the dimensions for colors and visual topography are available and textures can be described according to these. However, haptic content creation is one of the most imminent bottlenecks in current haptics technology for virtual reality (VR). Haptic feedback in a virtual environment usually requires a geometric model of the environment as well as haptic property models associated with the geometry [6]. For geometry modeling, many available tools, resources, and algorithms for computer graphics can be utilized for haptic modeling since a single geometric model is usually shared. However, models for haptic properties, e.g., stiffness, friction, surface texture, etc., are

1

much harder to obtain. The two most prominent methods for haptic modeling are data-driven modeling [7–10], and physics-based parametric modeling [11–13].

The physics based method has been a common approach employed by various researchers to render haptic content, where the haptic responses due to tactile properties of a virtual surface are determined by coefficients of physics-based parametric models. For example, high frequency textural vibrations were generated based on the simulation of contact dynamics of micro-scale geometry of surface made by parameterized cavity and bump models mapped into a surface [14, 15] or using stochastic surface geometry models [16, 17]. Although the designer usually has full control over all the parameters and aspects, such a method cannot replicate the complexity of real life surfaces due to simplification in the models. In addition, the designer has to manually incorporate the delicacies and nuances of real surfaces into a synthetic surface, which is quite a demanding task.

In data-driven modeling, the vibrations originating from interaction with different surfaces are recorded and are subsequently used for rendering tactile contents. For instance, the authors in [7] were able to generate virtually perceptible textures based on the scanning velocity and normal force. Similarly, Abdulali et al. extended this idea to recreate more complex textures (anisotropic textures) by incorporating the direction of scan velocity into the equation [18]. Recently, a more robust and efficient technique has been employed where Generative Adversarial Networks (GANs) have been trained to create vibrotactile signals based on texture images or attributes albeit using predefined and constrained tool-surface interaction [19]. The upside of data-driven modeling is that the created contents are highly realistic and computationally simpler. Data-driven modeling is efficient in comparison with manual tuning but it can still take a lot of time and effort to model a significantly large number of surfaces. For example, modeling all the surfaces in a complex virtual reality environment (e.g., 3D gaming environment, remote environment) can prove to be a difficult task using data-driven modeling. Second, it is evident that an object needs to be physically present in order to be modeled. Certain scenarios can arise where modeling an object without physical presence may be required. One such instance can be modeling all the fabrics in an online shopping outlet. Keeping these shortcomings in mind, we need to develop a method where haptic modeling is more robust, easy to adapt to new surfaces, and detached from dependence on physical presence

of the objects.

Our research thrust is originated from the need of efficient haptic content creation or haptic modeling. The broad goal of the current research is to build a "Haptic texture content library" – a collection of a large number of haptic models that describe a wide range of haptic surfaces and haptic attributes - and to develop a method that automatically authors the haptic properties of the environment with minimal effort using the library. We hope that with this tool, application-ready and haptic-enabled environment models can be easily generated without extensive modeling.

The haptic texture content library contains three sub-libraries. These are automatic data-driven haptic texture model assignment based on image features; haptic attribute space and haptic texture attribute prediction based on image features; and haptic texture authoring by interpolating data-driven real textures. Each sub-library attempts to solve one open challenges in the field of haptic content generation.

1.2   Haptic Texture Content Library

The current dissertation addresses three main problems under the umbrella of haptic texture content library. These will be described separately in the following paragraphs.

1.2.1   Automatic Assignment of Haptic Models

As one of the attempts to achieve this goal, this dissertation tests the concept of automatic content generation based on image textures with emphasis on haptic textures. It is reported that haptic texture correlates to some extent with image texture [20–22]. However, it is also known that two similar-looking surfaces can evoke completely different haptic perceptions. This means that pure image-based texture classification methods may not be able to distinguish surfaces with different haptic sensations. While images can sometimes be misleading, as mentioned earlier, there is definitely an overlap in the information conveyed by visual and haptic cues. This dissertation uses this information to cater for the perceptual aspects of each image and use it in the automatic assignment of haptic texture models. The main purpose of adapting this image-based approach is to make the process of haptic modeling more robust, intuitive, and easy to implement and

generalize.

The overall framework required to accomplish this task can be tabulated as follows:

1 - One time data driven modeling of texture surfaces to form a library. The range of surfaces should cover most of the daily life haptic interactions.

2 - A user study to establish a perceptual space where all the surfaces from the library are represented based on their perceptual characteristics of haptic texture.

3 - Extract image features of all the texture surfaces.

4 - Establish a relationship between haptic perception (step 2) and image features (step 3). Haptic texture models and image features are stored together.

5 - Based on the relationship established in step 4, carry out automatic haptic texture model assignment to newly encountered - outside library - texture surfaces, using the library.

6 - Render the assigned model from library as a haptic model for the newly encountered texture surface.

Data driven modeling and rendering are not addressed here due to scope of the study. However, the details of the modeling and rendering techniques used in this study can be found in [18] and [23], respectively. The three dimensional input space (2-d velocity and 1-d force) in [18] and [23] has been reduced to a two dimensional one (1-d velocity and 1-d force) for handling the isotropic surfaces used in this study. Focus of the present research lies in the process of automatic assignment, i.e., steps 2 - 5.

Expected Outcomes   The shortcomings in data-driven modeling mentioned in the above section can be overcome by adapting automatic assignment algorithm. First, since the assignment calculates image features from the new surface and then selects an appropriate model based on those image features, haptic models can be assigned to a large number of new surfaces in a very short time (within seconds) using the automatic assignment algorithm, as shown in Fig. 1.1. This process takes far less time as compared to physically interacting with a large number of surfaces and modeling them.
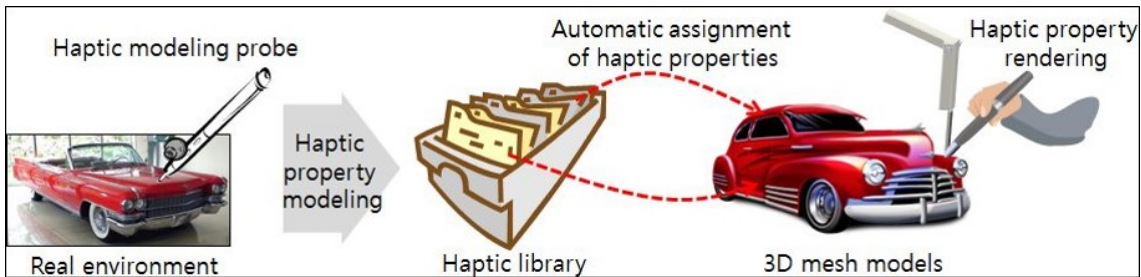
Figure 1.1: The process of automatic assignment of haptic models. Various haptic textures are recorded from real surfaces and stored in a library alongside their image features. The haptic models are then assigned to new surfaces based on their image features.

Haptic models are assigned using only images of the new surfaces. This eliminates the need for physical presence of the target object or surface. The significance of this technique is that we can render surfaces which are not physically available, such as the online shopping example discussed earlier or a 3D gaming environment.

Association of haptic property models with geometry can also be achieved using the proposed algorithm. Although it is not addressed in the thesis, the concept is rather straightforward to apply. Assume a mesh model with surface texture. A haptic model can be assigned to each vertex (or group of vertices) based on the surrounding texture. Such an approach can alleviate the need for manual assignment or tuning. Furthermore, a variety of 3D mesh models along with textures are available. These can easily be assigned haptic models based on the proposed algorithm. This idea can be particularly useful in VR environments or 3D gaming where a user has to interact with various objects/surfaces. Haptic interaction in VR or 3D gaming has been a focus of many researchers recently [24–28]. The overall VR scene can be segmented to capture and separate various textures and then use the automatic assignment algorithm to assign them haptic textures. The user can then interact with the haptic textures using a haptic device.

1.2.2 Haptic Attribute Space

There lies a need to establish standardized dimensions, akin to the RGB model for the visual sense, where haptic textures can be identified and populated based on their haptic attributes (roughness, hardness, etc). Such a space would make haptic textures more relatable to the general public and professionals working with haptic texture modeling. In the contemporary world, consumers buy
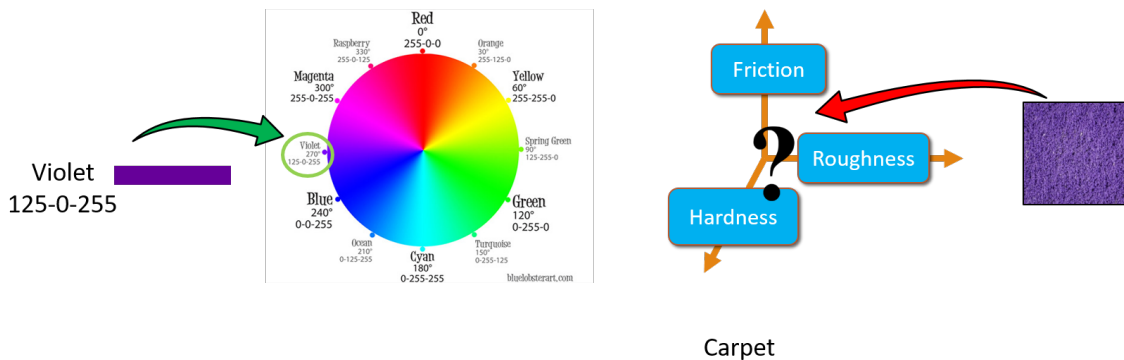
Figure 1.2: A conceptual illustration of the need of a Haptic Attribute space to standardize the haptic textures based on their attributes. Every color can be represented in terms of its RGB attributes, however, we do not yet have a similar system for representing haptic textures in terms of standard attributes.

online products without being able to touch them. Consumers are less likely to buy online products that have a strong tactile aspect [29]. A standardized system where products are rated according to their haptic attributes would allow the end user to make more informed decisions.

The current study aims to provide a Haptic Attribute Space (HAS) where haptic textures are defined by their haptic attribute values similar to how colors are defined by their RGB values. The HAS is a four dimensional space where the dimensions are haptic attributes of textures, i.e., rough-smooth, flat-bumpy, sticky-slippery, hard-soft. The study comprises of two parts. The first part of the study deals with establishment of the HAS from a dataset of 100 texture surfaces. The HAS is established by conducting psychophysical experiments with human subjects. They select a list of attributes that could define the haptic properties of the surfaces in the dataset, and then rate all the 100 surfaces in the datasets against those attributes. The four attribute pairs chosen as a result of this exercise become the axes of the HAS. The second part deals with generalizing the HAS to new textures by using images of new textures and predicting their attribute values. As mentioned earlier, there lies an area of intersection between visual and haptic texture perception [20–22], and this study aims to exploit that area of intersection. This study introduces a state-of-the-art multi-scale 1D-CNN model to predict haptic attribute values of new textures from their images. The 1D-CNN model is trained using the data from psychophysical experiments and image features of the 100 surfaces is dataset. The aim of the 1D-CNN model is to make it possible to assign attribute

values to newly seen and/or physically absent texture surfaces.

Expected Outcomes The HAS allows a texture surface to be defined by its haptic attributes as rated by human subjects. For example, how smooth or how bumpy a surface feels. A surface with a higher value of smoothness would intuitively mean a smoother surface. It would help in categorizing and defining textures based on their haptic attributes. Given that new textures can be effortlessly placed into the HAS without the need to remake the whole space, it is possible to scale the HAS using the 1D-CNN.

Another benefit from HAS could be the ease in online shopping. Users can judge the haptic attributes of online items from their images. This system would let the users make more informed decisions while shopping online. A possible application of the HAS could be in haptic mapping of remote environments. One of the benefits of the proposed system is that surfaces can be haptically labeled from images, without needing physical interaction with the actual surface. Once the images of a remote environment are available, its contents could be segmented and each segment could be haptically labeled using the proposed 1D-CNN model.

1.2.3 Haptic Texture Authoring

It would facilitate contents generation if we could freely edit the perceptual property of the real measurement, e.g., creating a new haptic texture having a slightly increased roughness from a real surface, a new texture where the roughness value is inherited from one and hardness from another, and a texture that can be perceived as lying exactly in the middle of two real textures. Efficiently creating such textures from real textures is the goal of present work, and we call this as haptic texture authoring. An example of texture authoring is shown in Fig. 1.3.

The goal of this study is to provide an effective method for haptic texture authoring using data-driven haptic texture modeling. We achieve this goal through two contributions. We first established an *authoring space* where 25 data-driven texture models build from 25 fully featured real surfaces are placed according to their affective properties. The space is made in such a way that it maximizes the correspondence between affective properties of the 25 models and features in the physical signals of the models. Axes of the space are the affective properties, and this
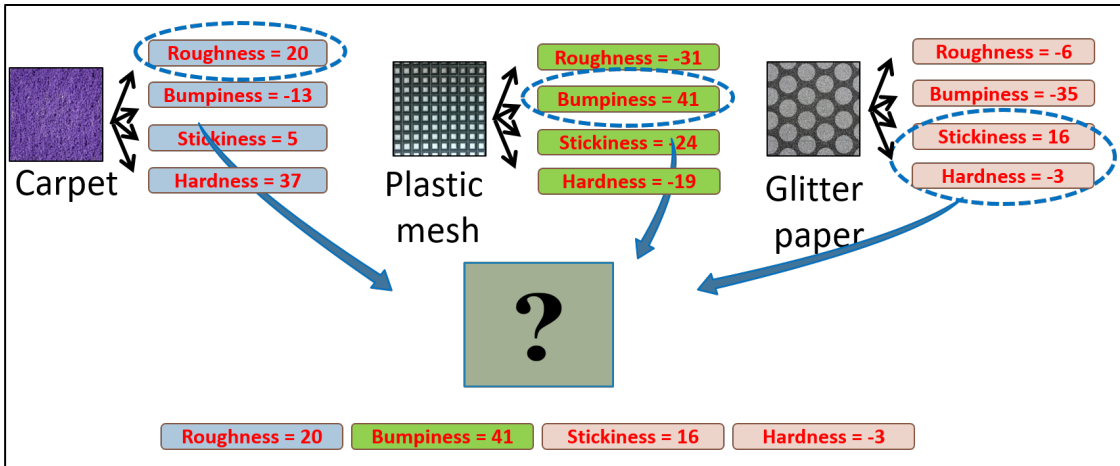
Figure 1.3: An example of one of the tasks possible with the help of haptic texture authoring. Creating a virtual texture that inherits the haptic properties of various real textures.

space plays the role of a perception-based descriptor of textures. Now, designers can freely select an arbitrary point in the space to author a texture, and the system automatically synthesizes a new texture signal corresponding to the selected affective properties. The second contribution lies in this part. The framework interpolates signals from adjacent data-driven models, so that two different haptic models are combined to form the new virtual texture. This step ensures that the new model inherits perceptual characteristics of the parent textures, allowing the aforementioned authoring scenarios. To the best of our knowledge, there is no such work which provides the approximation of physical properties across two different texture models.

The significance of this work can be explained through an analogy from the field of vision. It is well known that the RGB space can be used to create most of the colors perceivable to human eye. Image editing tools often provide an RGB color table where a designer can easily select a color to be used. In a similar way, through this work, we want to provide a unified haptic authoring tool comprising of the basic components or dimensions of haptic texture. Such a tool can be utilized by designers and researchers to create haptic models having arbitrary affective properties and would drastically reduce the time and effort required for haptic modeling.

Expected Outcomes The significance of this work can be explained through an analogy from the field of vision. It is well known that the RGB space can be used to create most of the colors

perceivable to human eye. Image editing tools often provide an RGB color table where a designer can easily select a color to be used. In a similar way, through this work, we want to provide a unified haptic authoring tool comprising of the basic components or dimensions of haptic texture. Such a tool can be utilized by designers and researchers to create haptic models having arbitrary affective properties and would drastically reduce the time and effort required for haptic modeling.

1.3 Contributions

The main contributions of each of the three sub-libraries are listed below:

Automatic Assignment of Haptic Texture Models

o Establishing a perceptual space by conducting a psychophysical experiment with 84 real life textured surfaces.

o Establishing a universal haptic texture library where the 84 surfaces are stored along with their associated image features.

o Proposing an automatic assignment algorithm for haptic texture model assignment, which can be readily used to assign data-driven haptic models to textured surfaces based on their images only.

o Drawing perceptual thresholds for haptic texture discrimination to validate the completeness of the library.

Haptic Attribute Space

o Collecting a dataset of 100 unique texture surfaces and establishing their perceptual space.

o Establishing a four dimensional Haptic Attribute Space from the dataset of 100 texture surfaces. The HAS describes the real textures based on their haptic attribute values.

o Proposing a multi-scale 1D-CNN model to predict haptic attributes of textures based on their images.

Haptic Texture Authoring

o Establishing an affective space through the combination of perceptual space and adjective rating. The texture surfaces in this space are scattered based on their haptic attributes.

o Creating an authoring space through the relationship between affective space and acceleration patterns from interaction with texture surfaces. Texture surfaces in authoring space inherit the perceptual as well as physical interaction properties.

o Authoring of textures in the authoring space by interpolation of neighboring textures.

o Rendering using weighted synthesization of data-driven models of haptic textures.

1.4   Thesis Outline

The three sub-libraries are detailed in the upcoming chapters of this dissertation. The background information which can facilitate the readers to better understand the current thesis is provided in Sect. 1.5. The steps required to establish the automatic assignment library and their details are provided in Chapter 2. The process of creating the haptic attribute space is presented in Chapter 3. The haptic texture authoring algorithm is introduced in Chapter 4. Lastly, the dissertation is concluded in Chapter 5 and the possible future research directions are discussed.

1.5   Related Works

This section covers three different aspects of literature. The first part deals with the perceptual dimensions of haptic texture, the second part briefly elaborates the relationship between visual and haptic texture, while the third part details the previous techniques used for texture classification.

1.5.1   Haptic Perceptual Space

A haptic perceptual space is an n-dimensional space used for an optimized visualization of haptic stimuli based on their mutual similarity of dissimilarity. It provides the backbone for classification and other haptic tendencies of stimuli in relation to one another [30]. The perceptual space is one

of the first landmarks that most studies strive towards, as it can lead to the unearthing of hidden perceptual relationships data.

The perceptual spaces established in the current thesis pertain to stimuli from haptic texture of real surfaces. Interaction with textured surfaces can occur in two ways: tool-based or bare-handed. Both these types of interactions have received a lot of attention from the research community. In case of bare-handed interaction, the researchers have focused on finding the underlying factors or perceptual dimensions that contribute towards the haptic texture perception. Yoshida et al. [31] were among the first in finding the perceptual dimensions for bare-handed interaction. They reported four main dimensions for haptic texture, i.e., hard-soft, heavy-light, cold-warm, and rough-smooth. Hollins et al. used bipolar adjective scales to define the basic dimensions in [32]. They identified smooth-rough and soft-hard as the two main dimensions in haptic texture perception. In summary, as corroborated by [33], haptic texture perception mainly consists of three basic dimensions, i.e., rough-smooth, hard-soft and cold-warm (e.g. [34, 35]). However, authors in [33] provide reasonable grounds to include friction as another dimension to cater for the stickiness-slipperiness of surfaces and that roughness dimension can be divided into macro and micro roughness. On the other hand, for tool-based interaction, Lamotte, in [36], showed that texture perception varies along the hard-soft dimension. It was concluded that participants were better at discriminating the differences in softness when they used active tapping. Other studies such as [37, 38] found that textural perception varies along the rough-smooth dimension.

All the perceptual spaces in the current thesis are a result of bare-handed interaction with textures surfaces. It can be argued that most haptic devices operate with a rigid link and users can feel the haptic stimuli through the parts in touch with the rigid link. However, the results in [39] showed that perceptual spaces created from tool-based and bare-handed interactions do not differ in principal. There are differences at the micro scale, however, the overall trend of stimuli in relation to one another largely remain intact.

1.5.2 Visual and Haptic Texture

Humans rely on both visual and haptic information when interacting with an object. Both the modalities contribute towards the identification of the object. Information about shape, color,

location, etc., is mostly provided by the visual sense, while, the haptic sense aids in attaining richer texture information [21, 40]. Contrary to popular belief, S.J. Lederman et al. and M.A. Heller showed, in separate studies, that vision and haptics perform equally well in texture perception tasks [20, 40]. In fact, it was argued that texture perception is intrinsically a bimodal (visual and haptic) phenomenon and perception degrades if observed through either of the individual modalities. Humans judge haptic and visual cues of real textures similarly, and the two modalities depict congruent perceptual characterizations [41, 42]. Functional Magnetic Resonance Imaging (fMRI) evidence shows that haptic and visual perception of texture activate same areas within the medial ventral temporal cortex of the brain [43]. Similarly, the fMRI based studies by Eck et al. indicated a crossmodal interaction in the somatosensory and visual cortices when humans process texture information [21]. Either of the visual or haptic sense can attain a dominating role in terms of texture perception depending on the nature of the task and the amount of variability available to either of the modality. To this end, Ernst et al. modeled the human nervous system responses using a maximum-likelihood integrator which accepted visual and haptic cues as inputs and estimated the role of each modality in perception [22].

All the above studies and numerous others suggest that visual and haptic texture perception operate in a flexible cooperation and that there exists a common ground between them. In this thesis, we exploit this common ground to associate visual information from images with haptic information in the form of haptic texture models.

1.5.3 Haptic Texture Classification

Texture classification using image features has remained the focus of several researches over the years. One of the pioneering efforts was presented by Haralick et al. [44]. They introduced the Grey Level Co-occurrence Matrix (GLCM) from which image features were calculated and used for texture classification. Various texture classification algorithms have been presented with ever improving prediction accuracy. These algorithms include but are not limited to filter bank features [45], binarized statistical image features [46], local binary pattern features [47–49], color maps [50], neural networks [51, 52], etc. All the above mentioned algorithms and many more such texture classification algorithms reported high accuracy on various texture datasets. How-

ever, these are purely based on image features and as such could not be applied to haptic texture classification.

A recent method of collecting sensorized data from haptic interaction with textures has been used for haptic texture classification. Customized interaction tools with various sensors are used to collect information from texture surfaces. Various features are calculated from this collected information. In this regard, Stresse et al. [53–55] used a custom built pen-like tool to interact with textures and collect acceleration signals, sound, frictional force, and images. These data are then used to collect various features that are used for haptic texture and material classification. Similarly, Romano et al. [56] used normal force, friction, scanning velocity and acceleration resulting from tool exploration. Kerzel et al. used a single force sensor to record the signals during lateral and vertical motions of the tool and trained a neural network using these data for compliance and texture identification [57]. Recently, Lima et al. used raw data from an inertial measurement unit (IMU) and deep barometer for texture classification using machine learning techniques [58].

In essence, the aforementioned techniques use physical vibrations from interaction with surfaces or mechanical properties of textures to classify haptic textures. It can be argued that such data could provide a high accuracy in haptic texture classification tasks. However, the process of collecting information from real textures every single time can be a tedious and time consuming process. One of the bottlenecks of such methods is the requirement of a physical surface for classification, as the signals are collected by interacting with a real surface, therefore, generalization or scalability of the system can be hindered. Using the proposed system, haptic attributes/properties of textures can be classified or identified based on their images only. Thus eliminating the requirement of a real texture, and making the process of haptic identification more robust and usable.

Chapter 2
Automatic Assignment of Haptic Texture Models

One of the emerging techniques for haptic modeling is the data-driven haptic modeling [7, 10, 59, 60]. In this technique, the signals originating from tool-surface interaction are recorded, e.g., high frequency vibrations generated by stroking a surface. These signals are subsequently used in rendering for approximation of the given surface. Based on data-driven modeling, the authors in [7] recorded the normal force and scanning velocity during interaction and rendered realistic isotropic haptic textures using that information. Similarly, more complex anisotropic textures were modeled and rendered in [18, 23] by including the direction of scan velocity along with normal force in the input data. One of the reasons for the huge popularity of data-driven modeling is that the model is created directly from interaction data regardless of the object properties or micro geometry of the surface. In case of manual tuning, these factors significantly influence the modeling and thus make it a cumbersome task.

Another positive aspect of data-driven modeling is the ease in generation of data. The model is captured by stroking a given surface and quality of the model is determined by comparing the error between the rendered and actual signal. On the other hand, the services of an expert are always required in manual tuning. All the parameters of the model have to be manually examined or felt by an expert or a designer and tuned according to the given surface.

With the introduction of data-driven technique, haptic modeling has become significantly robust but there still remain some underlying problems that renders model making a difficult task. First, every object has to be somehow probed by a sophisticated sensing hardware to get data for modeling. Data-driven modeling is efficient in comparison with manual tuning but it can still take a lot of time and effort to model a significantly large number of surfaces. For example, modeling all the surfaces in a complex virtual reality environment (e.g., 3D gaming environment) can prove

to be a difficult task using data-driven modeling. Second, as it is evident that an object needs to be physically present in order to be modeled. Certain scenarios can arise where modeling an object without physical presence may be required. One such instance can be modeling all the fabrics in an online shopping outlet. Keeping these shortcomings in mind, we need to develop a method where haptic modeling is more robust, easy to adapt to new surfaces, and detached from dependence on physical presence of the objects.

Another difficulty in haptic modeling is the association of haptic property models with the geometry. Currently, such property authoring is usually done manually by a haptic programmer directly in a rendering program code, e.g., openHaptics and CHAI3D. Some efforts exist for providing an intuitive tool for haptic authoring, e.g., [61, 62], but manual assignment and tuning still takes some efforts.

Our research thrust is originated from the need of efficient haptic modeling. The broad goal of the current research is to build a "Haptic texture library" – a collection of a large number of haptic models that describe a wide range of haptic surfaces – and to develop a method that automatically authors the haptic property of the environment with minimal effort using the library. We hope that with this tool, application-ready and haptic-enabled environment models can be easily generated without extensive modeling. The overall framework for automatic assignment is provided in Fig. 2.1.

2.1 Overview

The steps associated with automatic assignment are addressed in the following sections. Perceptual space is established using a similarity rating psychophysical experiment with 84 real life texture surfaces in Sect. 2.2. Section 2.3 is dedicated to extraction of image features and selection of the image features which best describe the perceptual space. A total of 98 image features are extracted using various well-known image feature extraction techniques. The image feature selection is carried out using sequential forward selection and parallel analysis. The haptic texture model library is established using the relationship between image feature space and perceptual space is discussed in Sect. 2.4. The procedure of assigning haptic models to unseen outside library texture surfaces is elaborated in Sect. 2.5. Furthermore, the system is evaluated using two psychophysical
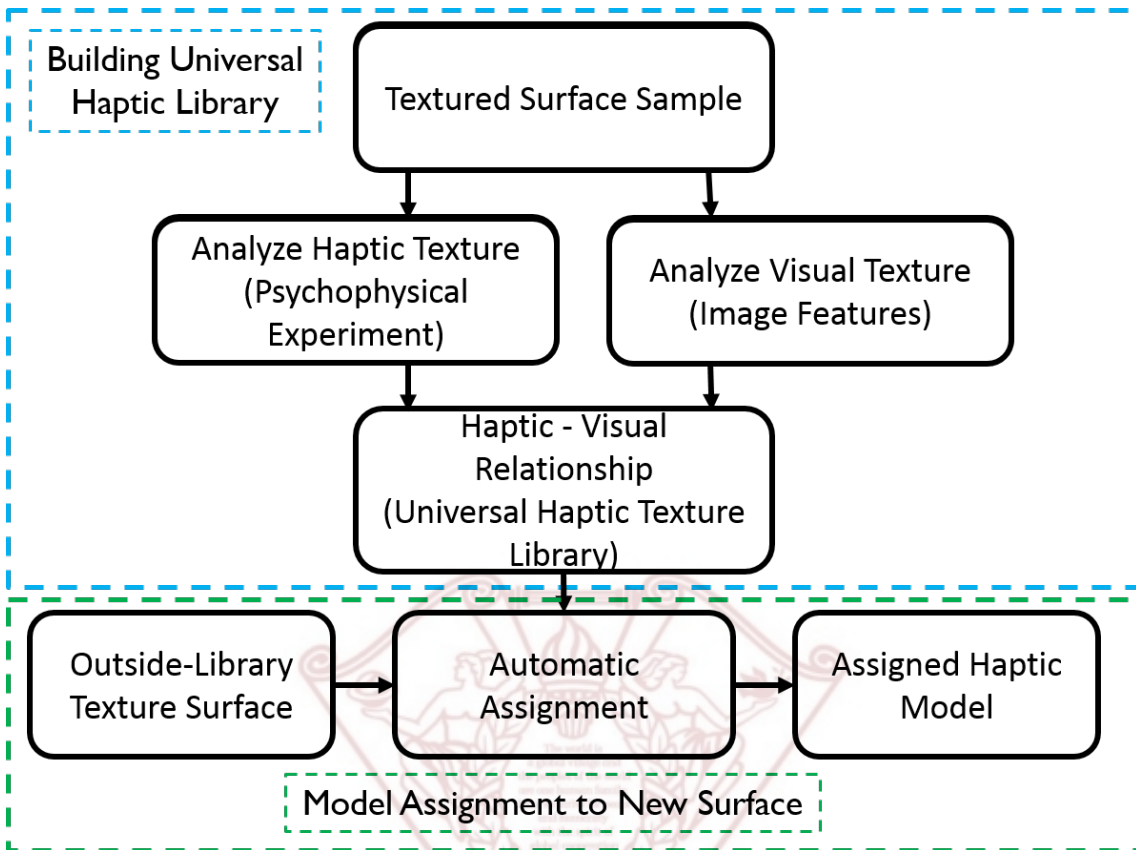
Figure 2.1: Overall framework of haptic library and automatic assignment.

studies. The first evaluation experiment in Sect. 2.6 is carried out to measure the accuracy of the proposed system when exposed to previously unseen textures The second evaluation experiment in Sect. 2.7 is conducted to judge the completeness of the library in terms of perception. In this experiment, convex hulls are created to find perceptual thresholds within the perceptual space. The discussion, based on the results, is given in Sect. 2.8. The chapter is concluded in Sect. 2.9.

2.2 Perceptual Haptic Texture Space

In the perceptual haptic texture space, real life textured surfaces are represented as points in an n-dimensional perceptual space. We use Multidimensional Scaling (MDS) analysis to represent the perceived texture of a textured surface. Each surface is represented as a point in the perceptual space. The distances among the textured surface locations are chosen such that they represent the
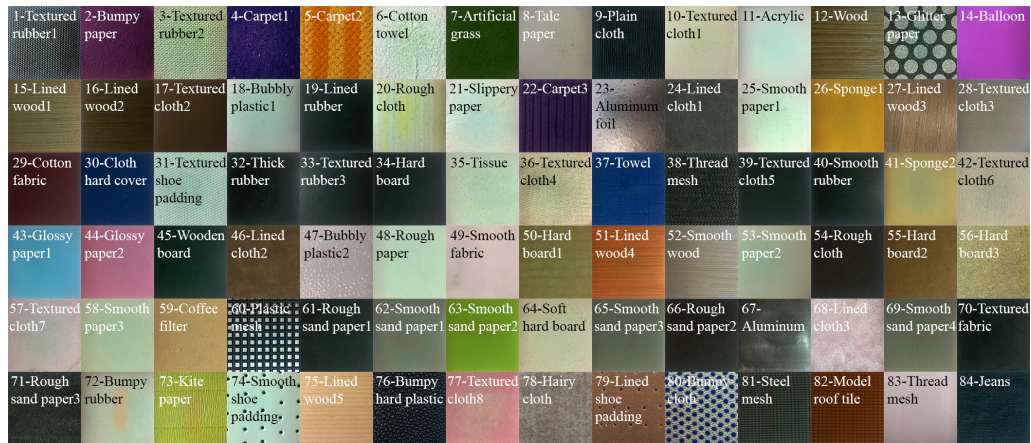
Figure 2.2: 84 real-life texture samples used in this study.

perceived dissimilarity between the them. A psychophysical experiment was conducted to find the dissimilarities between various real life textured surfaces.

2.2.1 Establishing Perceptual Space

A cluster sorting experiment was carried out to find the dissimilarities between the real life textured surfaces. The authors in [63] show that cluster sorting can accurately capture the dissimilarity data. This dissimilarity data was used to establish the haptic perceptual space.

Participants A total of ten participants took part in the experiment. They were paid for their participation. Their ages ranged from 22 to 31 years. The participants reported no disabilities and had little or no expertise regarding the experiment.

Stimuli The experiment consisted of 84 different real life textured surfaces. These 84 textured surfaces were subjectively selected in such a way that they captured the whole range of daily life haptic interactions that happen in a common office. The textured surfaces were glued to rigid acrylic plates of size $100 \times 100 \times 5$ mm. The real life textured surfaces will be referred to as 'samples' from here on for convenience. The details of all the textured surfaces can be found in Fig. 2.2.

It should be noted that the participants were asked not to judge the surfaces based on differ-

ences in stiffness, because, all the surfaces were mounted on hard acryl plates which augmented the actual stiffness of all the surfaces. Excluding stiffness, all the other haptic properties were considered for clustering the given surfaces.

Figure 2.3: Experimental setup for the cluster sorting task.

Procedure   A table was placed in front of the participants. Instructions to the participants were provided on a printed piece of paper. After reading the instructions, the participants were encouraged to ask any questions regarding the experiment. The participants wore a blindfold to restrict visual cues during the experiment. The participants also wore headphones playing pink noise. The volume of the pink noise was controlled such that it masked the sound of interaction of hand with the sample, while not obstructing normal conversation. The experimental setup is shown in Fig. 2.3.

The experiment was a cluster sorting task similar to the one carried out in [63,64]. Participants were asked to sort the 84 samples into predefined number of groups. They were asked to assign a given sample to a group based on the similarities with other samples in that particular group. A total of five trials were conducted per participant. The total number of groups in the five trials were 3, 6, 9, 12, and, 15, respectively. The order of trials was changed across participants to remove ordering bias. The total number of groups across trials were varied because, on one hand, a lower number of groups per trial ensured a broader classification of the samples, while, on the other hand, a higher number of groups ensured that the samples were classified more precisely. This ensured that the trials with lower number of total groups helped in forming major groups
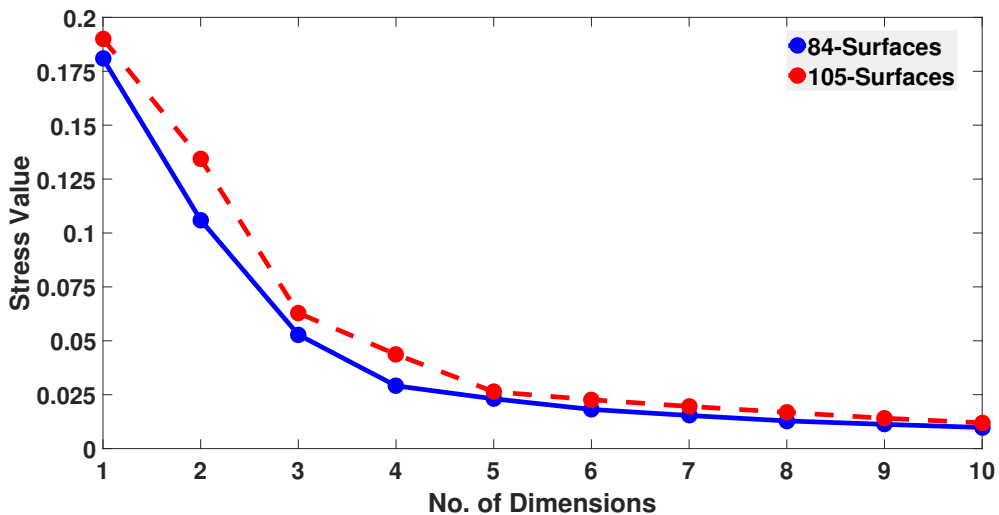
Figure 2.4: Kruskal stress values for the first ten dimensions of the 84-surface and 105-surface perceptual spaces.

in the sample set. The samples having a vague perceptual resemblance were grouped together. While, the trials with higher number of total groups helped in gathering very similar samples into the same groups, thus, providing groups with perceptually very similar samples. The participants were free to use any exploring strategy while interacting with the samples with their bare-hands. Once all the samples were classified, the participants were given a second chance to check all the groups for any errors in classification. In case of an error, they were allowed to assign it to a new group. The participants were allowed to take short breaks of five to ten minutes between trials. On average the experiment took 150 minutes per participant excluding the break times.

Data Analysis To convert the data into meaningful information, a similarity matrix was formed from the similarity scores of all the individual samples. Score to a pair of samples was assigned based on the total number of groups present in that particular trial, and subsequently, the scores across all the trials were added. For example, if a pair of samples was grouped together in the trials with total number of groups at 3, 6, and, 9, then the total score for that pair would be 3 + 6 + 9 = 18. The sample pairs which were perceptually very similar would be grouped across most of the trials and thus obtaining a higher similarity score. This data was used to form a similarity matrix for all the participants. Afterwards, the similarity matrix was converted to a dissimilarity

matrix , scaled from 0 to 1000, and averaged across all participants.

Results   Using the average dissimilarity matrix, non-metric MDS analysis was performed. Based on the Kruskal stress [65], a three dimensional representation was selected for the perceptual space. The stress value at dimension three is 0.05, which is considered as fair according to [66]. Furthermore, the decrease in stress values after dimension three is relatively small. The three dimensional MDS scatter graph of the perceptual space and the Kruskal stress for the first ten dimensions are shown in Fig. 2.5, and 2.4, respectively.

The MDS scatter graph of the perceptual space, in Fig. 2.5, shows distinctive trends and groupings, i.e., perceptually similar samples are clustered together. The scattering of the samples in the perceptual space follow a horseshoe curve. The roughest samples occupy the right side of the curve in the graph and as we move along the curve towards the left side, the roughness of the samples gradually decrease. Additionally, the curve exhibits some width also. The inner side tends to have softer samples as compared to the outer side .

It can be seen that the sandpaper samples which are distinctly different from all other surfaces, are located in a separate group in the right top corner of the graph. All other samples are located along a continuum. On one end, it starts with the surfaces having visible contours, e.g., steel and plastic meshes etc. These were deemed as the roughest samples. Next are the surfaces which have a visibly rough surface e.g., towel, carpet etc. The middle of the horseshoe curve is occupied by the mildly textured surfaces, most of them being fabrics. They include, cloth-hard-cover, jeans, fine sand paper etc. The other end of the horseshoe contains the smooth surfaces. Smooth surfaces are smooth shoe padding, aluminum, acrylic etc.

2.2.2   Completeness of Perceptual Space

The 84 surfaces used in this study are diverse and they cover a significant portion of haptic space. These surfaces represent various materials and their variants. However, the density or completeness of the library can be questioned. We need to check if the haptic space covered by this library is densely populated. If the space is sparsely populated, haptic texture assigned to any new texture could be prone to errors. For this purpose, a short analysis was carried out.
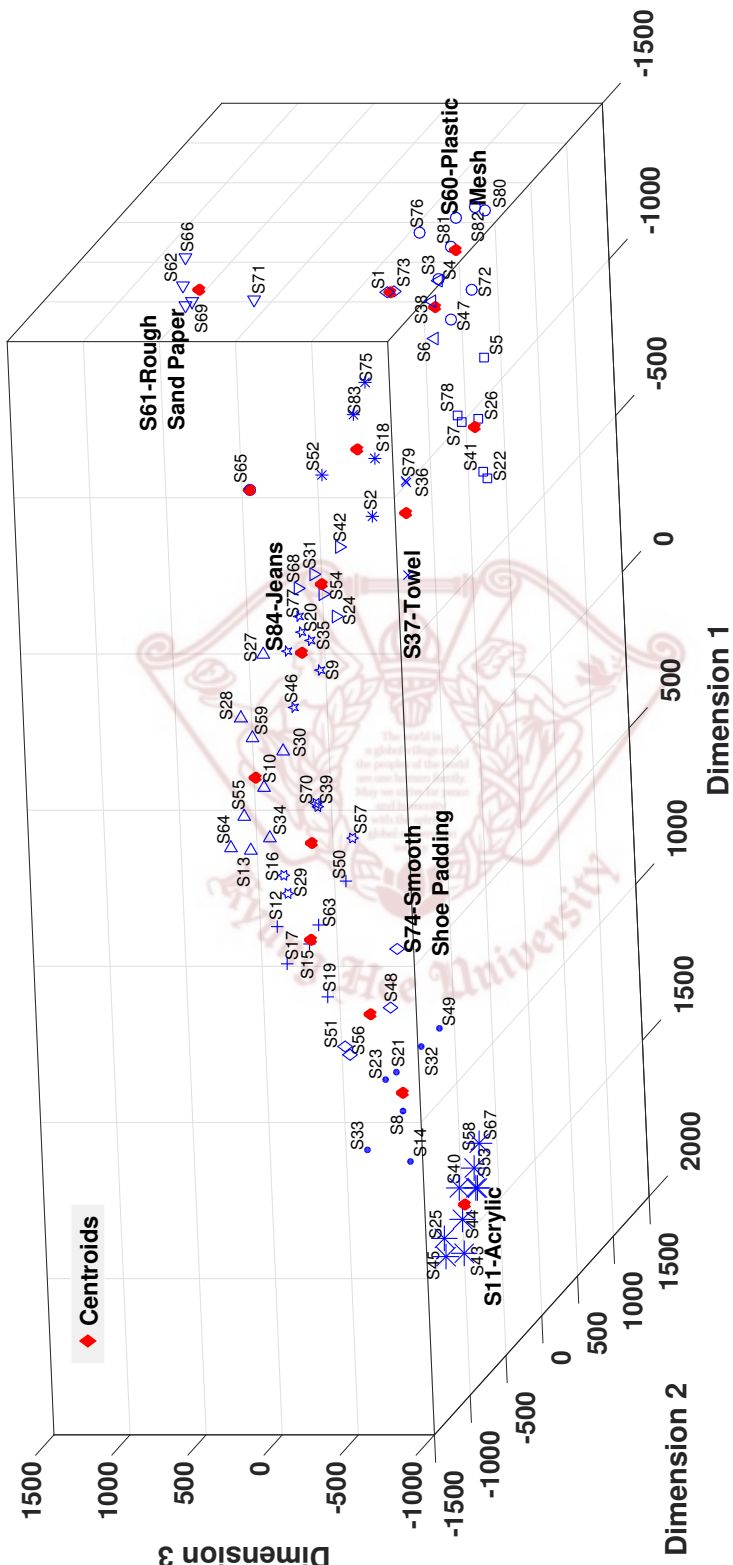
Figure 2.5: Three dimensional MDS of perceptual space. The different shapes represent the different groups as a result of K-means clustering. The filled red diamonds show the centroids of the groups.
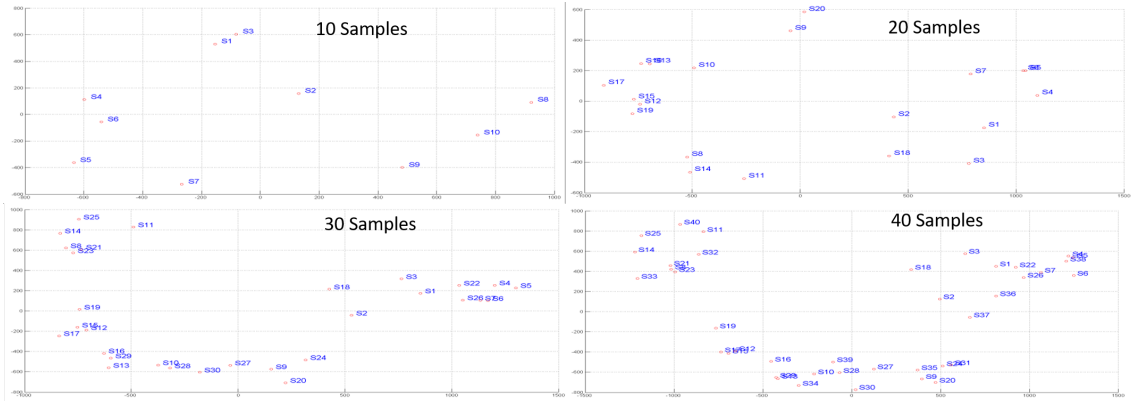
Figure 2.6: Step-wise population of the 84 surfaces to establish the perceptual space. 10 samples are added at a time.

Normally, the perceptual space is established considering the dissimilarities between all the given surfaces. In order to check the completeness of our library, we established the perceptual space in a step-wise manner. Only ten surfaces were used to build the space initially and MDS analysis was performed. Afterwards, ten more surfaces were added to the existing ones and MDS analysis was performed. This process was repeated until all the surfaces were included, as shown in Fig. 2.6 and 2.7 From the figure we can see that the first ten surfaces are scattered widely. As the number of surfaces increase, the overall coverage area increases. The coverage area increases up to around 40 surfaces. Afterwards, the addition of more surfaces only increases the density of the space. From this result we can deduce that around 40 surfaces are sufficient to cover the given subset of haptic space. The rest of the surfaces are used up in making the given space denser. Therefore, when new textures from similar haptic space are added into the perceptual space, they will most often reside within the area covered by the 84 surfaces.

2.3   Image Feature Space

In the image feature space, the visual texture of a surface is represented as a multidimensional feature vector calculated from an image of the surface. A total of 98 image features were calculated from each surface using well known image feature extraction techniques, constructing a 98 dimensional vector. The details of all the image features used in this study can be found in
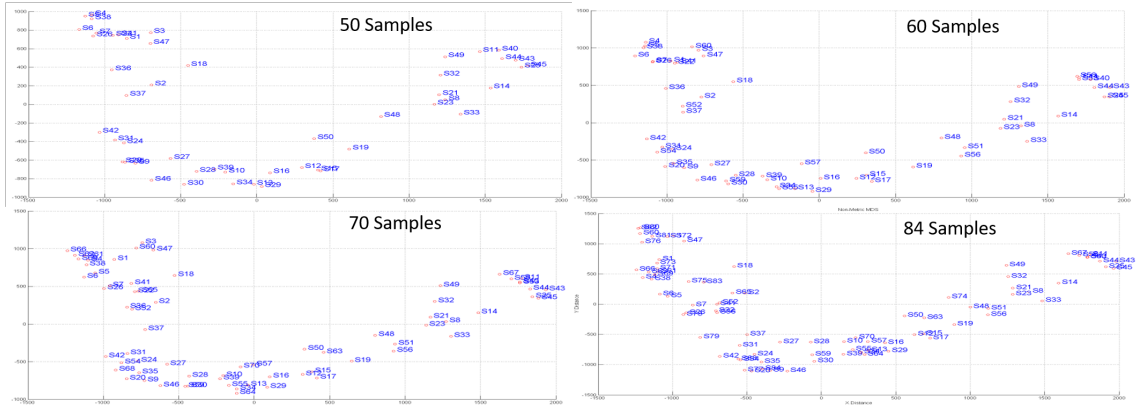
Figure 2.7: Step-wise population of the 84 surfaces to establish the perceptual space. 10 samples are added at a time (the last plot gets only 14 new surfaces.)

Table 2.1.

2.3.1 Image Capturing Setup

The finer details of image depend on the scale and resolution of the image. In an effort to remove the effects of scaling and resolution, all the images were captured with the same camera (SIGMA Digital Camera dp2 Quattro). The camera was mounted on a tripod and placed directly over the surface. The distance from the camera to the surface was kept constant at 300 mm. Standard room lighting was used during the capturing process. However, special care was taken to guard against any shadows in the images. The images were captured in high quality RAW format (loss less compression, 14-bit). The images were cropped to a size of $300{\times}300$ pixels. The images were also converted to gray scale in order to make them color independent.

2.3.2 Image Feature Selection

Given the large size of the image feature vector, it was infeasible to use all the features for prediction of perceptual haptic texture. Therefore, the most correlated image features with the MDS dimensions were selected through a sequential forward selection (SFS) algorithm. Afterwards, these features were put through a parallel analysis test to check if the resulting correlation values in the SFS are achieved by chance or they bare some significance. Features with the best predictive ability were highlighted as a result of parallel analysis. The process is shown in Fig. 2.8.

Table 2.1: List of all the image features used to establish the image feature space. The bold face image features are the ten best image features. * *Homogeniety (GLCM) was selecected for both d = 2 and 4.*

GLRLM Features [67–70]

- Short Run Emphasis
- Long Run Emphasis
- **Gray-Level Nonuniformity**
- Run-Length Nonuniformity
- Run Percentage
- Low Gray-Level Run Emphasis
- High Gray-Level Run Emphasis
- Short Run Low Gray-Level Emphasis
- Short Run High Gray-Level Emphasis
- Long Run Low Gray-Level Emphasis
- Long Run High Gray-Level Emphasis
- Gray-Level Variance
- Run-Length Variance

GLCM Features at d = 1,2,4 [44,71]

Sum of Squares	Energy
Sum Average	Entropy
Sum Variance	Dissimilarity
Sum Entropy	Contrast
Difference variance	Cluster Prominence
Difference entropy	**Correlation**
Maximum probability	**Homogeneity***
Information measures of correlation (1)	Autocorrelation
Information measures of correlation (2)	Cluster Shade
Inverse difference moment normalized	

GLSZM Features [67–70]

- Small Zone Emphasis
- Large Zone Emphasis
- **Gray-Level Nonuniformity**
- Zone-Size Nonuniformity
- Zone Percentage
- Low Gray-Level Zone Emphasis
- High Gray-Level Zone Emphasis
- Small Zone Low Gray-Level Emphasis
- **Small Zone High Gray-Level Emphasis**
- Large Zone Low Gray-Level Emphasis
- Large Zone High Gray-Level Emphasis
- Gray-Level Variance
- Zone-Size Variance

NGTDM Features [72]

- Coarseness
- Contrast
- Busyness
- Complexity
- Strength

Gradient Features

- Non-Zero
- Kurtosis
- Skew
- Percent 1
- **Percent 25**
- Percent 50
- Percent 75
- Percent 90
- Percent 99

Spatial Frequency
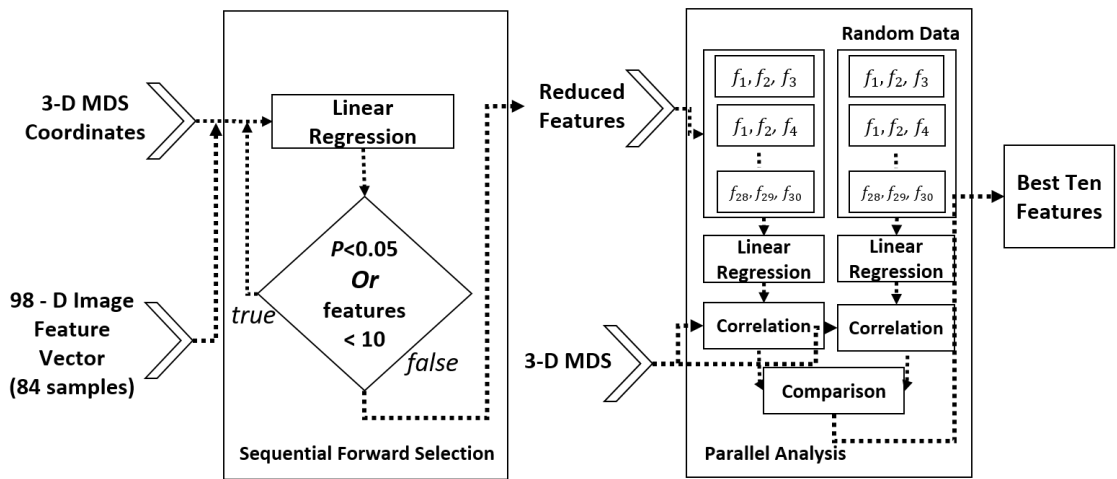
Figure 2.8: The two step process used for feature selection. Sequential forward selection reduces image feature vector from 98 to 30 dimensions based on correlation with perceptual space. Parallel analysis provides the ten most correlated and significant features among the given 30.

Sequential Forward Selection A sequential forward selection algorithm [73] was applied to reduce the dimension of the image feature vector (98 features). The input to the algorithm is the 98 dimensional image feature vector and the coordinate values of the first three dimensions given by MDS. For every single MDS dimension, the algorithm starts with the most correlated image feature and predicts the output. The output is in the form of the MDS dimension. A linear regression model was used to predict the output. Then it adds a second feature and predicts the output once again. It keeps on adding features until the termination criterion is met. The termination criterion in this case was either of, the prediction error being significantly reduced $p \geqslant 0.05$, using partial F-test) or a total of ten image features being selected for each dimension. The number ten was empirically determined. For all the dimensions, the prediction error was never significantly reduced for the first ten features. Thus, we had a reduced feature set of 30 distinct image features (ten per dimension), but once we go beyond ten image features per dimension, repetition starts to occur. Most of the new features are already present in the first ten features for the other dimensions. This fact was established after experimenting with varying number of features from each dimension, and it was decided to use ten features per dimension. The top 15 most correlated image features with each dimension are provided in Table 2.2

Table 2.2: The 15 most correlated image features with each of the dimensions of the perceptual space. The bold face numbers are the ones which are being repeated

S. No	Dimension 1	Dimension 2	Dimension 3
1	4	30	45
2	3	35	64
3	32	21	61
4	40	8	51
5	53	22	25
6	85	9	5
7	79	82	14
8	72	62	70
9	18	95	27
10	1	33	41
11	**30**	**4**	12
12	12	**79**	**21**
13	27	**45**	**53**
14	**14**	98	**72**
15	**45**	**85**	27

Parallel Analysis   Parallel analysis [74, 75] is carried out to see if the image feature is really related to the perceived haptic texture and to examine the predictability of the reduced feature compared to that of a random data set with the same dimensions. Our hypothesis is that the predictability of the reduced image feature subset should be higher than that of random data.

For the analysis, the reduced image feature subset of 30 image features was further divided into all possible subsets of three image features. The predictive quality of every subset was evaluated for the first three MDS dimensions using linear regression. The output from regression was the MDS coordinate values of the corresponding dimension. Subsequently, the correlations between the predicted values and the actual MDS coordinate values were measured.

The same process was repeated for a randomly generated data matrix which was of the same dimension as the reduced image feature vector. The correlations between the predicted output from random data subsets and actual MDS coordinate values were also recorded.

The correlation values measured from the randomly generated matrix are the values that can be achieved by chance and have no significance. Therefore, only those image feature subsets are significant which showed correlation values higher than the maximum correlation from randomly generated data. Figure 2.9 shows the correlation values for the image feature subsets (see green
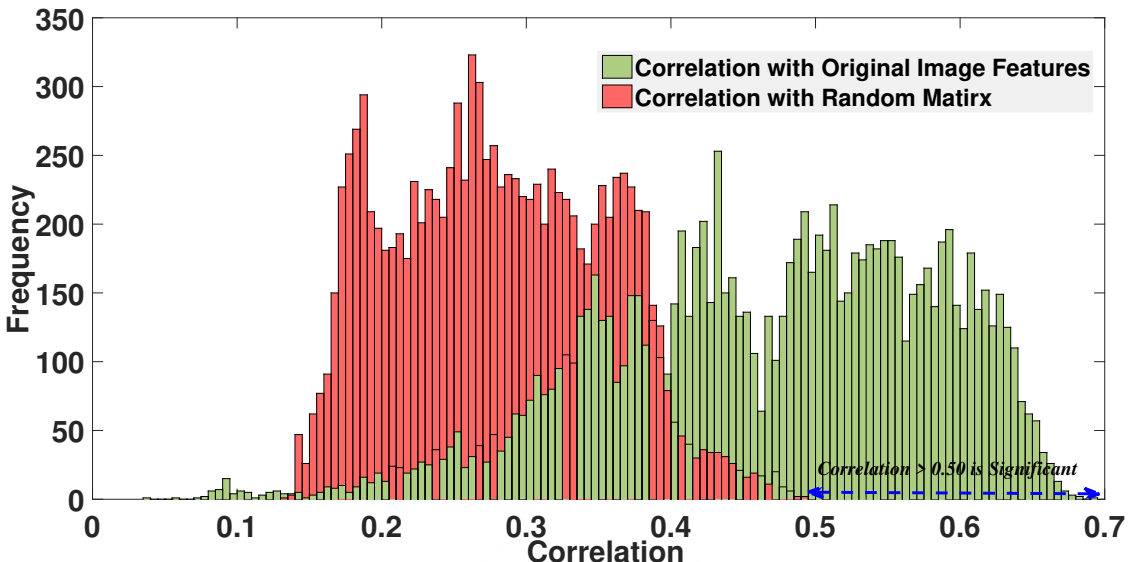
Figure 2.9: Correlation values for the image feature subsets and the randomly generated data subsets with the first three MDS dimensions.

bars) and the randomly generated data (see red bars).

The maximum correlation for a random data subset was 0.47. To be on the safer side, a value of 0.50 was considered. Image feature subsets with correlation higher than 0.50 were considered as significant. The frequency of features constituting the significant image feature subsets was calculated. The best features were the ones which occurred most frequently in the significant feature subsets. The ten features with the highest frequency were: Gray-level non-uniformity (GLRLM); gray-level non-uniformity and small Zone High Gray-level emphasis (GLSZM); gradient percentile 25% (Gradient); correlation, homogeneity, information measure of correlation (2), and inverse difference moment normalized (GLCM at d = 4); homogeneity and information measure of correlation (1) (GLCM at d = 2). These features were selected for the automatic haptic model assignment algorithm discussed in Sect. 2.4 and 2.5.

2.3.3 Description of the Selected Image Features

This section provides a brief overview of the ten image features obtained as a result of the image feature selection process.

The GLCM is a matrix which considers the spatial relationships between two pixels at a time

in the image. *Correlation* measures the linear dependency of gray levels on those of neighboring pixels. *Homogeneity* measures image homogeneity as it assumes larger values for smaller gray tone differences in pair elements. The weights decrease exponentially away from the diagonal. *Inverse difference moment normalized* is a linear measure which calculates the gray tone differences among pixels. *Information measure of correlation 1 and 2* are statistically derived from the correlation measure. The GLRLM looks at runs of pixels, rather than looking at pairs of pixels, i.e., how many pixels of a given gray value occur in a sequence in a given direction. *Gray level non-uniformity* measures the similarity of gray level intensity values in the run length matrix. The GLSZM looks at zones of connected pixels, i.e., how many pixels of a given gray value are connected in a single group. *Gray level non-uniformity* measures the similarity of gray level intensity values in the size zone matrix. *Small zone high gray level emphasis* is a robust and highly discriminative statistical measure since it includes the pixel information in addition to the rows and columns of the size zone matrix. The *25 percentile* gives the highest peak under which 25 percent of the pixels are in the image.

2.4   Haptic Models Library Using the Relationship Between Perceptual Haptic Texture Space and Image Feature Space

Figure 2.5 shows that the scatter graph of haptic perceptual space exhibits distinct grouping of perceptually similar samples while in Sect. 2.3, it was shown that there exists a relation between the image feature space and the haptic perceptual space. Based on this knowledge, it is assumed that the image feature space could also be classified into groups of haptic-perceptually similar images. For this purpose, a Multi-Class Support Vector Machine (MC-SVM) [76] was used in conjunction with K-means clustering [77].

Since the distribution of groups in image feature space cannot be predicted, a one-versus-rest Multi-Class Support Vector Machine (SVM) algorithm with a Radial Basis Function (RBF) kernel was used for clusterizing the image feature space. The use of RBF kernel was preferred since it can handle both linearly separable as well as inseparable data. Data in which clusters cannot be distinguished linearly is called as linearly inseparable. The multi-class SVM algorithm was

tested for different values of the parameter sigma, and the best results were obtained at sigma = 4. Another possibility was to use deep learning as it is used in various research areas and could provide better results, but in this case it was not applicable due to the limited size of our dataset. Similarly, other algorithms were also tried for the classification, however, MC-SVM provided the best results for our dataset. On the other hand, the clusterization of perceptual space was carried out using k-means algorithm. This clusterization falls under the umbrella of unsupervised learning, and k-means is one of the most powerful algorithm for unsupervised learning.

The reduced image feature set (ten image features) for all the 84 samples was used as input for training the MC-SVM. To provide labels for the SVM, k-means clusterization was applied to the haptic perceptual space. The labels are used to classify different samples into perceptually similar groups. As shown in Fig. 2.5, perceptually similar samples are in close proximity with one another. Therefore, as a result of the k-means classification, perceptually similar samples were grouped together. Since, the overall range of samples used in this study can subjectively be divided into 16 broad categories, the number of groups used in k-means was decided to be 16. This grouping can be seen in Fig. 2.5. The imbalance in the variance of the groups increases if the total number of groups are increased beyond 16. While, a lower number of total groups results in perceptually different surfaces being grouped together. As a result, the image features were labeled from perceptual clusterization and the MC-SVM was trained on this data. Consequently, a *Haptic Texture Library* was formed where image features of texture surfaces were directly associated with the perceptual haptic texture of the surfaces. The trained model of MC-SVM was used to classify new texture surfaces to perceptually similar groups based on the image features of the new surface.

2.5 Automatic Haptic Model Assignment

The relationship established between image feature space and the perceptual haptic texture space was used to automatically assign haptic models to newly encountered textured surfaces. The automatic haptic model assignment was a two-step process. First, the trained MC-SVM model was used to assign a perceptually similar group to the new sample based on its image features. Second, an exact match within the selected perceptually similar group was assigned based on an image classification technique, known as Binarized Statistical Image Features (BSIF) [46]. BSIF is a
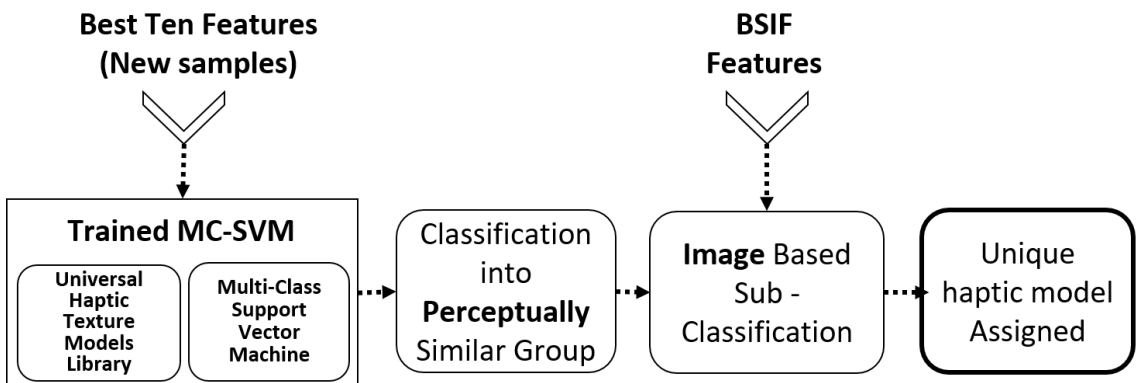
Figure 2.10: The process of assigning haptic models to newly encountered textures.

local image descriptor specifically designed for encoding texture information. It differs from other descriptors in the type of filters used for convolution. Usually, these filters are manually predefined, whereas, in BSIF, these filters are learnt from statistics of natural images. Since the surfaces used in this study can also be considered as natural, BSIF provides better modeling capacity as compared to other descriptors. The overall framework for automatic haptic model assignment is shown in Fig. 2.10.

The trained SVM model was used to assign a perceptually similar haptic model from the library to a new real life texture surface. As a first step, the reduced image feature set was calculated for the new sample. This image feature set was used as a test input to the SVM model. The trained SVM model then classified the new sample into one of the groups, which were made in Sect. 2.4.

As a pre-process to the second step, binarized statistical image features were calculated for all the surfaces in the perceptual space. In the second step, BSIF features were calculated for the new sample and compared to other samples within the group selected in the first step. The comparison was carried out using chi-squares distances. The haptic model of the sample, within the selected group, having the lowest distance to the new sample was assigned to it.

2.6 Evaluation Experiment 1

A psychophysical experiment was conducted for evaluation of the automatic assignment. The experiment was conducted to check if the haptic model assigned by the algorithm is perceptually

Figure 2.11: The 21 new textured surfaces used for evaluation.

similar to the new sample. The new sample over here is the surface to which we wanted to assign a haptic model using our algorithm.

2.6.1 Psychophysical Experiment

The design of the evaluation experiment was a cluster sorting task similar to the one conducted in Section 2.2. The aim of this experiment was to validate the authenticity of the automatic assignment algorithm. For this purpose, 21 new outside-library samples were used and the automatic assignment algorithm was used to assign them haptic models from the library. In the experiment, the 21 new samples in addition to the earlier 84 surfaces were used and participants were asked to classify them into perceptually similar groups. A perceptual space having these 105 samples was built using MDS. This provided us ground truth data about the 21 new samples in terms of their location in perceptual space. Afterwards, the automatic assignment algorithm was also used to assign haptic models to the new surfaces. If the model assigned by the algorithm appeared in the same perceptual group as in the experiment, the assignment was considered to be correct. The details of the experiment are provided in the following sub-sections.

Participants and Stimuli   A total of six participants took part in the experiment. None of the participants were part of the initial experiment for building the perceptual haptic texture space.

The participants reported no disabilities and had never been part of such an experiment. They were paid for their participation.

The stimuli for the evaluation experiment were a set of 105 real life textured surfaces. The 84 samples used in Section 2.2 and a new set of 21 real life textured samples constituted the 105 samples. Each sample was mounted on an acrylic plate of size $100 \times 100 \times 5$ mm. Figure 2.11 shows the new set of 21 samples.

Procedure The experiment was a cluster sorting task where the participants were asked to classify perceptually similar samples into groups. A total of three trials were conducted per participant, and the number of groups in these trials were 6, 9, and 12. The number of groups in a particular trial were randomly selected to avoid any bias. The rest of the details of the experiment were the same as the previous experiment.

Data Analysis and Results The data from the experiment was converted into a dissimilarity matrix and scaled from 0 to 1000. The dissimilarity values were calculated in the same way as in the initial experiment in Sect. 2.2. MDS analysis was performed on the dissimilarity matrix. The kruskal stress value for the first ten dimensions is shown in Fig. 2.4. The stress value for three dimensions is 0.062, which is considered as fair according to [65]. Therefore, a three dimensional space was established to visualize the new samples in relation to the old samples. The space obtained as a result of MDS analysis was also divided into 16 perceptually similar groups using K-means. The scatter graph of the new space can be seen in Fig. 2.12.
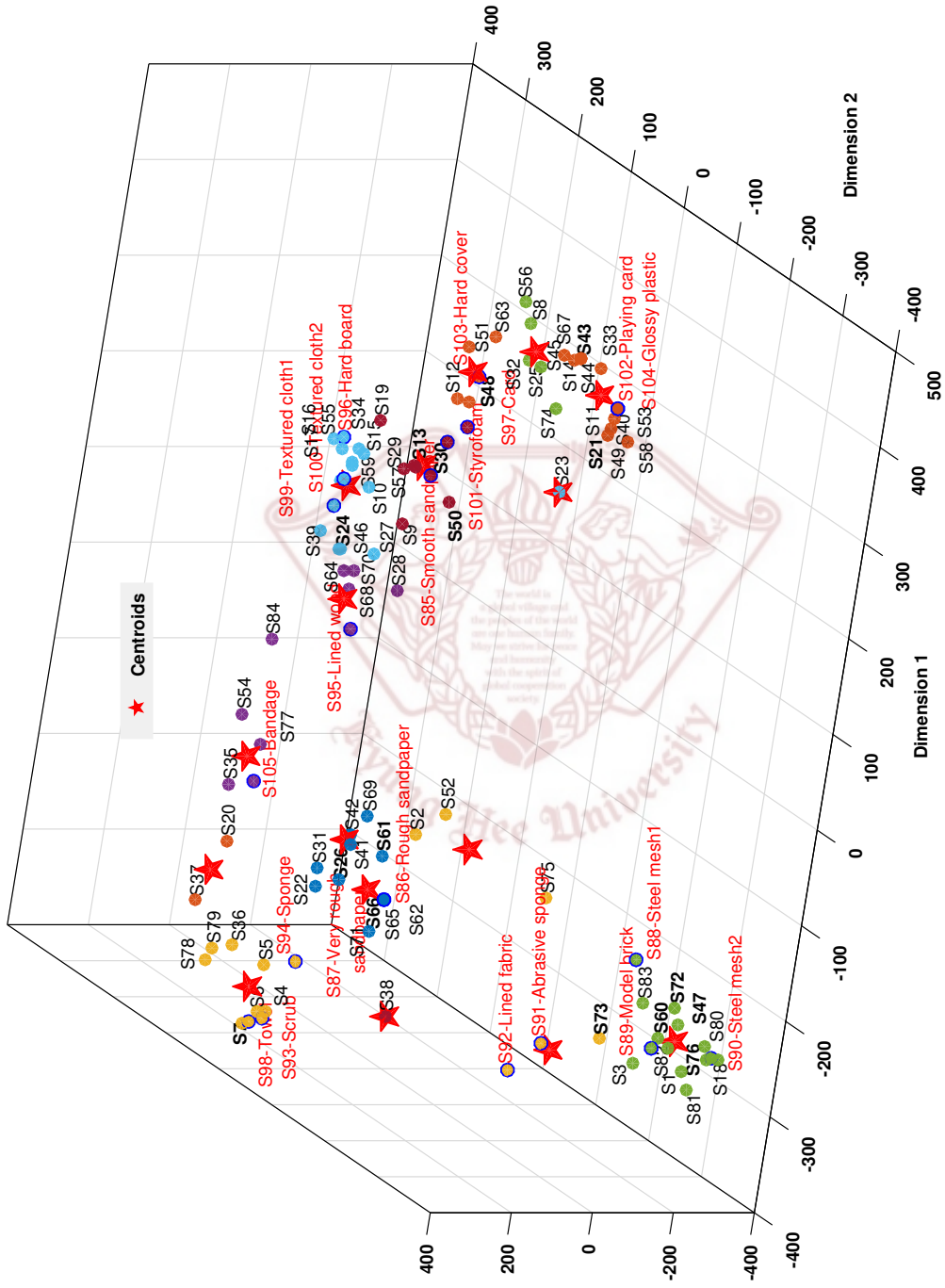
Figure 2.12: The new perceptual space made up of 21 new and 84 old texture surfaces. The different colors (of circles) represent the different groups as a result of K-means clustering. The stars show the centroids of these groups. The new surfaces are written in red color while the assigned models are shown in bold black color.

2.6.2 Evaluation Criterion

On one hand, the automatic haptic model assignment algorithm was used to assign haptic models to the new samples based on their image features. On the other hand, in the experiment, the participants classified the new samples into different groups along with the old samples. After applying K-means to the new space, all the samples were classified into perceptually similar groups. The new samples also appeared in these groups along side the old ones. These groups would provide the ground truth for the automatic haptic model assignment algorithm. An automatic assignment of a haptic model would be deemed as correct only if both the new sample and the corresponding assigned model appeared in the same perceptual group in the new space.

The haptic models assigned to all the new samples were evaluated based on the above strategy. A total of 15 out of the 21 new samples were assigned perceptually correct models i.e., the new samples and corresponding assigned model appeared in the same perceptual group. The haptic models assigned to the 21 new samples are presented in Table 2.3. Figure 2.12 shows the new samples and the corresponding assigned models inside the new perceptual space.

After checking for the correct perceptual group assignment, it was important to check if the assigned models and new samples appear closer to each other inside a group. This was checked in relation to the overall variance of the groups. The average normalized variance all the groups was 0.24 units in perceptual space. Based on this variance, the new samples having smaller distances as compared to average variance are considered as perceptually very similar to their assigned model. The histogram in Fig. 2.13 shows that the majority of samples exhibit far less distances as compared to average variance. This means that the majority of assigned models are perceptually very similar to the new surfaces.

2.6.3 Comparison Between the 84-Surface and 105-Surface Perceptual Spaces

Figure 2.14 shows the comparison between the perceptual spaces for 84 surfaces and 105 surfaces. The perceptual spaces are represented in two dimensional cross sections for better visualization for comparison purposes. To remove scaling artifacts, both the spaces were scaled from zero to one. All three dimensions of both the spaces largely follow the same trends. Especially, the first two dimensions exhibit remarkable similarity. This shows that the addition of 21 new surfaces

Table 2.3: Haptic textures models assigned to the 21 new texture surfaces.

New Texture Surface	Assigned Model	Remarks	Distance from Assigned Model (normalized 0-1)
85	30	Correct	0.05
86	26	Correct	0.07
87	61	Correct	0.04
88	47	Correct	0.09
89	60	Correct	0.01
90	76	Correct	0.02
91	73	Correct	0.07
92	73	Correct	0.12
93	7	Correct	0.04
94	7	Correct	0.14
95	73	Wrong	0.52
96	21	Wrong	0.86
97	50	Correct	0.13
98	7	Correct	0.01
99	24	Correct	0.08
100	66	Wrong	0.61
101	13	Correct	0.10
102	72	Wrong	0.95
103	48	Correct	0.06
104	61	Wrong	0.88
105	43	Wrong	0.92
Average correct classification rate	**71.4%**		
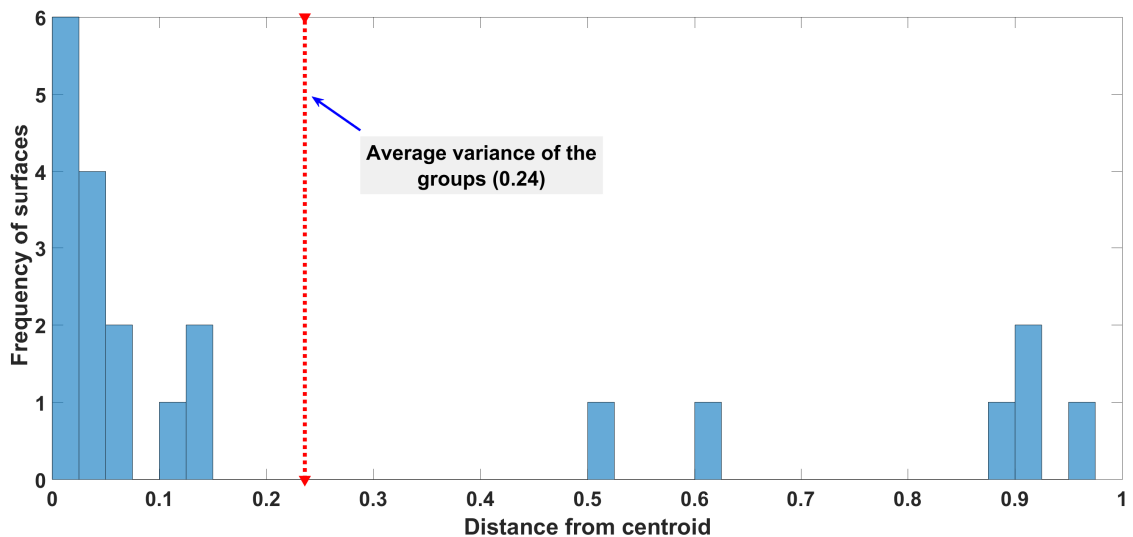
Figure 2.13: Histogram of the distances between new surfaces and the assigned haptic models from the library.

did not alter the basic shape of the perceptual space. The new surfaces either fitted inside or lie immediately outside the boundary of the convex hull created by the original 84 surfaces.

Both spaces were divided into 16 clusters having variable number of surfaces in each cluster. After examining the clusters, it was evident that most of the groups largely carried the same surfaces in both the perceptual spaces. Only 11 (out of the original 84) surfaces in the 105-surfaces perceptual space, residing on the cluster boundaries, had jumped into the adjoining clusters. this behavior was expected since multidimensional scaling and kmeans optimize each point in the space. However, it must be noted that the haptic library is established based on the 84-surface perceptual space and the 105-surface perceptual space was established for evaluation purposes only, i.e., to check if the new surface and its assigned surface resided in the same group.

2.7 Evaluation Experiment 2

Haptic texture perception is similar to visual color perception in many ways. We interact with various textures in our daily life similar to the many colors we see. It can be a trivial task for us to distinguish among the various texture that we come across. However, in some cases where any two given textures exhibit a high degree of similarity in some aspects, distinguishing them
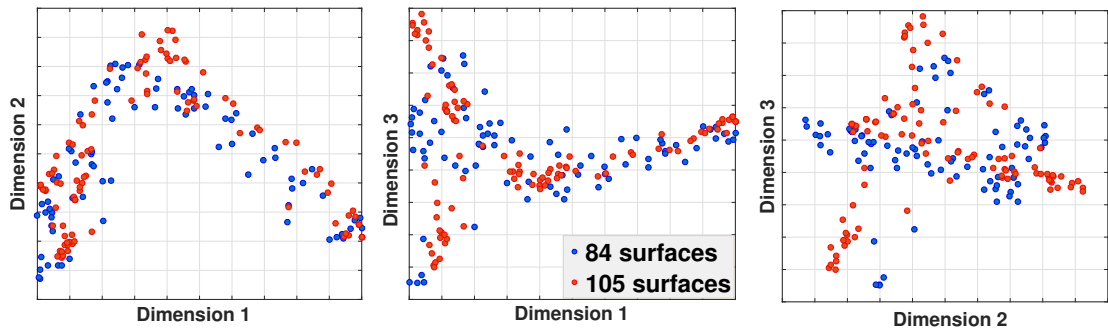
Figure 2.14: Comparison between 2-dimensional cross sections of the 3D perceptual spaces for 84 and 105 surfaces.

apart can become a challenging task. This means that humans can only distinguish textures up to a certain extent beyond which all the textures appear to be perceptually similar, we can call this limit as the haptic texture discrimination threshold.

A lot of research has been done in trying to find out the human haptic sensitivity thresholds for textured surfaces of different kinds of roughnesses and various frequencies. But the shortcoming in these researches is that the textured surfaces used were either virtually constructed or physically controlled surfaces. In the virtually constructed surfaces friction, frequency and viscosity were varied and the thresholds were determined [78]. On the other hand, the surfaces used in the physically controlled surfaces were dot-patterns [79, 80], gratings [80–82] or sandpapers [83]. They provided accurate thresholds for these surfaces but the application of this information in real life scenarios is not possible. Since, in real life we don't often encounter such surfaces. Real life textured surfaces are a mix of complex attributes and physical dimensions. Therefore, a unified study addressing the classification of real life textures based on the perception thresholds is highly required.

In an effort to achieve this goal, this study focuses on finding out the threshold levels below which two real life textured surfaces are considered to be perceptually similar. Two surfaces located close to one another in the perceptual space are considered to be similar to one another. Despite this information, there appears to be no clear boundary beyond which two surfaces can be considered as perceptually different.

In order to find the perceptual threshold for different kinds of textures, we carried out another

psychophysical experiment. In this experiment, a subset of the 84 surfaces, i.e. 16 surfaces, was used, and the perceptual thresholds were marked by enclosing the given surfaces in a convex hull. Subsequently, the standard convex hulls were extended, using a new method, to make them applicable to perceptual thresholds. It was considered that surfaces inside this perceptual convex hull are perceptually similar to the given surface.

2.7.1   Psychophysical Experiment

In the previous experiment conducted, we asked participants to classify 84 real life textures into various groups based on the similarities between them. There were five trials in that experiment and the total number of groups in the trials were 3, 6, 9, 12, 15, respectively.

In the current experiment we analyzed that grouping data for further processing. In order to find the best candidates for establishing a convex hull for a given surface, we calculated the grouping frequency of all the other surfaces with a particular surface. This calculation was done for all group sizes. Afterwards, scores were assigned to each surface based on this calculation. The scoring system is defined with the help of an example as follows; two given surfaces which were grouped together in group sizes of 3, 6, and 12 were assigned a score of 3+6+12 = 21. After calculating the scores for all the surfaces, the scores were normalized from 0 to 100. A score of zero means that the surfaces were never grouped together and a score of 100 means that the surfaces were grouped together across all the trials. In the current study, both the extremes appeared. This normalized score is called as the weighted sum of grouping frequency (WSGF). As an example, Fig. 2.15 shows the WSGF scores for surfaces 44 and 81.

Experimental Procedure   A total of six participants took part in this experiment. The first step was to select a subset of surfaces from the total of 84 surfaces for which thresholds were to be calculated. For this purpose, the perceptual space was divided into various number of groups using K-means algorithm. It was empirically found out that 16 groups sufficiently represented the perceptual space. Increasing the groups beyond 16 would cause unnecessary division of groups, while less than 16 groups would leave some groups to be very large. The perceptual space after K-means grouping is shown in Fig. 2.5. Afterwards, the surfaces nearest to the centroid of each group

Table 2.4: Baseline surfaces along with selected candidate surfaces

S. No	Baseline Surface	Perceptually Similar Candidates
1	81	76, 60, 3
2	44	58, 53, 67, 43, 45, 25
3	28	59, 64, 55, 30, 34, 27
4	17	64, 15, 16
5	36	6
6	65	-
7	51	56, 70
8	68	24, 28
9	83	73
10	26	41
11	69	69, 62, 61
12	10	39, 34, 59
13	21	74, 56, 48, 33, 14, 8
14	84	54, 46, 39, 35
15	79	26, 22
16	38	6, 73

was selected for the experiment. Thus, a total of 16 surfaces were selected from the perceptual space for which perceptual thresholds were to be calculated inside the perceptual space.

The second step for the experiment was selecting candidate surfaces for comparison with the above 16 surfaces. For this purpose, a baseline criterion was defined. The surfaces having a WSGF score of 50% or higher with a given surface were used as candidates for comparison.

The participants were provided with the baseline surface with which all other candidate surfaces were to be compared. If the candidate surface was perceptually same, it was considered as lying inside the perceptual threshold for the given surface. This procedure was repeated for all the 16 selected surfaces.

Results   The list of all the 16 surfaces used in the experiment along with the selected candidate surfaces is given in Table 2.4. Figure 2.15 shows the result of this experiment for two baseline surfaces i.e., S44, and S81. The surfaces above the 50% line were used in the experiment as candidates. The surfaces enclosed in a green outline are the ones positively identified by participants as perceptually the same.

(a) Weighted sum of grouping frequency for surface 81

(b) Weighted sum of grouping frequency for surface 44
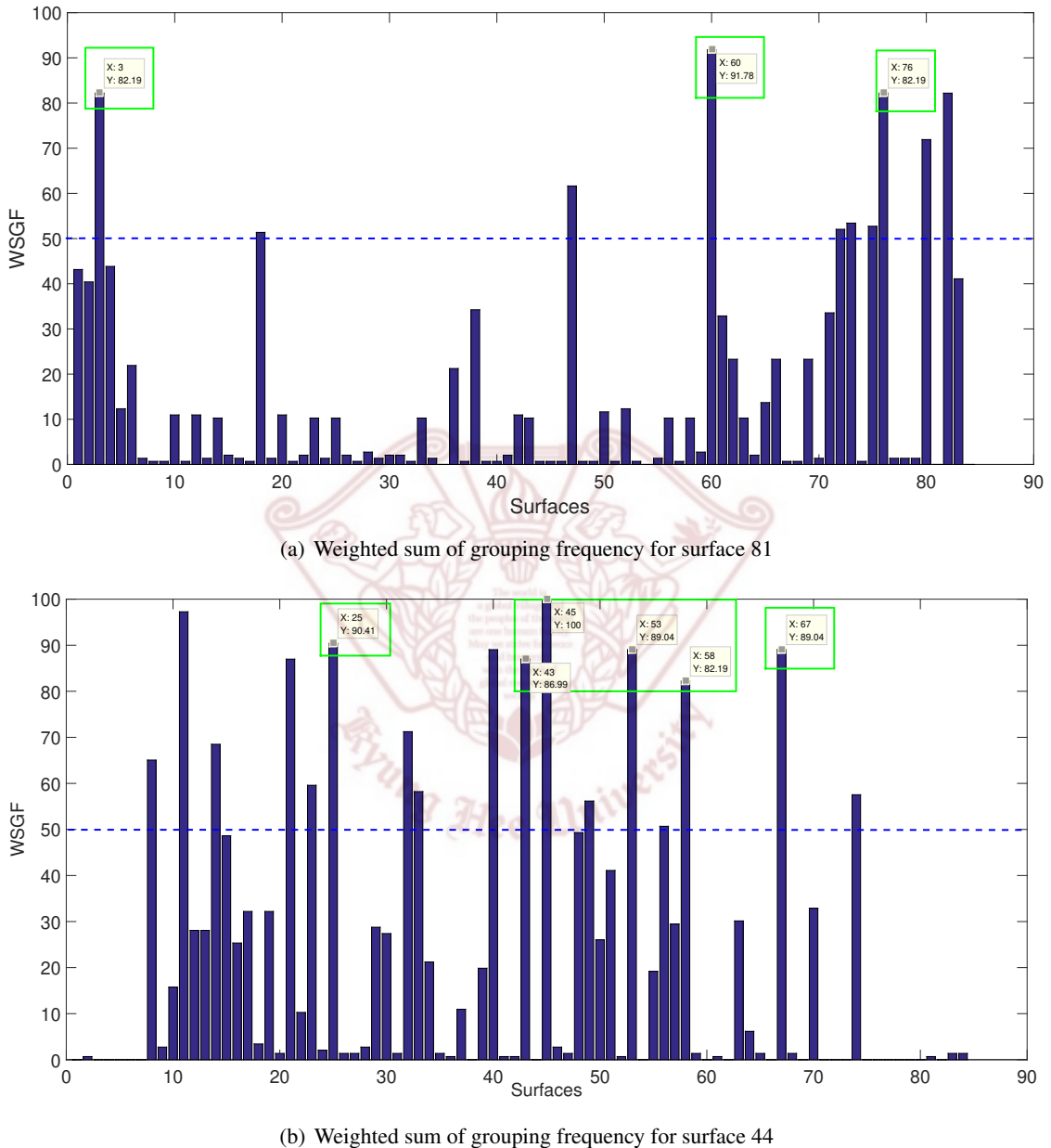
Figure 2.15: The surfaces having WSGF higher than 50 were used as candidate surfaces for comparison with baseline surfaces. The green boxes highlight the surfaces selected as perceptually similar by participants.
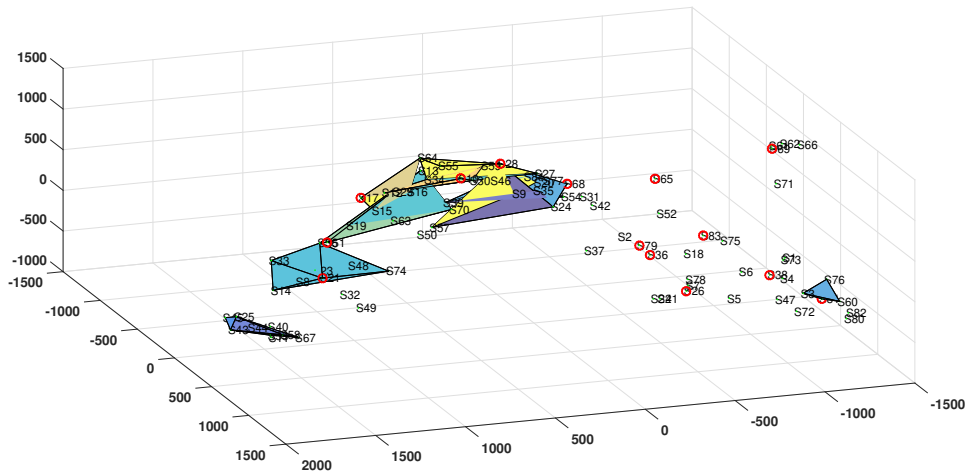
Figure 2.16: Normal convex hulls for the 16 selected surfaces. The red circles show the selected 16 surfaces. It can be seen that some of the selected surfaces are not bounded by convex hulls due to lack of perceptually similar textures.

2.7.2 Convex Hulls as Perceptual Thresholds

Based on the psychophysical experiment, we found out the perceptual boundaries for surfaces in the perceptual space. These boundaries were in the form of nearby surfaces which were perceived as same by participants. A convex hull was drawn for each of the 16 mentioned surfaces based on its perceptually similar neighbors. The 16 surfaces along with the perceptually similar neighbors are given in Table 2.4. As a result of this exercise, the perceptual space was converted into a cluster of convex hulls. Figure 2.16 shows the perceptual space with the convex hulls for 16 surfaces.

Analysis of Convex Hulls   From Fig. 2.16, we can see that most of the selected textured surfaces are bounded by convex hulls which show the perceptual threshold for a given textured surface.

However, as we know that a convex hull requires at least four non-coplanar points in space. But from Table 2.4 we can see that some of the selected surfaces had two or less perceptually similar textured surfaces. As a result of this, it was impossible to form a threshold in the form of a convex hull. From Fig. 2.16 it is visible that some of the selected surfaces are not bound by convex hulls. The fact that some surfaces had very few other perceptually similar surfaces can be attributed to the method of collecting the surfaces for making the perceptual space. While establishing the perceptual space, a conscious effort was being made to include as many diverse

surfaces as possible, therefore, some of the surfaces were perceptually very different from all or most other surfaces.

Thus it was concluded that the current approach of making convex hulls exhibited two major drawbacks:

- It used the perceptually similar surfaces, for a given selected surface, as the vertices of the convex polyhedrons for forming the convex hulls. In most cases such a bounding box would suffice. But since we are dealing with perceptual thresholds, it can be argued that the threshold level for a certain texture cannot be limited to the farthest perceptually similar textured surface. Since, the vertices of the convex hulls are deemed as perceptually similar, it would be fair to assume that the perceptual threshold lies somewhere beyond that vertex.

- The textured surfaces with two or less perceptually similar surfaces also needed to be bounded by a threshold. Since, the current implementation of convex hulls could not find a solution for this, a new method was formulated for finding the thresholds for them.

Extended Convex Hulls   A new approach for forming convex hulls was applied in order to incorporate the two major drawbacks of the standard approach. Both the drawbacks were countered with just a single tweak in the standard algorithm for making a convex hull. The details of the modified algorithm are given as follows.

Each vertex of the standard convex hull was extended into three vertices. To achieve this, the three nearest neighbors for every surface in the convex hull, for a given selected surface, were identified. Afterwards, the center point from each neighbor to a given point in the convex hull was selected as the perceptual boundary between the two points. Thus, as a result of this exercise, the boundaries of the standard convex hulls were extended to incorporate the first drawback discussed in the previous section.

The second drawback was countered automatically using the above approach. After extending each point into three new points, the problem of having four or more points no longer remained. And thus the surfaces with two or lesser perceptually similar surfaces could also be bounded by a perceptual threshold in the form of a convex hull.

The extended convex hulls are shown in Fig. 2.18. It can be seen that all the convex hulls
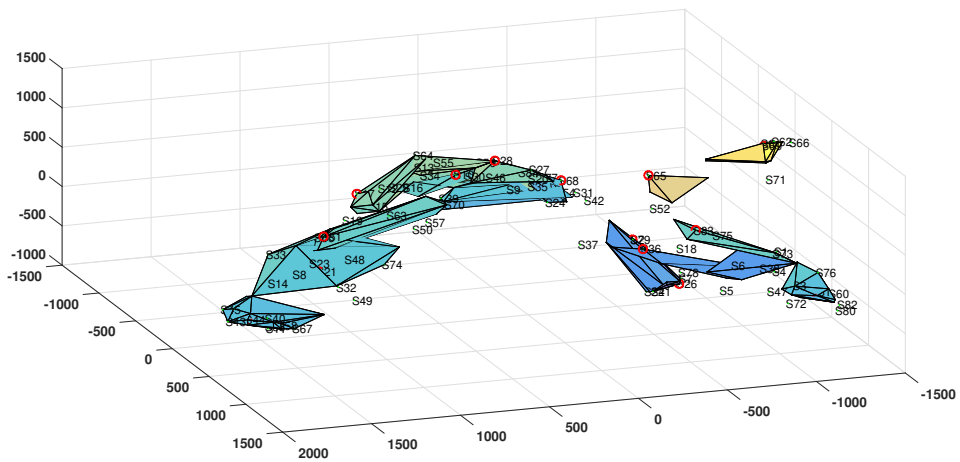
Figure 2.17: Extended convex hulls for the 16 selected surfaces. The red circles show the selected 16 surfaces.

are larger than the normal convex hulls. Additionally, the surfaces with two or less perceptually similar surfaces also have convex hulls. Thus all the surfaces now exhibit a perceptual threshold.

Comparison Between Standard and Extended Convex Hulls Figure 2.18 shows the comparison between the extended and standard convex hulls for one of the test cases (one selected surface). It can be seen that the vertices of extended convex hulls cover more area as compared to the standard ones. It is only logical that the perceptual boundary cannot lie on a perceptually similar textured surface. For instance, if we look at the standard convex hull for dimension 1, it shows four distinct vertices. All these four vertices are perceptually similar textured surfaces. While, in the extended convex hull, the above mentioned vertices are stretched further to extend the threshold and to incorporate some area beyond the perceptually similar surfaces. Same is the case for the other two dimensions also.

As mentioned earlier, this approach was selected because the vertices of the given convex hull are perceptually similar textures. Now lets assume that another imaginary texture were to be inserted right next to a vertex but on the outside of the convex hull. In most likelihood, this new texture would be perceptually similar to the textures inside the convex hulls. But if we use normal convex hulls, this texture would be deemed as outside the convex hull and thus perceptually not similar. Therefore, the convex hulls were extended beyond the farthest perceptually similar
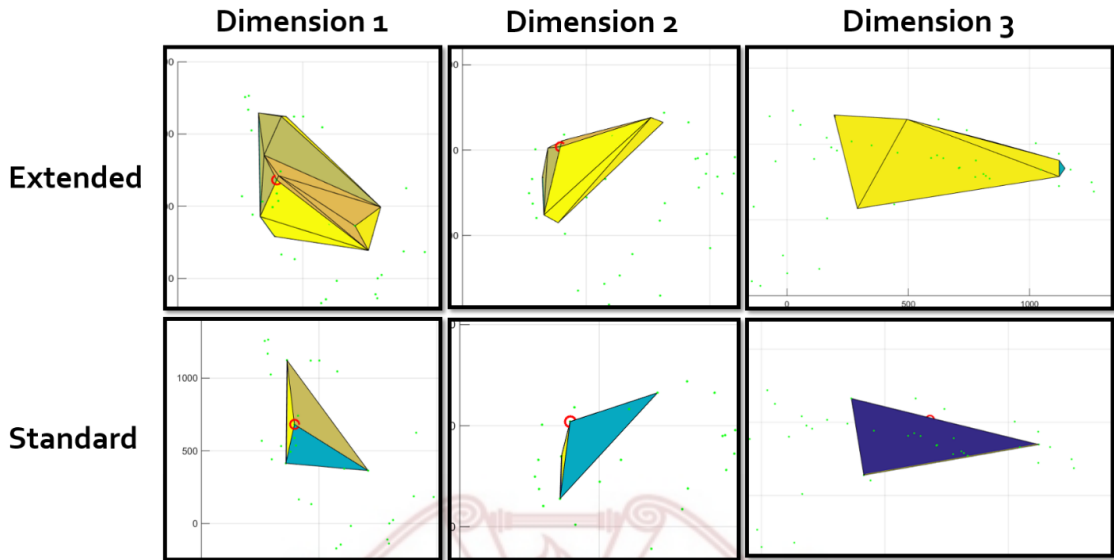
textures.

Figure 2.18: Comparison between extended and standard convex hulls

2.8   Discussion

From Fig. 2.12, it can be seen that texture surfaces having visible rough texture (S88-Steel mesh1, S89-Model brick, S90-Steel mesh2 etc.) or the ones having some degree of roughness in texture (S86-Rough sandpaper, S87-Very rough sandpaper, S93-Scrub etc) are quite accurately classified. The image features from these surfaces were very clear and the algorithm could readily differentiate the surfaces from one another. On the other hand, the smooth surfaces (S102-Playing card, S104-Glossy plastic) were incorrectly classified due to the fact that the images captured from these surfaces could not portray the surface micro geometry. This can be accredited to the limitation of hardware since the camera could not capture the surface details for these texture surfaces. Thus the image features from these surfaces were not clear and the algorithm classified them incorrectly.

Another set of surfaces that was wrongly classified was the set of textured cloth2 (S100) and lined wood (S95). The algorithm assigned a moderately rough sandpaper (S66) to textured cloth2 (S100). Upon a closer inspection it was revealed that the actual surface texture of the two surfaces was quite similar and that the two should have been assigned to the same group by the human

subjects, while building the actual perceptual space. Same was the case for lined wood (S95) to which the algorithm assigned S73 (kite paper). These two also resemble each other and should have been placed in the same group.

After careful deliberation on the experimental process it was noted that since S66 was a sandpaper and as soon as it was encountered, human subjects would directly assign it to the group where other sandpapers were previously placed. This assignment usually took place without considering the actual surface details, instead the basis for assignment were the material properties of the surface. Additionally, sandpapers have a very peculiar surface and are easily recognizable. This fact also aided the material based assignment process. At the same time, textured cloth2 (S100) was equally rough but it was a fabric. The fact that it was a fabric played a major role in it being assigned to a completely different group as compared to the given sandpaper.

The phenomenon where surfaces are classified based on their material properties instead of actual textural differences is called as *Pre-Judgement* in [39]. In pre-judgment participants use their previous knowledge for classifying a surface. A similar scenario developed for the lined wood (S95) and kite paper (S73) pair, where S95 was a wood (classic case of pre-judgement) and S73 was a kite paper.

The database of surfaces used in this study mostly comprises of everyday office/household materials. Furthermore, the textures of the surfaces was uniform and natural to a large extent. Similarly, the 21 surfaces used for evaluation also exhibited roughly the same properties. However, in real life we encounter a multitude of surfaces which are not represented in the current study. For example, organic surfaces, oily or wet surfaces, surfaces with artificial patterns, etc. Thus, it can be said that the current library covers some portion of the overall haptic space. Keeping this in mind, if we test a surface which belongs to the same portion of the overall haptic space as the library, the assigned model would mostly be perceptually similar. However, if we test a surface which lies far away from the library surfaces in the haptic space, the assigned model despite being the closest surface (among the library surfaces) would be perceptually dissimilar to the test surface.

In case of a surface containing artificial patterns, the success or failure of the algorithm depends on topography of the surface. If the artificial patterns are significant enough to mask the topography (or the surface is too smooth for the camera to capture the topography), the algorithm

would fail to assign a perceptually similar surface. The playing cards (S102) is an example of this phenomenon. On the other hand, if the surface exhibits camera visible texture, the algorithm can successfully assign a perceptually similar surface from the library. For instance textured cloth1 (S99) was successfully classified despite having artificial patterns. It contains visible micro geometry which was readily detected by the camera and the algorithm could assign a perceptually correct model from the library.

It can be noted that the psychophysical experiment to establish the perceptual space is based on bare-handed interaction with the surfaces. The participants rated the dissimilarities between different surfaces by directly interacting with the surfaces using their hands. This data played a significant role in formulating the automatic assignment algorithm. On the other hand, most haptic rendering and modeling algorithms consider a tool-based interaction with the surfaces. It can be argued that this difference in mode of interaction might cause different perceptual sensations. However, in a previous study it was shown that the sensations perceived through bare-handed and tool-based interactions are largely similar [39]. It is also highlighted that the different dimensions for both types of interactions bare a high degree of correlation. Thus, it can be safely assumed that the classifications provided by the automatic assignment algorithm will readily translate into perceptually correct haptic models for tool-based haptic modeling and rendering environments. Here we would like to state that the textures used in [39] were a subset of the textures used in this study. The perceptual space in [39] showed four dimensions, while the perceptual space in the current study comprises of only three dimensions. Upon a closer inspection it becomes evident that one of the four dimensions in [39] was related to hardness-softness, which is not considered in this study. Although adjective rating analysis of the current perceptual space has not being carried out in this study, as the scope of this article is different, it is safe to assume that the three dimensions of the current perceptual space should relate highly with the dimensions highlighted in [39].

Image feature extraction is one of the core parts of the current system. During the course of this research it was found that the image capturing process should be deliberated carefully. The image capturing mechanism should be robust and repeatable in order to extract meaningful image features. Especially, the lighting conditions and clarity of texture play a vital role. The images

should be captured with a good quality camera in good lighting conditions.

It can be seen from Fig. 2.17 that the convex hulls for very smooth (extreme left side) or very rough (extreme right side) textured surfaces were rather small. As it was very easy for participants to judge the differences for the two extremes. For example, a very smooth surface can be easily distinguished from a surface which is a little rougher. While, the convex hulls in the center of the perceptual space are rather inflated, meaning it was difficult for participants to clearly define perceptual boundaries in that region. As a consequence, a given texture surface was adjudged similar to more than one baseline textured surface and the respective convex hulls overlapped at certain regions. Another reason for this overlap could have originated from the nature of surfaces residing in the center of the perceptual space. Most of these surface are fabric based (which are soft) or have low stiffness. Therefore, even if the textures are different, it is being masked by the compliance of the material and thus the difference between the textures becomes perceptually less pronounced. This effect is called as pre-judgment, which is explained in greater detail in [39].

2.9 Chapter Summary

Our research concludes that visual features extracted from the image, if carefully selected, can reveal important physical characteristics related to perceptual haptic surface texture. Based on this relation, perceptual haptic models library was established and haptic models were assigned automatically to a given surface. The proposed system showed reasonable accuracy in assigning perceptually similar haptic texture models. This research can help in standardization and simplification of the haptic texture modeling and rendering process. It can eliminate the need for building a haptic model for every surface, instead, a perceptually similar model can be assigned to a given surface from the library.

Chapter 3

Haptic Attribute Space

The sense of vision has been thoroughly studied throughout the years. Different dimensions of visual attributes of a texture are objectively describable and accurately capturable. For instance, colors are readily describable by the RGB (or CMYK in case of pigments) model. Surface topography can be accurately described using parametric or non-parametric descriptors [2]. Similarly, capturing an image in terms of its constituent colors is easily achievable, and a large number of techniques are available to capture visual surface topography of a texture [3–5]. In essence, the dimensions for colors and visual topography are available and textures can be described according to these. On the other hand, most attempts at describing haptic attributes deal with perceptual dimensions. The relation between physical attributes of texture and the perceptual dimensions is not clearly defined. Therefore, researchers have focused on the relation between haptic attributes of texture (roughness, stiffness, etc) and the perceptual dimensions. The haptic dimensions and attributes of texture have been successfully identified [31, 37, 84, 85], however, the goal of these studies was the dimensions/attributes only and no further investigation was done.

There lies a need to establish standardized dimensions, akin to the RGB model for the visual sense, where haptic textures can be identified and populated based on their haptic attributes (roughness, hardness, etc). A space akin to the RGB model for the visual sense, where haptic textures can be readily populated and identified based on their haptic attributes, as illustrated in Fig. 3.1. Such a space would make haptic textures more relatable to the general public and professionals working with haptic texture modeling. In the contemporary world, consumers buy online products without being able to touch them. Consumers are less likely to buy online products that have a strong tactile aspect [29]. A standardized system where products are rated according to their haptic attributes would allow the end user to make more informed decisions.
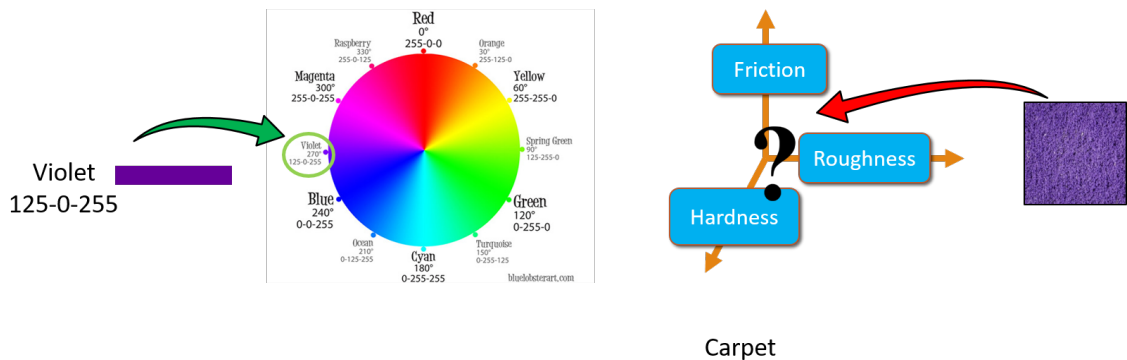
Figure 3.1: Colors can be easily defined in terms of their RGB values, however, there is no standardized system for categorizing haptic texture attributes.

The current study aims to provide a Haptic Attribute Space (HAS) where haptic textures are defined by their haptic attribute values similar to how colors are defined by their RGB values. The HAS is a four dimensional space where the dimensions are haptic attributes of textures, i.e., rough-smooth, flat-bumpy, sticky-slippery, hard-soft. The study comprises of two parts. The first part of the study deals with establishment of the HAS from a dataset of 100 texture surfaces. The HAS is established by conducting psychophysical experiments with human subjects. They select a list of attributes that could define the haptic properties of the surfaces in the dataset, and then rate all the 100 surfaces in the datasets against those attributes. The four attribute pairs chosen as a result of this exercise become the axes of the HAS. The second part deals with generalizing the HAS to new textures by using images of new textures and predicting their attribute values. It is proclaimed that there lies an area of intersection between visual and haptic texture perception [20–22], and this study aims to exploit that area of intersection. This study introduces a state-of-the-art 1D-CNN model to predict haptic attribute values of new textures from their images. The 1D-CNN model is trained using the data from psychophysical experiments and image features of the 100 surfaces is dataset. The aim of the 1D-CNN model is to make it possible to assign attribute values to newly seen and/or physically absent texture surfaces.

3.1 Overview

Figure 3.2 presents the overall system and the interaction of individual components. The constituent components of the system and their relationship will be briefly defined in this section.

The main aim of the current study is to provide a haptic RGB space where texture surfaces are located based on perceptually meaningful haptic attributes. This is achieved by accurately predicting the haptic attributes of texture surfaces from their images and subsequently locating the haptic textures in terms of quantifiable haptic characteristics in a haptic attribute space. The overall study can be divided into two major parts, i.e., establishing the haptic attribute space, and establishing a relationship between the haptic attributes and the image feature space.

The study starts with the collection of 100 different texture surfaces (see Sect. 3.2.1) which are rated by human users to establish the haptic perceptual space (see Sect. 3.2.3) and the haptic attribute space. The haptic perceptual space is a 3D space achieved from the multidimensional scaling (MDS) of similarity ratings from human subjects. The haptic attribute space is established based on user ratings of texture surfaces according to different perceptual properties. The haptic attribute space is a four dimensional space where each dimension defines a perceptual characteristic of the 100 haptic textures used in this study. All the textures are located in this four dimensional space according to user ratings.

The next step is to establish an image feature space (see Sec. 3.3) where each surface is defined by its image features. A combination of Various algorithms is used to extract meaningful textural features from the 100 texture surfaces used in this study.

A relationship between the haptic attribute space and the image feature space is established using a novel 1D convolutional neural network (1D-CNN) (see Sect. 3.4). The 1D-CNN takes the image features extracted from texture surfaces as input, and predicts the corresponding haptic attributes. The haptic attribute space established as a result of this exercise can potentially be scaled by populating it with new unseen textures.
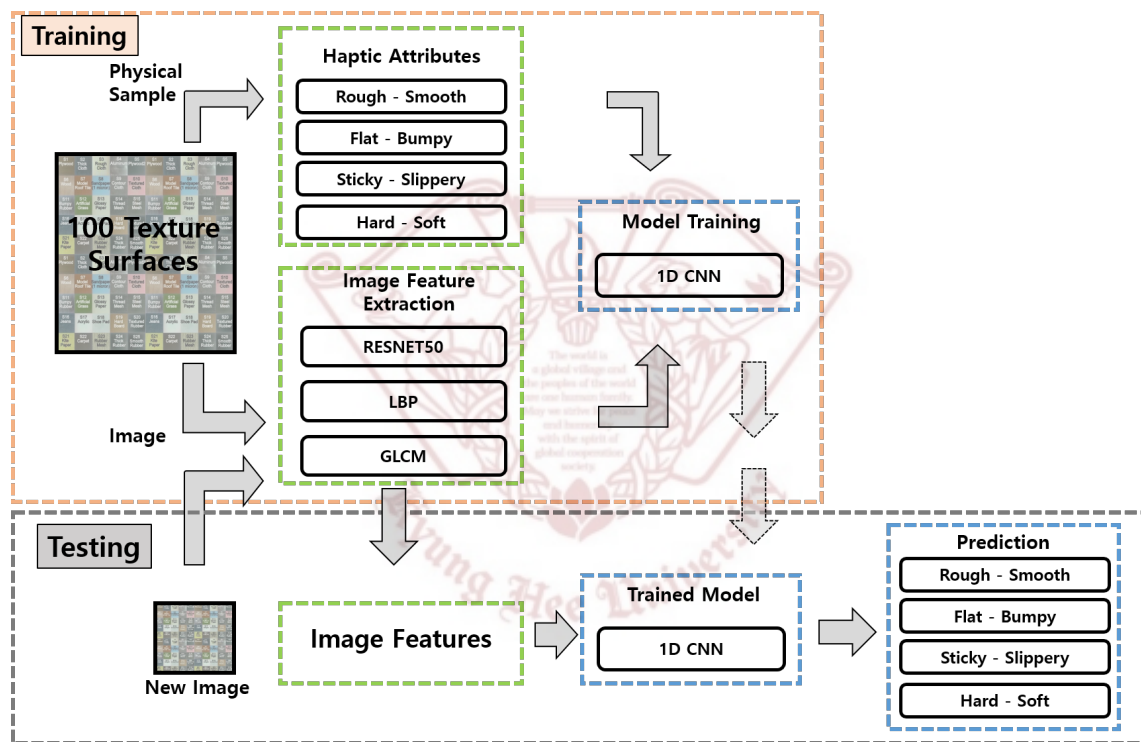
Figure 3.2: A block diagram of the overall framework.

3.2   Haptic Attribute Space

The Haptic Attribute Space (HAS) is a four dimensional space where haptic textures are located based on the differences in their physical characteristics and properties. Each axis of HAS represents a particular attribute that defines the textural properties of surfaces. Psychophysical experiments are conducted on a large dataset of versatile textures to establish the HAS space. In one experiment, human subjects rated all the textures according to various attributes that define the haptic properties of textures. These ratings were used to establish the four dimensional HAS space. In another experiment, the human subjects rated the texture surfaces based on their perceived dissimilarities. The result of the second experiment created a three dimensional perceptual space where texture surfaces are placed based on their dissimilarities. The details of the texture dataset, the psychophysical experiments and their purposes are provided in the following sections.

3.2.1   Texture Dataset

A total of 100 different texture surfaces were collected to be used as stimuli in both the psychophysical experiments. An effort was made to collect texture surfaces in such a way that they captured a wide variety of daily life haptic interactions. The 100 texture surfaces are provided in Fig. 3.3. The textures in the dataset can be subjectively categorized into varied categories based on material or textural/surface properties. The material categories are wood, rubber, plastic, fabric, leather, sandpaper, paper, sponge, and metal. Each of these categories contain multiple texture surfaces, i.e., flat surfaces with varying degrees of smoothness, metallic and fabric meshes, fabric with visible threads, flat fabrics, wooden surfaces with different textures, and many more. Some of the textures in these subjective categories are similar in haptic perception, while others are completely different. There are surfaces present with similar textural properties across different categories.

All the texture surfaces were cut to a size of 100 x 100 x 5 *mm* and mounted on hard acryl plates of the same size. This was done to provide a uniform base for all the surfaces, otherwise the stiffness of the underlying table-top could influence their perception. Some of the metallic and thick wooden texture surfaces were not mounted on top of acryl plates, as the participants could not perceive the affect of the underlying table-top through these surfaces.
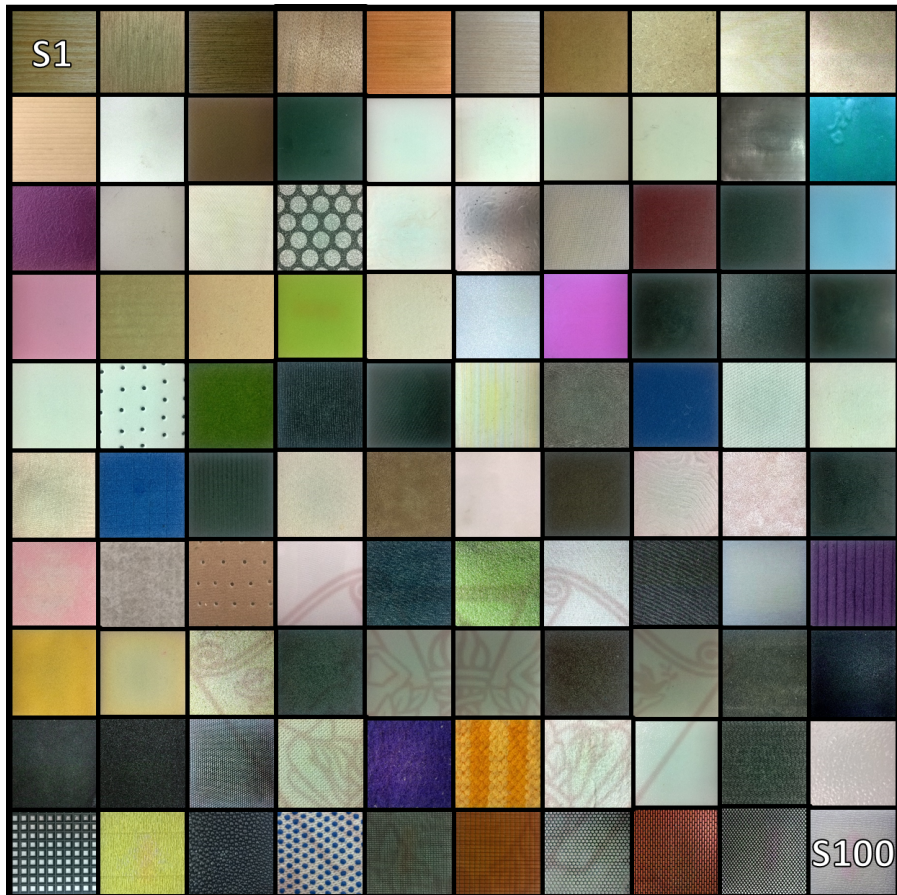
Figure 3.3: The 100 texture surfaces used in this study. 1 Artificial wood , 2 Lined-wood1 , 3 Lined-wood2 , 4 Lined-wood3 , 5 Lined-wood4 , 6 Smooth-wood , 7 Hard-board2 , 8 Lined-Wood5 , 9 Lined-Wood6 , 10 Hard-Board4 , 11 Hard-board3 , 12 Styrofoam , 13 Textured-cloth2 , 14 Wooden-board , 15 Acrylic , 16 Smooth-paper1 , 17 Smooth-paper2 , 18 Smooth-paper3 , 19 Aluminum , 20 Glossy-paper3 , 21 Bumpy-paper , 22 Talc-paper , 23 Textured-paper , 24 Glitter-paper , 25 Slippery-paper , 26 Aluminum-foil , 27 Textured-cloth3 , 28 Cotton-fabric , 29 Hard-board1 , 30 Glossy-paper1 , 31 Glossy-paper2 , 32 Hard-board2 , 33 Coffee-filter , 34 Smooth-sandpaper2 , 35 Soft-hardboard , 36 Card , 37 Balloon , 38 Thick-rubber , 39 Textured-rubber , 40 Smooth-Rubber , 41 Rough-paper , 42 Smooth-shoe-padding , 43 Artificial-grass , 44 Plain-cloth , 45 Lined-rubber , 46 Rough-cloth , 47 Lined-cloth1 , 48 Cloth-hard-cover , 49 Textured-shoe-padding , 50 Tissue , 51 Textured-cloth4 , 52 Towel1 , 53 Textured-cloth5 , 54 Textured-cloth6 , 55 Lined-cloth2 , 56 Smooth-fabric , 57 Rough-cloth , 58 Textured-cloth7 , 59 Lined-cloth3 , 60 Textured-fabric , 61 Textured-Cloth8 , 62 Hairy-cloth , 63 Lined-shoe-padding , 64 Thread-mesh , 65 Jeans , 66 Scrub , 67 Towel2 , 68 Textured-Cloth9 , 69 Hard-Cover , 70 Carpet3 , 71 Sponge1 , 72 Sponge2 , 73 Sponge3 , 74 Rough-sandpaper1 , 75 Smooth-sandpaper1 , 76 Smooth-sandpaper3 , 77 Rough-sandpaper2 , 78 Smooth-sandpaper4 , 79 Rough-sandpaper3 , 80 Smooth-Sand-Paper5 , 81 Rough-Sandpaper4 , 82 Very-Rough-Sandpaper , 83 Textured-rubber1 , 84 Textured-rubber2 , 85 Carpet1 , 86 Carpet2 , 87 Cotton-towel , 88 Bubbly-plastic1 , 89 Thread-mesh , 90 Bubbly-plastic2 , 91 Plastic-mesh , 92 Kite-paper , 93 Bumpy-Hard-Plastic , 94 Bumpy-cloth , 95 Steel-mesh1 , 96 Model-roof-tile , 97 Steel-Mesh2 , 98 Model-Brick , 99 Steel-Mesh3 , 100 Lined-Cloth4
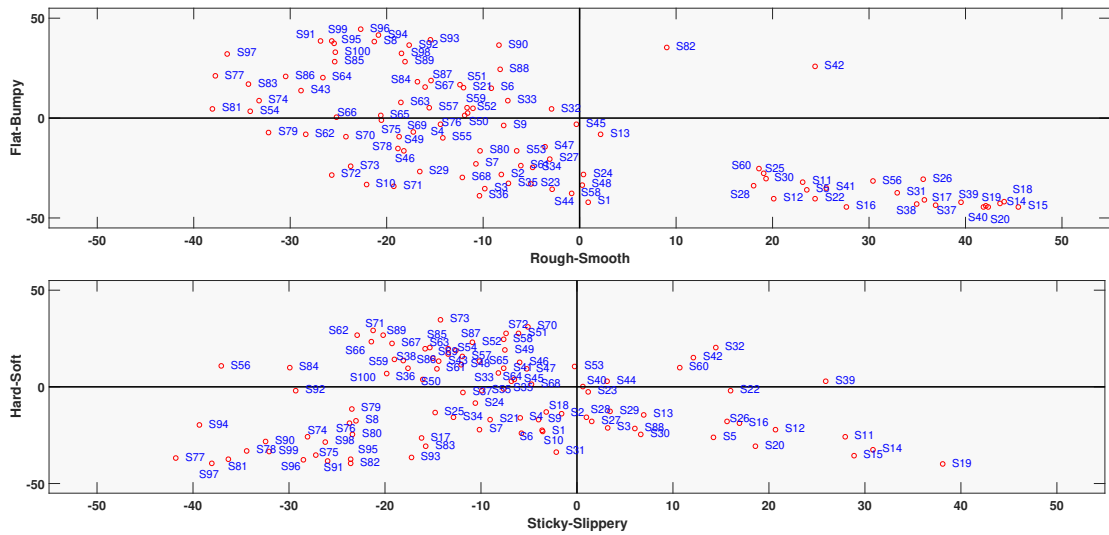
Figure 3.4: The four dimensional haptic attribute space shown as two 2-dimensional spaces. The texture surfaces are scattered around in the haptic attribute space.

3.2.2 Experiment 1: Haptic Texture Attribute Space

The main aim of this experiment was to identify the prominent haptic attributes that can be used to explain the textural properties of the 100 surfaces. The identification of these prominent haptic attributes was a multi-step process. First, a comprehensive list of attributes/adjectives was compiled that could potentially describe texture surface properties. Second, the list was narrowed down to 8 attributes (4 attribute pairs) based on participant responses. Third, the 100 texture surfaces were rated according to these four attribute pairs. The four attribute-pairs formed the four axes of the four dimensional HAS where all the surfaces were located according to their corresponding attribute values.

Participants and Stimuli The 100 texture surfaces detailed in Sect. 3.2.1 were used as stimuli in this experiment. A total of 20 participants took part in the experiment (16 male and 4 female) with an average age of 27 (ranging from 24 to 31).

Procedure The participants sat in a chair in front of a table. They wore headphones playing white noise at a volume which blocked interaction and environment noises but experiment instructions could be heard. The texture surfaces were provided one at a time. The surfaces were placed

under a cardboard box with a small opening for the participant's hand at one end and another larger opening for the experimenter to replace the surfaces. The participants were not able to see any of the surfaces throughout the experiment.

The first part of the experiment was to collect a comprehensive list of haptic attributes. A total of 60 haptic attributes were collected. Some of these came from literature [86–89], while the others were selected by human participants keeping in mind the type of textures present in the dataset. The participants were encouraged to express the textures with words or attributes that they felt were associated to the texture or which were relevant to the dataset. The full list is provided in Table 3.1. After compiling the list, the participants were asked to select attributes that they felt could describe the haptic properties of the texture surfaces. The decision was either a 1 for yes or a 0 for no. This process was conducted to filter out the particular attributes that were dominant among the 100 surfaces used in this experiment.

A total of 11 attributes were short listed for the next experiment. Among these 11 attributes, four pairs of attributes with an antonymous relation were selected as they could represent opposite extremes of the same physical property. The four pairs were rough-smooth, flat-bumpy, sticky-slippery, and hard-soft. It must be noted that hard-soft in this experiment referred to texture and not compliance of the surface. All the surfaces were mounted on acryl plates to minimize the compliance bias. These four pairs were used in the next part of the experiment.

In the next part of the experiment, participants rated all the texture surfaces according to the four attribute pairs selected in the first part. A GUI (graphical user interface) displayed each of the four attribute pairs on opposite sides of a slider, as shown in Fig. 3.5. The slider had no scale marks and spanned a length of 127 *mm* [87] on the screen. The participants were asked to perceive the surfaces and slide the marker in the direction of the attribute. The slider values were mapped from zero to hundred and averaged across all participants.

Analysis And Results   The data for all the participants is averaged. The y-axes of the plots are marked with attribute pairs. Originally the participant responses were rated between zero and 100 with 50 being the center point, however, in Fig. 3.4 the attribute values are centered around zero. The shifting of the ratings does not have any affect on their perception. It has been done to provide an easier visual understanding of the plots. The four attribute pairs acquired as a result of this
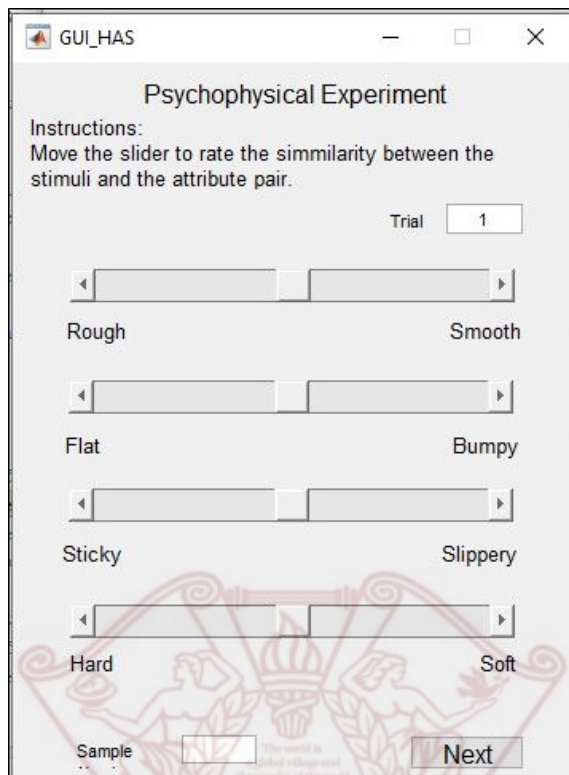
Figure 3.5: The graphical user interface used for rating the texture surfaces according to the four selected attribute pairs.

experiment were used to establish the HAS. Each attribute pair represents a unique dimension. The four-dimensional HAS is shown in Fig. 3.4 in the form of two two-dimensional plots.

3.2.3   Experiment 2: Haptic Perceptual Space

The haptic perceptual space is a multi dimensional space where surfaces are scattered based on their perceptual similarities. Perceptually similar surfaces are grouped together while perceptually different surfaces are located away from one another. The similarities among surfaces are determined by human participants using a cluster sorting psychophysical experiment.

Participants and Stimuli   The 100 texture surfaces detailed in Sect. 3.2.1 were used in this experiment. The 20 participants who took part in the previous experiment also took part in this experiment.

Table 3.1: The list of attributes provided to participants for the attribute rating experiment. The four selected attribute pairs are in bold-face font.

Abrasive	Granular	Bald	Cold	Warm	Pointy	**Sticky**	Jarred
Bouncy	Grating	**Hard**	Wooden	Sharp	Hatched	Patterned	**Bumpy**
Glassy	**Flat**	Mild	Wavy	Deep	Solid	Grainy	Dark
Fast	Refined	Furry	Shallow	Fizzy	**Slippery**	Thin	Angular
Irritating	Spongy	Slick	Mushy	Slow	Malleable	Blurry	vague
Smooth	Silky	Metallic	Fine	Jagged	Thick	Distinct	Rough
Pleasant	Prickly	Rigid	Soft	Bright	Blunt	Heavy	Light
Even	Dense	Sparse	Bubbly				

Procedure   The participants sat in a chair in front of a table. They were headphones playing white noise to block out interaction and environment noise. The participants were blindfolded to avoid visual bias.

This experiment was in the form of a cluster sorting task. The participants were asked to group perceptually similar textures into a predefined number of groups. They were free to use their preferred method of texture exploration. Every participant conducted a total of five trials where the total number of groups were 3, 6, 9, 12, and 15. The order of the trials was counter-balanced using latin square. The lower number of total groups results in somewhat perceptually similar surfaces being grouped together, thus, capturing the large scale difference. The higher number of total groups means that surfaces that are perceptually very similar are grouped together, hence, capitalizing on the finer differences among the surfaces.

One surface was provided at a time which was assigned to a group by the participant. The next surface, if perceptually similar, could be assigned to the same group, otherwise it could be placed in a new group. Once the allotted number of groups for a particular trial were reached, the participant had to assign all the remaining surfaces into one of the created groups. It was possible to merge two or more already created groups into a single group to make room for a new group of perceptually different textures. After assigning all the surfaces to the predefined number of groups, the participants were asked to reevaluate the groups for any errors. They were allowed to change the groups as many times as they deemed necessary. The five trials on average took 160 minutes per participants excluding break times.

Analysis and Results The data from the experiment was in the form of groups made across various trials by participants. Scores to a pair of surfaces in the same group were assigned based on the total number of groups in that trial. Scores for the surfaces across all trials were subsequently added together to get a similarity score. For example, a pair of surfaces were grouped together in the trials with total groups at 6, 9, and 15. The similarity score for this pair would be $6 + 9 + 15 = 30$. This method ensures that the surfaces that were grouped together across more trails receive a higher similarity score. The surfaces are assigned scores based on the total number of groups in that trial. This strategy is important because the total number of groups plays a vital role in terms of the surfaces resulting in each individual group. A trial with three total groups would have perceptually different surfaces within each group. On the other hand, the groups of a trial with a fifteen total groups would have perceptually very similar surfaces. The scoring system capitalizes on this phenomenon and rewards the surfaces in higher total groups trials with higher scores. The data across all participants were averaged and used to form a similarity matrix. The similarity matrix were converted into dissimilarity matrix and scaled from zero to one.

Multi-dimensional scaling (MDS) analysis was performed on the dissimilarity data to establish the perceptual space. The number of dimensions for MDS were determined by running a Kruskal stress test on the MDS data. The stress test results in Fig. 3.6 show a stress value of 0.048 at third dimension which is considered as fair according to [66], therefore, a three dimensional space is sufficient to describe the variation across the data in our dataset. The perceptual space is provided in Fig. 3.7. In this space, as mentioned earlier, the surfaces located close to one another are perceptually similar while those located away from one another are perceptually different. The surfaces follow a U-shaped curve in the 3D space with the width and depth of the U varying at various points. The dimensions obtained from the MDS analysis do not portray any physical meaning. These are the result of an optimization algorithm used to locate the given surfaces at optimum distances to maintain their dissimilarities ratings.

Attribute Projection In order to make sense of the dimensions of MDS in terms of physical attributes of a surface, the four attribute pairs from Sect. 3.2 are regressed into the perceptual space. Multi-linear regression was performed where the perceptual space dimensions were the response variables, whereas, the attribute scores were used as the predictor variables. Fig. 3.7
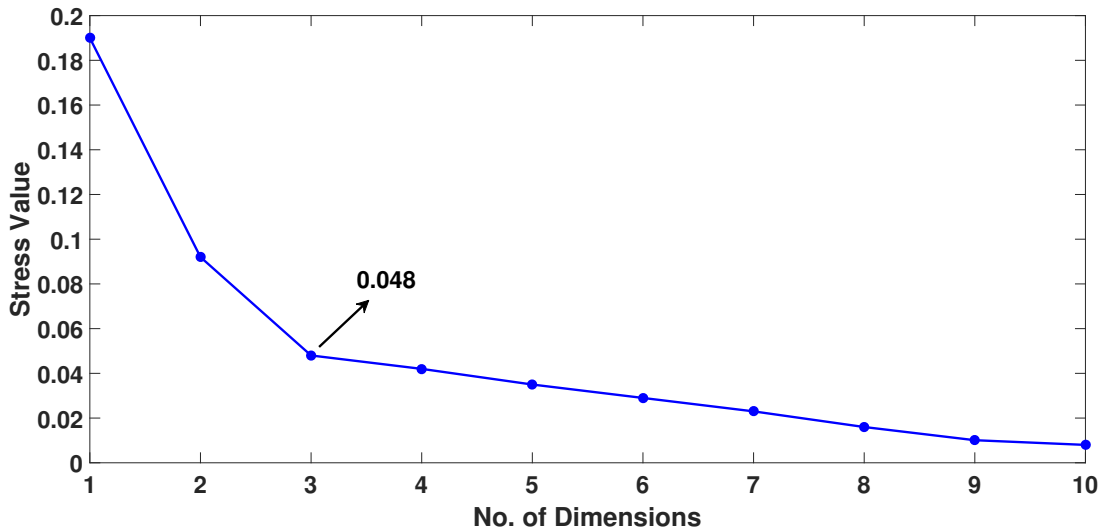
Figure 3.6: The kruskal stress value for the first ten dimensions of the perceptual space.

Table 3.2: The 3D angles for the four attribute pairs regressed into the perceptual space.

Attribute Pair	Elevation	Azimuth
Rough-Smooth	324.48	99.93
Flat-Bumpy	70.66	52.0
Sticky-Slippery	228.96	47.77
Hard-Soft	345.58	338.09

shows the four attribute pairs regressed into the perceptual space. The length of each attribute pair shows the goodness of fit of the regression model.

The HAS is the combination of the four attribute pairs, and ideally, one would want the four dimensions to be perpendicular to one another. However, Fig. 3.7 shows that the attribute pairs are not perpendicular. This analysis further emphasizes the fact that haptic perception is not a linear phenomenon. Furthermore, it shows that haptic attributes of texture are dependent on one another up to varying degrees. This non-linearity is carried and contained in the HAS dimensions. The angles of the four attribute pairs with respect to origin are provided in Table 3.2.
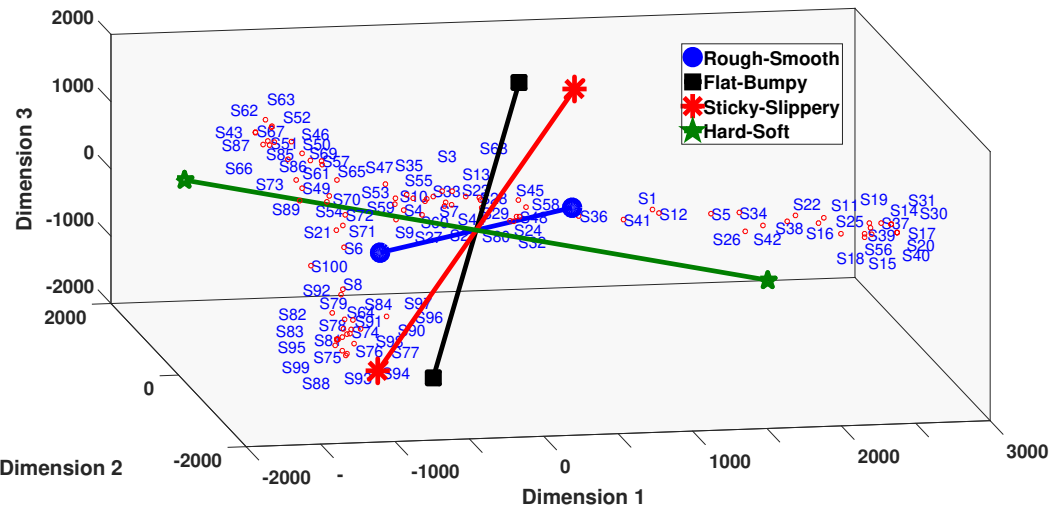
Figure 3.7: The four attribute pairs are regressed into the three dimensional perceptual space. Length of the attribute pair shows the goodness of fit.

3.3 Image Feature Space

The main aim of the current study is to establish a system which enables us to identify the haptic attributes of a texture only by examining its image (visual texture). To this end, images of the textures in our dataset were used to collect meaningful features that will be used in training the 1D-CNN model. A large variety of image feature extraction techniques are available in literature. In the current study we decided to use an amalgam of classical and deep learning based image features. Three image feature extraction techniques were used, i.e., Gray Level Co-occurrence Matrix (GLCM), Local Binary Pattern (LBP), and ResNet50. A wide variety of other feature extraction techniques were tested before steeling down on the aforementioned three methods. The three methods chosen in this study contain a complementary modus operandi. LBP captures the local spatial patterns in an image, GLCM has the ability to capture local and intermediate level features, while, ResNet50 progressively extracts higher level deep features from the input images. A combination of these three features covers diverse aspects of an image and the resulting image features show high discrimination ability. The details of the image capturing setup and image features are provided in the following sections.

3.3.1 Image Capturing Setup

All the images used for training were captured using a standardized and uniform procedure to guard against any scaling or resolution bias. It is important to capture the finer details of the surface with clarity and in high enough resolution so that the algorithm can extract meaningful features from the images. All images were captured using dp2 Quattro SIGMA digital camera and saved in in high quality RAW format (14 bit lossless compression). The camera was mounted on top of the surfaces using a tripod stand. The distance between the camera lens and the surfaces was kept constant at 300 *mm*. The images were taken in standard room lighting, however, special care was taken to guard against any shadows. Color does not affect the haptic perception, therefore, all the images were converted into gray scale before using them in training to remove/reduce color bias.

3.3.2 Gray Level Co-Occurrence Matrix

In [44], Grey Level Co-occurrence Matrix (GLCM) based texture feature descriptor was proposed for surface classification. Recently, for haptic texture assignment in [90], GLCM was utilized as one of the texture features because of its higher performance in this area. Motivated by this, we employed the GLCM, which considers the spatial relationships between two pixels at a time in the surface texture image. First, the surface images are resized into 1568×1568. Then, the GLCM method is applied to this resized surface image, which produces a matrix of 8×8. Then, this matrix is flattened to generate a feature vector of size 1×64.

3.3.3 Local Binary Pattern

Local pixel information from an image can be calculated by using Local Binary Pattern (LBP). The LBP is performed by comparing the pixel values of an image by thresholding a circular neighborhood area [47]. In this work, we applied the LBP method on the surface image to calculate the local spatial patterns. First, the resized input images are divided into multiple cells with sizes 224×224. Then, the LBP operation is performed on each cell, which generates a feature vector with the size 1×59. Subsequently, the feature vectors obtained from each cell are combined to produce the final feature vector with size 1×2891 using the LBP.
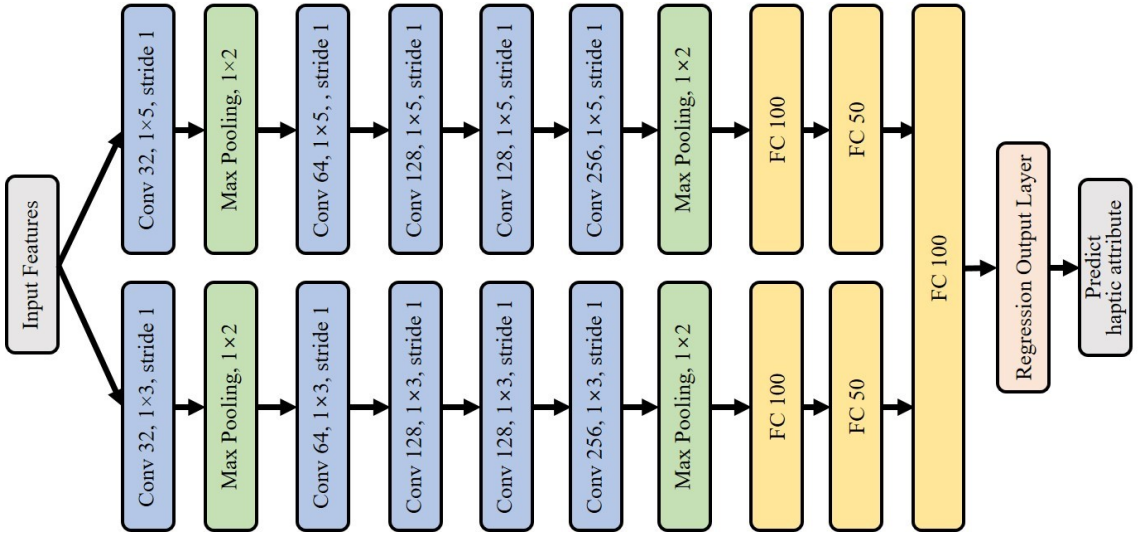
Figure 3.8: The structure of the proposed multi-scale 1D-CNN.

3.3.4 ResNet50

ResNet model was presented in [91] for the image classification task, which is trained on the ImageNet dataset. The network achieved state-of-the-art performance in image recognition due to having residual learning support. In our work, we used the pre-trained ResNet-50 model to capture the higher level deep features from the surface images. At first, the surface images are resized into 224×224 in order to match the input of the ResNet-50 model. Then, the processed surface images are fed into the pre-trained ResNet-50 model, which gives us the feature vector with size 1×1000 containing the deep spatial information of the surface texture.

After capturing surface features by employing the GLCM, LBP and ResNet-50, we concatenate the features and produce a feature vector with size 1×3955, which is then used as input to the multi-scale 1D-CNN.

3.4 1D-CNN

Recently, deep learning-based approaches have become popular for haptics applications, i.e., tactile understanding [92], texture signal generation from surface images [51], perceptual similarity learning from haptic textures [93] and so on. In light of the aforementioned work's success, here,

we design a multi-scale 1D-CNN to establish a relationship between haptic attributes of surface texture and its image features. The infrastructure of the 1D-CNN is similar to that of a conventional CNN. The difference is the use of the input data and trainable kernels of the one-dimensional (1D) vector. As a consequence, during the training phase, the forward propagation and backpropagation procedures are modified. The structure of the proposed multi-scale 1D-CNN is presented in Fig. 3.8. The model takes the image features captured using the previously discussed methods. Then, we train the model with respect to the given haptic attribute values. Ultimately, the model is able to predict the haptic attribute values for the given surface image features. The details of the proposed multi-scale 1D-CNN are as follows.

The network contains two sub-1D CNN. Each 1D-CNN has five 1D convolutional layers, two 1D max-pooling layers, and two fully connected layers. The convolutional layers are in charge of extracting the features, while the max-pooling layers reduce the dimensionality of each feature map. In the convolutional layers, different numbers of kernels are applied with different scales. Therefore, local spatial information in different scales is captured. In the convolution operation, we operated 1×3, and 1×5 sizes of kernels, while the max-pooling process is performed on 1×2 blocks. Additionally, we utilize multiple kernels to obtain the diverse aspects from each scale of local information in convolutional layers. For instance, the first convolution layer operates 32 kernels, the second convolution layer uses 64 kernels, the third and fourth involve 128 kernels, while the fifth convolution layer operates 256 kernels. More specifically, in a 1D convolution layer, the computation is performed as follows.

$$g_i = f(w_i^T a_n + b_i) \tag{3.1}$$

$$f(z) = \begin{cases} z; & if z > 0 \\ 0; & otherwise \end{cases} \tag{3.2}$$

where g_i is the calculation result of the ith filter, a_n is the input data of size $1 \times N$, w_i is the ith convolutional kernel vector with size $1 \times N$, b_i is the bias of the ith filter and the ReLU nonlinear activation function is denoted as f.
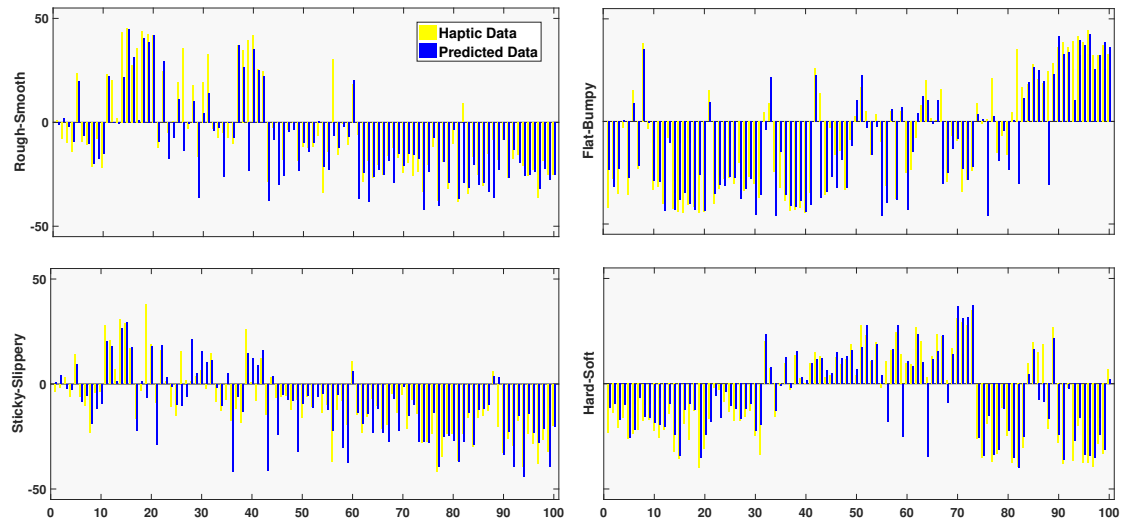
Figure 3.9: The attribute values from the psychophysical experiment plotted alongside the attribute values predicted by the 1D-CNN.

Each sub-1D CNN model ends with two fully connected (FC) layers having 100 and 50 neurons, respectively. Finally, another FC layer with 100 nodes is engaged to concatenate the features achieved through different 1D CNN modules. The loss function in this study is the mean-square error (MSE), while the activation function is the Sigmoid function. To train the model, the ADAM optimizer is used.

In most cases, the number of samples is significantly less than the number of features when it comes to sampling cost in real-world applications. Due to the lack of samples, the complex model can easily lead to overfitting problems without considering the model's generalization ability. In other words, the fitted model can correctly predict the adjective rating for the training data, but the test set's prediction results are poor. Therefore, to balance prediction performance and speed up the deep network training process, the rectified linear unit (ReLU) and batch normalization (BN) techniques are used after convolution operation in this study.

3.5 Evaluation

The main goal of the proposed system is to predict accurate and reliable haptic attributes of textures based on their images. It is important to reliably predict these attributes and that the errors in haptic
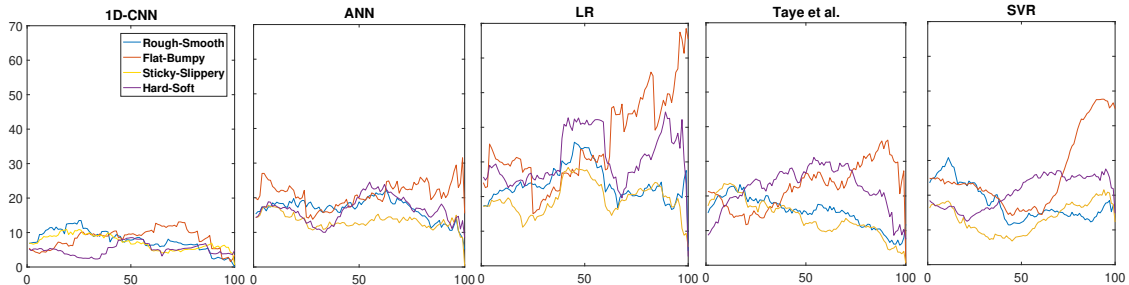
Figure 3.10: The Mean Absolute Error (MAE) values for the proposed and four other algorithms.

attribute value prediction stay below human perception. In this section, a numerical evaluation of the proposed model is carried out using the Leave-One-Out Cross-Validation (LOOCV). The evaluation assesses the prediction capability of the system in terms of how well it can predict haptic attribute values for unseen textures.

The proposed model was also compared against other prominent classical and neural network algorithms in terms of prediction accuracy. Linear regression and Support Vector Regression were chosen among the classical algorithms. There are two of the most commonly used regression techniques. In case of neural network models, Artificial neural network and state-of-the-art 1D CNN by Taye et al. [94] were selected .

3.5.1   Leave-One-Out Cross Validation

Cross validation is an evaluation method used to verify the estimation capability of a trained model on unseen data. It tests the generalization ability of a trained model on a dataset that was not used in training the model. One of the most common form of cross validation is the *k*-fold cross validation, where the dataset is split into *k* subsets. A fix number of subsets are used for training and the remaining are used for testing. The process is repeated until all the subsets are used for testing. LOOCV is a special case of the *k*-fold cross validation where *k* = 1. The number of subsets is equal to the number of instances in the dataset. In every cycle all the instances are used for training baring one which is used for testing. The process is repeated until all the instances in the dataset have been used as a test instance. LOOCV provides accurate and unbiased evaluation of a model as every item in the dataset is used for testing. LOOCV was chosen to perform an exhaustive evaluation of the proposed model. LOOCV can be computationally expensive for large

datasets, however, the dataset used in this study in not large by machine learning standards.

The dataset described in Sect. 3.2.1 was used in LOOCV. The model was trained using 99 of the textures in the dataset, and the remaining one was used as a test set. The same process was repeated until all the textures were used as test sets. The point by point prediction results from LOOCV for the proposed model are provided in Fig. 3.9. Using LOOCV as an evaluation metric reduces the need to test the model on surfaces outside of the original. It must be noted that in every iteration the 100th instance is an unseen surface for the model as if the testing was being done with textures outside the original dataset.

Figure 3.9 shows that the predicted value and the value assigned by human subjects to each of the texture surfaces. It can be seen that in most cases the prediction result is very close to the haptic value assigned by human subjects. In order to gain a better understanding of the prediction results, Mean Absolute Error (MAE) was calculated with a window size of 20, as shown in Fig. 3.10. MAE for all 100 surfaces is provided in Table 3.3. The MAE provides a more direct and intuitive summary of the prediction results. It can be seen that the max MAE (for average of 20 surfaces) of 11.2 is achieved by Rough-Smooth towards the beginning of the curve. MAE for the other three attributes mostly stays below this value. It should be noted that MAE provided the absolute value of error and, thus, an error of 10 means 10 out of 100.

3.5.2   Accuracy Comparison

In this section, the proposed algorithm is compared against other popular and state-of-the-art algorithms. These algorithms are linear regression, support vector regression, artificial neural net, and state-of-the-art 1D CNN [94]. Note that, linear regression and support vector regression algorithms are used from the Scikit-learn machine learning library. On the other hand, ANN is designed with two fully connected (FC) layers and a regression output layer. The FC layers having 200 and 100 nodes, respectively. To train the ANN, an ADAM optimizer is used along with the MSE loss function. The same LOOCV evaluation strategy was used for all the four algorithms to keep the comparison fair. Table 3.4 shows the root mean square error (RMSE) for the four algorithms and the proposed algorithm. The Root Mean Square Error (RMSE) is measured as

follows.

$$RMSE = \sqrt{\frac{1}{N}\sum_{i=1}^{N}(y_i - \bar{y_i})^2} \tag{3.3}$$

where $\bar{y}_i$ represents the actual rating of the ith sample, y_i denotes the predicted rating and N is the total samples. This experiment shows that linear regression has an RMSE of 29.9, 57.05, 25.04 and 42.18 for Rough-Smooth (R-S), Flat-Bumpy (F-B), Sticky-Slippery (S-S) and Hard-Soft (H-S), respectively. On the other hand, ANN has an RMSE of 20.41, 30.52, 16.74 and 20.29 for R-S, F-B, S-S and H-S, respectively. However, SVR shows better RMSE for F-B and S-S compared to the other existing algorithms.

The LR and SVR are good models for training linearly separable data. However, the dataset in this study consisted of images, and the configuration of the image feature space could have been linearly inseparable. Therefore, the LR, and SVR failed to offer a higher accuracy as compared to our model. From Table 3.4 it can be observed that in most cases, the deep learning algorithm (i.e., 1D CNN) proposed in [94] failed to produce lower RMSE (see Table 3.4) than the simple machine learning algorithms (i.e., ANN). This is because the 1D CNN [94] applies kernels with larger window sizes; therefore, this 1D CNN fails to capture the local features adequately. Besides, the number of kernels applied to the 1D CNN [94] is also fewer compared to the proposed multi-scale 1D-CNN. Because of capturing the local spatial information in different scales as well as utilizing a large number of kernels helps to boost the performance of our model. Hence, the proposed algorithm has significantly lower RMSE values as compared to the other four algorithms.

3.5.3   Individual Feature Accuracy

In the aforementioned comparisons, the proposed model was trained using a concatenated 1D vector comprising of ResNet-50, LBP, and GLCM features. In this subsection, the three features were individually used to train the 1D-CNN model and predict the output. This exercise was conducted to figure out the individual accuracy of each feature and whether a single feature could perform better than the concatenated version.

Table 3.5 shows that the model trained with feature concatenation provided the highest accu-

Table 3.3: The mean absolute error (MAE) values for the proposed system and four other algorithms. The values are written for each of the four attribute pairs.

	R-S	F-B	S-S	H-S
Linear Regression	23.11	32.43	19.17	30.21
Support Vector Regression	17.81	23.85	12.94	20.28
Artificial Neural Network	16.96	20.62	13.31	16.59
1D CNN (Taye et al. [94])	15.57	22.16	14.43	21.44
Proposed 1D-CNN	**8.13**	**8.47**	**7.12**	**5.15**

Table 3.4: The root mean square error (RMSE) values for the proposed system and four other algorithms. The values are written for each of the four attribute pairs.

	R-S	F-B	S-S	H-S
Linear Regression	29.9	57.05	25.04	42.18
Support Vector Regression	22.78	26.38	15.97	21.46
Artificial Neural Network	20.41	30.52	16.74	20.29
1D CNN (Taye et al. [94])	20.79	27.70	19.70	26.59
Proposed 1D-CNN	**13.39**	**14.30**	**9.59**	**7.91**

racy as compared to the individual features. This result was expected, as the ResNet-50 captures higher level spatial information, while LBP and GLCM focus on micro level spatial arrangement of texture. The concatenated features had the advantage of using both higher level and micro level information for predicting the attributes of textures and thus performed better than the individual features.

3.6   Discussion

Figure 3.10 shows that different attribute pairs perform differently for certain texture surfaces. The R-S attribute pair has the highest MAE value all others for the first 25 textures, and the F-B

Table 3.5: The RMSE of each individual feature in comparison with the concatenated features.

	Rough-Smooth	Flat-Bumpy	Sticky-Slippery	Hard-Soft
GLCM	17.91	14.51	15.21	10.81
LBP	18.92	19.16	16.91	11.50
ResNet-50	18.62	15.26	19.00	10.40
Concatenated features	**13.39**	**14.30**	**9.59**	**7.91**

attribute pair performs the worst for textures 50 to 85. Similarly, the best attribute pair for the first 50 textures turns out to be H-S, while for the last 50 textures three attribute pairs (R-S, S-S, H-S) predict with similar accuracy.

As mentioned earlier, the prediction error for R-S attribute pair is relatively higher for the first 25 texture surfaces. A majority of these textures are polished surfaces, as seen in Fig. 3.3. It is probable that the camera used in this study could not capture images detailed enough to fully encapsulate the micro geometry of the surfaces. The prediction values for F-B attribute pair for textures 74 to 83 are have a very high error rate. It can be seen from Fig. 3.3 that all these surfaces are sandpapers with different grit ratings (80 to 3000). The algorithm predicted their attribute values based on the image features, however, it is highly likely that the participants judged these surfaces as sandpapers only without going into too much detail about the texture itself. This phenomenon is called as pre-judgment, where a participant judges the haptic qualities of a texture based on their past experience rather than the textures available at the time. Pre-judgment is defined in greater detail in [39]. The fact that the MAE is shown in terms of a moving window of 20 surfaces may have resulted in the outliers affecting the average. MAE for all the 100 surfaces is available in Table 3.3, and it can be seen that the highest MAE is 8.47 for F-B. The exact value for human JND (Just noticeable difference) for haptic attributes of real textures is unknown, however, an earlier research [95] showed that perceptual similarity boundaries extend a fair distance beyond a given surface. Therefore, it can be assumed that a difference of around 10 or less (10 out of 100) should be perceived as haptically similar by most humans.

In Fig. 3.4 the four quadrants in each plot represent specific types of texture surfaces. For instance, in the first plot of HAS (Rough-Smooth and Flat-Bumpy), the first quadrant has smooth and bumpy surfaces, second quadrant represents rough and bumpy surface, third quadrant contains rough and flat surfaces, and the fourth quadrant is populated with smooth and flat surfaces. It is intuitive to assume the the rough and bumpy and smooth and flat are densely populated as these attributes often occur simultaneously. The rough and flat is also well populated, however, most of the surfaces are close to the origin. This shows that some flat surfaces were perceived as mildly rough, for example, high grit sandpapers or some wooden surfaces. The least populated quadrant is the smooth and bumpy one. The current dataset contained very few textures that could represent

these two attributes. The two surfaces in this quadrant are the ones with clearly perceivable bumps on an otherwise smooth surface.

A similar pattern can be seen in the third and fourth dimensional plot of HAS in Fig. 3.4. The first quadrant contains slippery and soft surfaces and is the least populated. The second quadrant has sticky and soft surfaces, the third one containing hard and sticky surface, and the fourth quadrant containing slippery and hard surfaces. The second and third quadrants are the most populous quadrants which means that a high number of surfaces were perceived as more sticky as compared to slippery. It can be seen that in the second quadrant the surfaces do not reach extreme values and are rather situated more towards the origin. It can be argued that we do not encounter such surfaces in most of daily life interactions. Some examples can be organic surfaces (chewing gum, clay etc) or silicone, which are not a part of this texture dataset. The third quadrant consists of sticky and hard surfaces. The extremes in this quadrant are some sandpapers and metallic meshes. The fourth quadrant contains slippery and hard surfaces. This quadrant incorporates metals or polished hard-wood surfaces in the extreme.

In the current study, a total of 60 attributes were selected for the attribute rating experiment. It must be noted that selecting an attribute list can have some limitations. It is possible that certain dimensions of texture might be left unextracted due to lack of associated attributes in the overall list. Another possible limitation of missing texture dimensions could be the difficulty of participants in verbalizing their perceptive experiences [96, 97]. In order to guard against this, an effort was made to collect a high number of attributes from literature and from the participants.

Incorporating new textures into the HAS is based on their image features. This emphasis the image capturing setup and the quality of the image being captured. It is a well-known fact that better quality images lead to better image features. The algorithm (1D-CNN) can also predict haptic attributes with higher accuracy if the image features are well collected and correctly capture the micro and macro texture information of a surface. It is of utmost importance that the image is captured without shadows, the texture should be clearly visible (not blurred), and with high resolution.

3.7   Chapter Summary

In this chapter, we established a four dimensional Haptic Attribute Space (HAS) from psychophysical experiments. The axes of the 4D HAS are haptic attributes of texture which were chosen by participants to best represent the 100 textures used in this study. The 100 textures are then scattered in the 4D HAS according to their corresponding attribute values. In order to populate the HAS with new textures, a multi-scale 1D-CNN was trained to predict haptic attributes of texture based on their image features. The HAS in combination with the multi-scale 1D-CNN provide a universal space where all textures can be represented based on their attribute values. This provides an intuitive way to classify or identify textures based on their images, without the need to physically interact with them.

Chapter 4

Haptic Texture Authoring

Imagine that you are designing multimedia contents of an immersive virtual reality (VR) based game where players can see, hear, and touch virtual objects. You assign a faded wooden image texture to a virtual prop used in the game play and try to create a realistic haptic texture (roughness) for it as well. One straightforward way is to find a real surface having haptic properties same as that you want to assign, measure/copy its haptic responses, and replay it during interaction (analogous to photos taken from real scenes used as image textures in 3D graphics). Furthermore, it would facilitate contents generation if we could freely edit the perceptual property of the real measurement, e.g., creating a new haptic texture having a slightly increased roughness from a real surface, a new texture where the roughness value is inherited from one and hardness from another, and a texture that can be perceived as lying exactly in the middle of two real textures. Efficiently creating such textures from real textures is the goal of present work, and we call this as haptic texture authoring.

In the contemporary world, the above examples are not quite possible yet, and this leads to a sub-standard level of realism and immersion for VR and augmented reality (AR) applications. This lack of realistic tactile contents is one of the major hindrances for haptics technology to become widely applicable. The main reason of this bottleneck is that haptic signals are relatively difficult to author compared to other modalities. They are usually based on very complex dynamics of very subtle physical characteristics of a surface, which usually need huge effort to measure, model, parameterize, and simulate in real-time [98]. Data-driven approach, which reproduces haptic signals based on interpolations of pre-measured data, can be an alternative, but this also has inherent drawbacks: the major one being lack of flexibility [7] . This naturally leads us to the need of an authoring tool that allows for creating rich and realistic tactile contents with little effort.

In general, successful authoring of sensory contents needs two technological prerequisites. First, final stimuli to be delivered to the user should be objectively describable. Stimulus that a content designer desires to create should be defined in a description space, so that it can be accurately replicable. The description space can be based on either physical dimensions, e.g., RGB space in color, or perceptual dimension, e.g., decibel space in sound, but authoring needs a way of transforming one space to the other. Second, according to the given description of the desired sensation, its corresponding physical stimuli should be accurately synthesized. Synthesizing can be a combination of various processes: physical simulation of a signal, e.g., computer graphics and modifying/merging existing signals, e.g., sound synthesizer.

In this section, we first select *surface haptic texture* as the subject of authoring among various haptic properties (e.g., stiffness, friction, and so on), as it is one of the perceptually important tactile properties of a surface. With regards to haptic texture, there are a few attempts at examining the first prerequisite, i.e., objective description of haptic texture. Unlike other properties that use physical dimensions for description, e.g., stiffness in N/m, color in RGB, most attempts for haptic texture use *perceptual* dimensions, since physical attributes involved in haptic texture perception are multidimensional, and the relationship between physical signals and their perception is not clearly revealed. Thus, many researchers have focused on the perceptual dimensions and affective properties of touch. Perceptual dimensions are the characteristics based on which humans are able to differentiate various textures. Affective properties of touch are the characteristics that quantify feeling of a given texture. Pioneering work in identifying perceptual texture dimensions was done by Yoshida et al. [31]. They found out that the main dimensions of haptic textures were hard-soft, heavy-light, cold-warm, and rough-smooth. Others extended his work to tool-surface interaction. In [36], Lamotte showed that tool based texture perception is highly related to the hard-soft dimension, while, authors in [37] showed that rough-smooth dimension is also of great importance. Similarly, various affective properties of texture were presented in [84]. Although these studies successfully identified the dimensions and affective properties of tactile perception, their goal was the dimension itself, and no further study was carried out to find the relationship between perceptual space and corresponding physical signal space, which is necessary for actual authoring, i.e., creation, manipulation, or control of tactile stimuli.

The second prerequisite has been extensively studied under the name of haptic texture modeling. Physics based modeling [11, 12] and data-driven modeling [7, 10] are the two prominent ones, and both techniques come with their own advantages and limitations. The physics based method has been a common approach employed by various researchers to render haptic content, where the haptic responses due to tactile properties of a virtual surface are determined by coefficients of physics-based parametric models. For example, high frequency textural vibrations were generated based on the simulation of contact dynamics of micro-scale geometry of surface made by parameterized cavity and bump models mapped into a surface [14, 15] or using stochastic surface geometry models [16, 17]. Although the designer usually has full control over all the parameters and aspects, such a method cannot replicate the complexity of real life surfaces due to simplification in the models. In addition, the designer has to manually incorporate the delicacies and nuances of real surfaces into a synthetic surface, which is quite a demanding task.

In data-driven modeling, the vibrations originating from interaction with different surfaces are recorded and are subsequently used for rendering tactile contents. For instance, the authors in [7] were able to generate virtually perceptible textures based on the scanning velocity and normal force. Similarly, Abdulali et al. extended this idea to recreate more complex textures (anisotropic textures) by incorporating the direction of scan velocity into the equation [18]. Recently, a more robust and efficient technique has been employed where Generative Adversarial Networks (GANs) have been trained to create vibrotactile signals based on texture images or attributes albeit using predefined and constrained tool-surface interaction [19]. The upside of data-driven modeling is that the created contents are highly realistic and computationally simpler. However, the recorded model is an arbitrary signal having no physical meaning and is hard to modify meaningfully. This indicates that the number of feedbacks that a designer can generate are limited. In addition, it is impossible to create contents that are not physically available, and model building is a highly time consuming process. In summary, on one hand, the physics based models do not guarantee a high level of realism but can be controlled easily. On the other hand, data-driven models ensure higher realism with limited controllability and authoring power. Increasing realism of physics based approaches generally come at a very high computational cost, which often make a system non-practical. Instead, it seems that more feasible solution would be to keep the data-driven approach
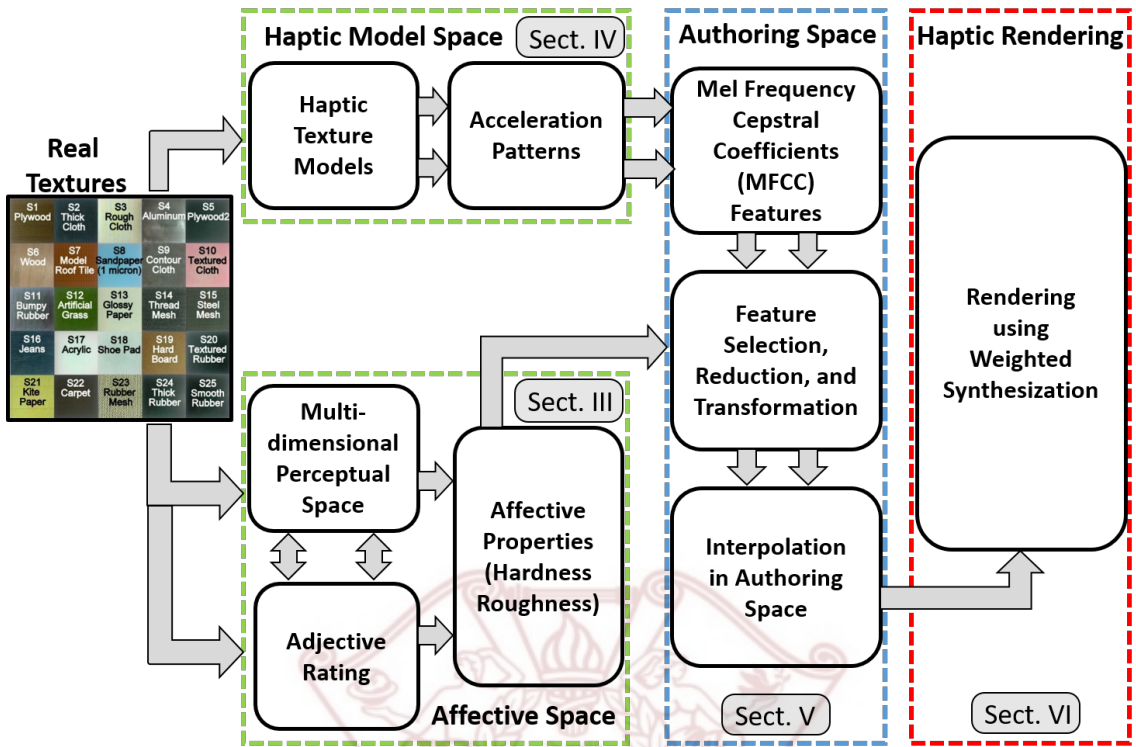
Figure 4.1: Block diagram of the overall system.

and to focus on improving controllability of data-driven models.

The goal of this chapter is to provide an effective method for haptic texture authoring using data-driven haptic texture modeling. We achieve this goal through two contributions. We first established an *authoring space* where 25 data-driven texture models build from 25 fully featured real surfaces are placed according to their affective properties. The space is made in such a way that it maximizes the correspondence between affective properties of the 25 models and features in the physical signals of the models. Axes of the space are the affective properties, and this space plays a role as a perception-based descriptor of textures. Now, designers can freely select an arbitrary point in the space to author a texture, and then the system automatically synthesizes new texture signal corresponding to the selected affective properties. Our second contribution lies in this part. Our framework interpolates signals from adjacent data-driven models, so that two different haptic models are combined to form the new virtual texture. This step ensures that the new model inherits perceptual characteristics of the parent textures, allowing the aforementioned

---

Algorithm 1 Flow of the overall system

1: **Input:** Real textures and acceleration patterns from tool-surface interaction
2: **Step 1:** Affective Space
3:      Create Perceptual space from psychophysical experiment
4:      Establish attribute ratings for all textures
5:      Regress attribute ratings onto Perceptual space to form Affective space
6: **Step 2:** Haptic Model Space
7:      Create haptic models from interaction vibrations
8:      Approximate 25 uniquely spaced acceleration patterns
9:      Concatenate the 25 patterns to form raw features
10: **Step 3:** Authoring Space
11:      Calculate MFCC features from raw features
12:      Reduce features based on correlation with affective space
13:      Create new textures by Delaunay triangulation and interpolation in Authoring space
14: **Step 4:** Haptic Rendering
15:      Synthesize new textures using interpolation weights
16:      Render new textures
17: **Finish**

---

authoring scenarios. To the best of our knowledge, there is no such work which provides the approximation of physical properties across two different texture models.

4.1   Overview

Figure 4.1 presents a holistic view of the overall system, while Algorithm 1 provides the flow of the system. The methods used to approach our goal are detailed in the following sections.

The current study aims at providing a platform that can manipulate existing data-driven haptic textures in a perceptually meaningful manner. Since a data-driven model is just a recording of haptic-related signals, it is not a trivial task to find a connection between a certain modification in signals and its perceptual result, and vice versa. This relationship is essential for our goal. This study first tries to establish this relationship. To this end, we first build an affective space where 25 data-driven models are scattered in a two dimensional space defined by two perception-based affective properties (see Sect. 4.2). Another space called haptic model space is built from the multi-dimensional features extracted from the acceleration signals of the same 25 data-driven models (see Sect. 4.3).

Now, the two spaces are merged based on the correlation between them, yielding an authoring space (see Sect. 4.4). The main characteristic of the authoring space is that all textures are scattered in this space as a function of their affective properties while also maintaining their connection to the physical acceleration patterns. Each point in affective space is linked with a corresponding acceleration pattern, and a change in affective values is instantly reflected in the acceleration patterns.

However, we only have acceleration patterns for a few points (the points where 25 real surfaces are located) in the authoring space. Therefore, interpolation is carried out to generate acceleration patterns for any arbitrary point within the convex hull of real surfaces in the authoring space (see Sect. 4.5). In order to do this in a perceptually correct manner, we did a time-domain acceleration signal interpolation based on distances to the nearest real samples. This results in a new virtual texture having arbitrary affective properties.

Finally, the newly authored virtual textures are evaluated using a psychophysical experiment (see Sect. 4.6).

4.2   Affective Space

Real life textures used in this study are scattered in the affective space as a function of their affective properties. Two psychophysical experiments are carried out to establish the affective space. The first one is a cluster sorting experiment to form a perceptual space and the second one an attribute rating experiment. The first experiment, with the help of multidimensional scaling (MDS), resulted in a two dimensional perceptual space where textures are scattered based on differences in textural perception. The second experiment, called as attribute rating, is carried out to find affective properties that best describe the given textures. These affective properties are in the form of attribute pairs. The attribute pairs are regressed into perceptual space to establish an affective space, and the perceptual space is projected onto each attribute pair.

Consequently, we are left with two affective axes (one from each attribute pair) where all surfaces are aligned according to one specific property. Furthermore, the two affective axes are combined to form affective space.

Figure 4.2: Texture surfaces used to establish the perceptual space.

4.2.1   Experiment 1: Perceptual Space

This experiment was performed using a set of 25 real life textured surfaces. The variety of surfaces in this set was such that they encompassed a majority of the surfaces encountered in daily life haptic interactions. Details of all surfaces are shown in Fig. 4.2. Ten participants took part in this experiment. They were blindfolded and wore headphones playing white noise. The participants had little prior experience about haptics, and were paid for their participation.

The participants interacted with the surfaces using a pen shaped aluminum tool with a solid plastic tip, as shown in Fig. 4.3. The length of the tool was 14 cm while the diameter of the tip was 7 mm. The participants were asked to use free hand motion and to vary their hand velocity and penetration force during interaction. The vibrations emanating from the interaction propagate through the tool and help the users to identify various characteristics of texture. The main aim of using a tool was to emulate exactly the same situations encountered while interacting with a
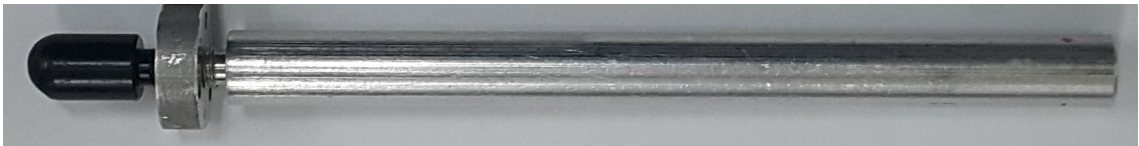
Figure 4.3: Tool used for interaction during the psychophysical experiments.

Table 4.1: The list of attributes provided to participants for the attribute rating experiment. The four selected attribute pairs are in bold-face font.

Hard	Flat	Bumpy	**Sticky**	Even
Slippery	**Irritating**	Sparse	Dull	Sharp
Rough	Thin	**Soft**	Prickly	Uneven
Thick	**Smooth**	Dense	**Pleasant**	Soothing

virtual texture, where interactions mostly occur through a stylus or other such media.

The experiment was a cluster sorting experiment similar to the one in [63,90]. Each participant carried out three trials where total number of groups were 3, 6, and 9. They interacted with surfaces using active touch and assigned perceptually similar surfaces to same groups.

Readers can refer to [63,90] for in-depth details of the experiment. Data from this experiment were in the form of a similarity matrix calculated by averaging the clustering data of all participants. A similarity score, equal to total number of groups in the trial, was assigned to a pair of surfaces when grouped together in a trial. Similarity scores for all pairs of surfaces were added and scaled from zero to 100. The similarity matrix was converted to a dissimilarity matrix and analyzed using non-metric MDS. Kruskal stress values for the first ten dimensions of MDS were calculated. The stress value of 0.09, at dimension two in Fig. 4.4, is considered as fair according to [66]. Hence, a two dimensional perceptual space was established, shown in Fig. 4.5.

4.2.2 Experiment 2: attribute Rating

Same participants took part in this experiment and interaction was through the same tool. A total of twenty attribute were provided (provided in Table 4.1) among which participants selected the ones which could be used to describe the surfaces in this experiment. The remaining attribute were discarded. Within the selected attribute, the ones having a corresponding attribute with an opposite meaning were paired together. As a result four pairs of attribute were formed. attribute
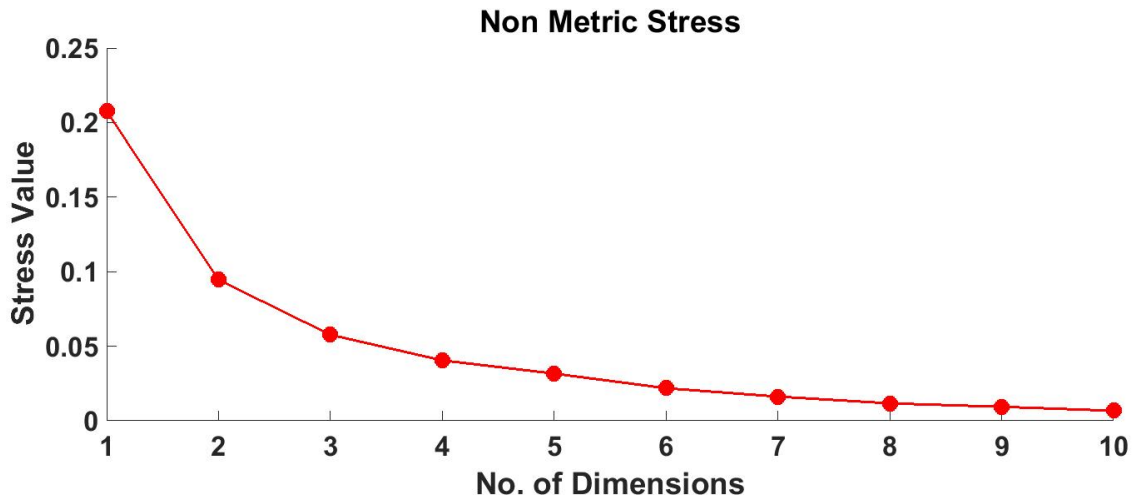
Non Metric Stress

Figure 4.4: Nonclassical (nonmetric) Kruskal stress values for the first ten dimensions of MDS

pairs selected as a result of this experiment are given in Table 4.2. Participants were asked to quantify affective attributes of the textured surfaces based on these attribute pairs. An unmarked scale was provided on a computer screen containing attribute pairs on opposite sides. Participants adjusted a slider on the scale to evaluate surfaces according to each of the attribute pairs. Slider values were scaled from zero to 100 and averaged across of all participants. Detailed procedure of this experiment can be found in [39].

Correlation of attribute pairs with the dimensions of MDS was calculated to evaluate the correctness of these attribute pairs, given in Table 4.2.

4.2.3   Regression and Projection

Multi-linear regression is performed to interpret the attribute pairs according to the perceptual space. The attribute pairs are linearly regressed into the perceptual space, where the length of the line shows its goodness of fit, as shown in Fig. 4.5. For simplicity, we selected only the highest correlated attribute pair for each dimension.

After regressing the two attribute pairs, all the surfaces in the perceptual space are perpendicularly projected onto the given regressed lines. The main characteristic of projecting points onto the attribute pair line is that all points on the line are in an increasing or decreasing order of that particular attribute. Finally, we are left with two lines i.e, hard-soft and rough-smooth line. These

Table 4.2: The correlation values of different attribute pairs with the two dimensions of the perceptual space

attribute Pair	Dimension 1	Dimension 2
Rough - Smooth	**-0.7565**	0.2603
Sticky - Slippery	-0.7286	0.0580
Hard - Soft	-0.0717	**-0.5906**
Irritating - Pleasant	-0.7220	0.0142

lines are considered as independent axes and are combined to form the Affective Space, since angle between the lines is 90.01 degrees.

4.3 Haptic Model Space

The model space must be based on the characteristics of physical interaction with surfaces because the psychophysical experiments were also based on physical interaction. Since the model space will be mapped with the affective space, these physical characteristics must be the ones that are perceivable by humans. The most common source of haptic texture perception is the high frequency vibrations (acceleration patterns) originated during interaction with a surface. Hence, we decided to use the acceleration patterns for the haptic model space establishment. Various scanning parameters were also taken into consideration while collecting the acceleration patterns, since different scanning parameters affect the spectral characteristics of the resultant vibration signal [99].

Since the aim of establishing the model space is to find a relationship between acceleration patterns and affective space, it is important to maintain a controlled environment while scanning textures. Same scanning parameters must be used across all texture models. There are two possible ways to collect such data; use a special machine for data collection; or simulate the signal using very sophisticated haptic modeling and rendering framework that accurately reflects real signals, e.g., data-driven haptic texture modeling and rendering. In [18], authors provided a haptic texture modeling algorithm which showed reasonable performance. More importantly, the authors claim that their models are perceptually sound, therefore, it is decided to build haptic texture models based on [18] and use it to simulate the vibration output for a given combination of input param-

eters, by using the complementary rendering algorithm [23]. The data acquisition setup used for model building was similar to the one provided in [23]. The device used for data collection is provided in Fig. 4.3. The overall haptic model gains were manually tuned to provide perceptually correct rendering output.

The signal recording time for each texture is 40 seconds. Since all the textures in the current study are isotropic in nature, the directionality of the sample texture is deemed irrelevant. Therefore, the input space for the algorithm provided in [18] is reduced to two-dimensions, i.e., velocity magnitude and normal force. Lastly, 25 response signals are approximated using each texture model with a predefined input vector. The responses resulting from combining each value in the velocity vector (50, 100, 150, 200, 250) with each value in force vector (0.1, 0.2, 0.3, 0.4, 0.5) are approximated.

After calculating the responses, the 25 acceleration patterns are concatenated together to form a single feature vector for each texture. Employing such a strategy ensured that the signal preserves the delicacies induced due to varying scan parameters. This concatenated signal will be used for feature extraction in the next section.

4.4   Authoring Space

The main aim of this work is texture authoring, which means that a change in affective space should be replicated accordingly in the haptic model space. For this purpose, the authoring space is established by combining the two spaces. In authoring space, surfaces are scattered based on their affective properties, while at the same time it carries information about physical properties of the surfaces.

Physical acceleration signals collected from the modeling of various surfaces carry redundant information in addition to useful haptic information. It is required to distill that information and to represent it in a meaningful and reusable way. Therefore, a feature extraction algorithm is used, called as Mel Frequency Cepstral Coefficients (MFCC) [100].

The MFCC features are used to predict the affective properties calculated in Section 4.2. In order to find out which of the MFCC features can be useful for predicting the individual affective axes, further feature reduction and transformation algorithms were used. Sequential Forward
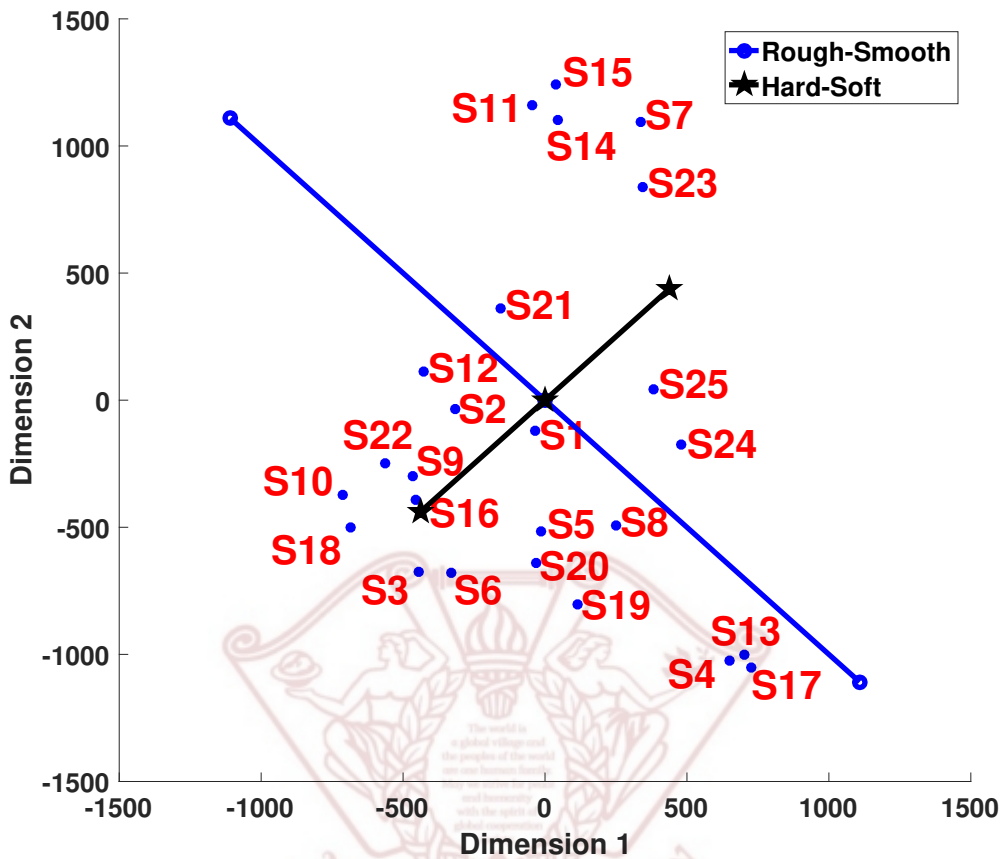
Figure 4.5: Two dimensional MDS of the perceptual space. The lines show the regressed attribute pairs. The length of the line shows the goodness of fit for that attribute pair with the perceptual space

Selection (SFS) [73] and Parallel Analysis (PA) [75] are performed to obtain the MFCC features that are highly correlated with the respective affective axes. Afterwards, Principal Component Analysis (PCA) is applied to further reduce the feature dimension. As a result, we are left with a one-to-one correspondence between the features and affective axes, i.e., one feature representing one affective axis. These two features are combined to form a two dimensional authoring space.

4.4.1 Mel Frequency Cepstral Coefficients

MFCC has been widely used in audio signal processing. It is fine tuned to be compatible with the human perception of audio. Therefore, it is a suitable choice to be used as the primary feature

extraction technique. Additionally, the authors in [101] showed that MFCC provides a high level of accuracy in representing haptic perception data from tool based interaction.

The overall signal is broken down into segments of 25 ms with an overlap of 10 ms . The higher and lower frequency thresholds are set at 500 Hz and 10 Hz, respectively. A total of 13 MFCC coefficients are calculated from each segment. Afterwards, all the 13 MFCC coefficients for every sample are aligned in a single row to represent one instance i.e., one given texture surface. At the end of this process we are left with a matrix of 25 rows which represented the texture surfaces and its columns representing the features.

4.4.2 Feature Reduction

The number of features after concatenating the MFCC coefficients is very large, therefore, SFS in combination with PA and PCA is used to reduce the size of feature vector. This reduction in size of the feature vector is carried out while keeping the affective space in perspective. The unnecessary features are removed while the ones which showed high correlation with the affective space are kept.

Sequential Forward Selection   The correlation between each feature and the individual axis of affective space is calculated. One axis of the affective space is considered at a time. SFS starts by selecting the most correlated feature and predicts the affective axis using linear regression. Afterwards, the next most correlated feature is combined with the first one and the affective axis is predicted. This process continues until a termination criterion is met. The termination criterion in this case is the prediction error of the linear regression model being significantly increased i.e., $p \geqslant 0.01$.

As a result of SFS, we are left with 11 significant features for the rough-smooth axis and 16 significant features for the hard-soft axis. Since these features are selected based on correlations, it is possible that these correlations are achieved by chance. In order to prove that the correlations are significant, parallel analysis is carried out.

Parallel Analysis   PA compares the predictive ability of the significant features against random data. If the features are truly significant, correlation of features with affective axis will be higher as

compared to the correlation between random data and affective axis. PA is carried out separately for both the affective axes using their respective features.

The features obtained as a result of SFS are divided into subsets of three features. Each subset is used to predict the associated affective axis. Correlation between the predicted values for the affective axis and the actual values of affective axis is calculated. Concurrently, a random data matrix having the same dimensionality as the feature vector is created and divided into subsets of three features. Similar to the significant features, the random features are used to predict the affective axis. The correlations between the predicted and actual values are calculated. In the next step, the correlation values from the significant features and random features are compared. Only those subsets are selected for further processing that show correlation values higher than the highest correlation value achieved by random features. After selecting these subsets, the features which appear most frequently in these subsets are selected as the most significant features. Seven features for the rough-smooth axis and six features for the hard-soft axis appeared most frequently in the significant subsets.

Principal Component Analysis   A cubic polynomial model is trained using the affective space as response while features are used as predictors. This model is iteratively trained for all combinations of the features and it is found out that even a single feature can provide reasonable accuracy. Therefore, we further reduced the features obtained after PA. PCA is used to convert these features into just one feature to represent the associated affective axis. The affective axis is predicted using the cubic polynomial model to check the validity of this feature. Furthermore, five fold cross validation is used to check the robustness in prediction when using a single feature. Five surfaces are used as test samples, while 20 surfaces are used as training samples. Average cross validation root mean squared value for rough-smooth axis is 91.59% while that for the hard-soft axis is 92.49%. Average cross validation correlation between the predicted and actual affective axes is 0.93 and 0.94 for the rough-smooth and hard-soft axes, respectively.

4.4.3 Establishing the Authoring Space

In the previous section we calculated two features which could predict the affective axes with reasonable accuracy. These two axes are combined to form a two dimensional authoring space. Since the authoring space is established from both the spaces, it can be argued that it inherits the properties of both spaces. All textured surfaces are scattered into this two dimensional space. The authoring space is shown in Fig. 4.6.
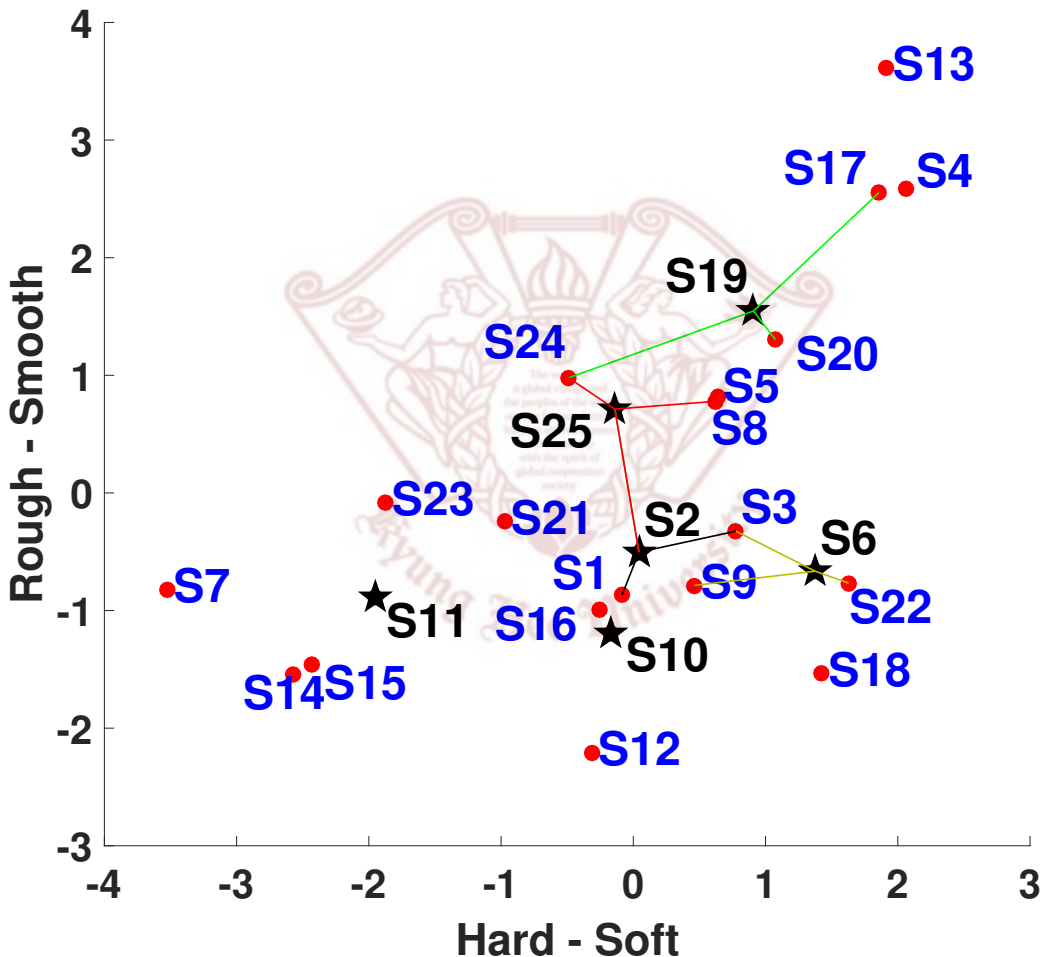
Figure 4.6: The two dimensional Authoring space established by combining the affective and haptic modeling spaces. The surfaces represented by black stars are the ones used in the evaluation section. The colored lines show the three samples which are interpolated to render the authored texture at the location of black stars.

4.4.4 Interpolation in Authoring Space

Now, new virtual surfaces can be authored based on any given affective values from the authoring space. A point in authoring space can be represented by a pair of rough-smooth and hard-soft values. Using these values, a new texture signal can be synthesized by interpolating neighboring real textures.

For instance, Fig. 6 shows the interpolation of a model at the location of S25. The three nearest neighbors from P25 are S2, S24, and S8, and we assume that a weighted interpolation among these three real models would yield a new texture model that properly represents the perceptual characteristic of the location of P25.

Finding nearest neighbors and calculating weight is done as follows. Any certain location can be enclosed by performing Delaunay triangulation. This gives us three nearest neighbors, and distances to them can be computed. These distances are used to assign weights to the three neighboring models using the inverse distance method. Using these weights, haptic models for the three surfaces are combined to render the virtual authored texture, which will be further discussed in Section 4.5.

It can be argued that perception is a non-linear phenomenon, whereas, the weights being used here are calculated linearly. It must be noted that the authoring space in itself is considered as a non-linear entity and thus the interpolation weights being calculated in this space inherit the same non-linearity.

4.5 Haptic Rendering Using Weighted Synthesization

The three haptic models selected as a result of Delaunay triangulation in the authoring space are combined to author the new texture by weighted synthesization. The weights are calculated, using inverse distance method, from the vertices of the Delaunay triangles (the vertices are the three nearest neighbors). The weighted synthesization is carried out in two steps. In the first step, under the given current interaction parameters (stroking velocity and normal force) three vibration wave forms from the three selected models are virtually generated using the rendering algorithm (see first three signals in in Fig. 4.7 and Fig. 4.8). Note that these signals are not physically rendered
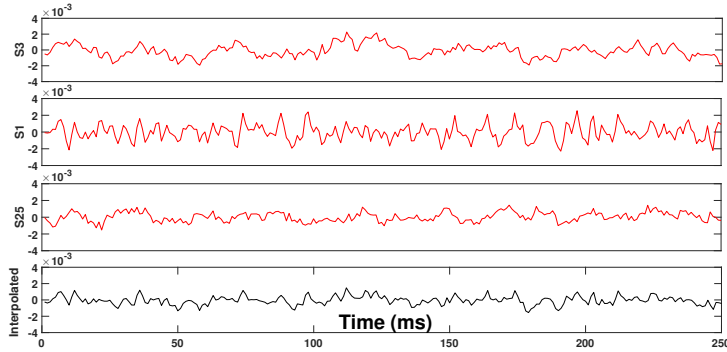
Figure 4.7: S2 = 0.28*S3 + 0.54*S1 + 0.18*S25.
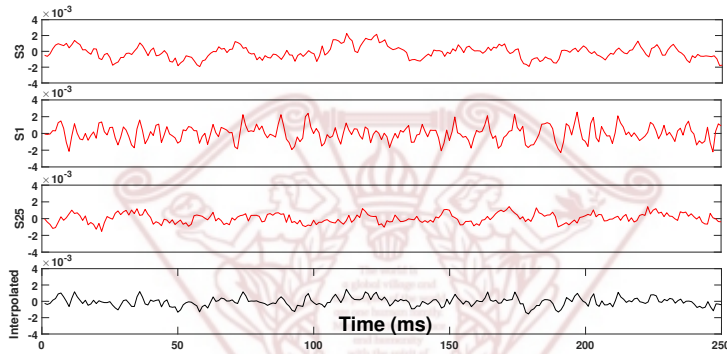

Figure 4.8: S6 = 0.59*S22 + 0.18*9 + 0.23*S3.
The two dimensional Authoring space established by combining the affective and haptic modeling spaces. The surfaces represented by black stars are the ones used in the evaluation section. The colored lines show the three samples which are interpolated to render the authored texture at the location of black stars.

but only simulated internally. In the second step, these signals are added together in time domain using the weights associated with them (see the last signal in Fig. 4.7 and Fig. 4.8). Finally, the synthesized signal is sent to a haptic interface to be rendered. It must be noted that in general such signal synthesization takes place as parametric interpolation in frequency domain [7, 18]. Signal addition is usually carried out in frequency domain since it breaks down the signal into individual frequencies and it is easy to keep track of these frequencies. However, weighted addition in time domain has the same effect on the signal according to [102], and the time domain signal can easily be reconstructed from its Fourier transform. Additionally, superposition of time domain signals was also carried out in [103] to study its effect on the neural system.

The rendering we used for simulating the signals is based on the algorithm in [23]. The original algorithm takes in a three dimensional input, i.e., two dimensional velocity and force to deal with dimensionality in texture. Since all the textures in the current study are assumed to have an isotropic texture, the original algorithm is modified to reduce the input dimension from three to two i.e., velocity magnitude and normal force.

In certain cases adding two sinusoids having very similar frequency (but not exactly the same) can cause an interference pattern. Such an interference pattern is called as a *beat*, and it can positively or negatively affect the amplitude of the signal over time [104]. If we add two sinusoids having frequencies f_1 and f_2, a beat frequency equal to the difference $|f_1 - f_2|$ of the two is generated. The beating effect becomes quite pronounced when we are adding two pure sinusoids. However, the amplitude of the beat frequency decreases as the number of sinusoids increase. Similarly, addition of noise can also dilute the effect of beating. Further details about this are provided in supplementary materials.

Theoretically, this phenomenon can occur in our system when we synthesize signals during rendering, since we are interpolating nearby models having similar characteristics, and it could destroy the haptic feeling of texture. However, it is very rare to encounter such a phenomenon in real life due to the complex nature of the stochastic signals generated during rendering. The signals used in this study on average contain frequencies from one to 1000 in addition to being stochastic. Additionally, there is some mechanical noise added to the signals during tool-surface interaction. These two factors effectively nullify the effect of any beating phenomenon that might occur. It has been shown that perceivable beats occur mostly in favorable conditions, i.e., high power beats can only be perceived in a specific noise band and through the superposition of a limited number of sinusoids [103, 105].

Furthermore, rendering of authored haptic textures, based on weighted synthesization, is perceptually evaluated in the next section.

4.6 Evaluation

The overall texture authoring framework was evaluated using a psychophysical experiment. Some of the textured surfaces were removed (one at a time) from the authoring space and new tex-

tures were authored using the affective values of the removed textures. These affective values were located in authoring space, and three nearest haptic models were selected based on Delaunay triangulation. Afterwards, new virtual haptic textures were synthesized with the given affective properties using the models selected in the authoring space. Finally, participants were asked to compare the authored textures against the associated removed textures. The details of the experiment are provided in the following sub sections.
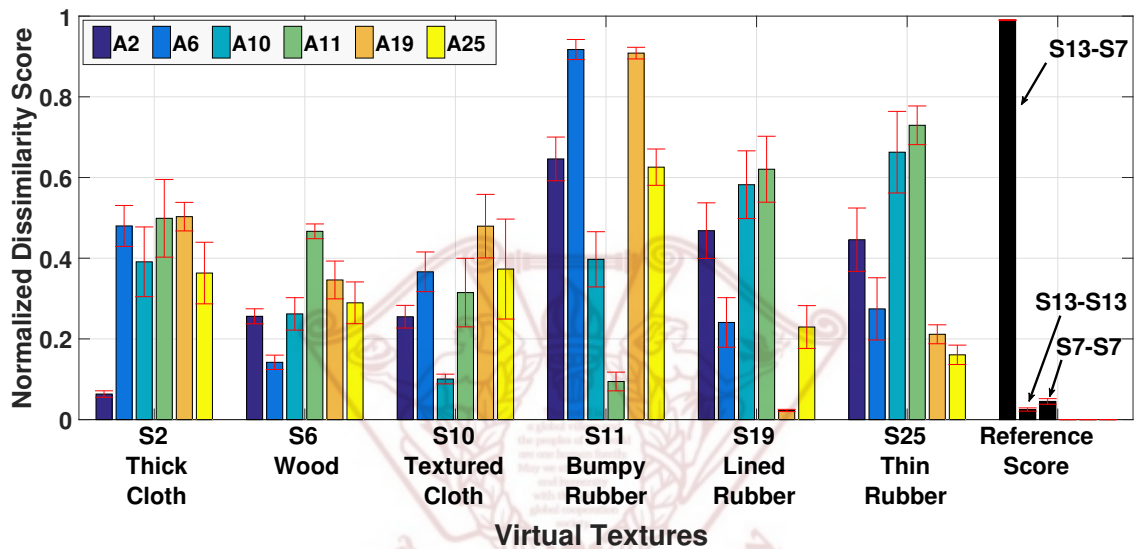
Figure 4.9: The x-axis shows the original haptic models of real life textured surfaces, while the six bars against each one of them show the authored textures. The A in the legend stands for authored.

Participants and Stimuli A total of 10 participants took part in the experiment. During the experiment, the participants were blind folded and wore headphones to restrict visual and auditory cues.

A tablet PC (Microsoft Surface Pro 4) and a voice coil actuator (Haptuator Mark II; Tactile Labs) mounted on top of the Microsoft Surface Pen were used as a rendering device in this experiment. The experimental setup was same as the one provided in [23]. A total of six surfaces were removed (one at a time) from the authoring space. After removing a surface, a virtual texture was authored at its location. Thus, stimuli for the experiment was a total of six virtual textures which were generated at the locations of the six removed textures. The removed surfaces were S2,

Table 4.3: Normalized realism scores for the corresponding pairs of authored and original haptic textures.

	A2-S2	A6-S6	A10-S10	
Normalized Realism Score	0.97	0.89	0.93	**Average**
	A11-S11	**A19-S19**	**A25-S25**	0.94
Normalized Realism Score	0.94	1.00	0.87	

S6, S10, S11, S19, and S25. These surfaces were randomly selected from different parts of the space. Comparisons between two extreme samples (S7 with S13) and two same samples located at extremes (S7 with S7, and S13 with S13) in the authoring space were also evaluated to provide reference for the dissimilarity scores. It should be noted that the virtual textures closer to a real texture should inherit a higher degree of its affective properties.

Procedure   The experiment was a pairwise comparison task using magnitude estimation without modulus. Every authored texture was compared against every removed (haptic model of real texture) texture. Thus, a total of 36 combinations were provided to the participants, one at a time. The participants were asked to rate the dissimilarities between two given textures at a time. A same pair of surfaces was presented to the participant two times. The order of stimuli presentation was randomized across participants and trials. The experiment took 30 minutes on average per participant.

Data Analysis   Data from the experiment are in the form of dissimilarity values. A value of zero means that two models are same, while a higher score shows a higher dissimilarity. Data are normalized (0-1) for each participant and averaged across all. Our hypothesis is that a pair of authored texture and its original haptic model should receive a dissimilarity score of zero.

Results   Fig. 4.9 shows the dissimilarity scores of the six authored textures against the six original haptic models of real life textures. It can be seen that the participants rated each one of the authored textures as the most similar to its associated original haptic model, e.g., A2 and S2, A6

and S6 and so on. In case of the reference comparisons, the two farthest models received the highest dissimilarity score (0.99 for S13-S7) while the two same models received extremely low scores (0.025 for S13-S13, 0.045 for S7-S7). The dissimilarity scores for all the same real-real and authored-authored texture pairs (A1-A1, S1-S1 and so on) were also calculated, however, all the pairs showed values in the vicinity of zero (a value of zero means the two surfaces are exactly the same) and as such did not provide any further insights. This is also evident from the two same texture reference points provided in Fig. 4.9 which show extremely low dissimilarity values. Therefore, the scores for all similar texture comparisons (real-real and authored-authored) are not reported here.

4.7 Discussion

From Fig. 4.9 it can be seen that haptic model of Bumpy Rubber (S11) received a very low dissimilarity score against its associated authored texture (A11), while all other authored textures (A2, A6, A10, A19, and A25) received significantly higher dissimilarity scores. This means that participants could easily associate them together. This can be due to the fact that S11 lies far away from the other surfaces in the authoring space, and its affective properties are significantly different from the other surfaces in the experiment.

The haptic models for the Thick Cloth (S2) and Hard Board (S19) also received very low dissimilarity scores with respect to their associated authored textures. However, the dissimilarity scores for most of the other authored textures were not as significantly large as that for the Bumpy Rubber. This is also a reflectance of the fact that the other authored textures are relatively closer to S2 and S19.

Normalized realism scores (NRS) for all the corresponding pairs of authored and original haptic textures were calculated to find out the perceptual authenticity of the authored textures. These scores are provided in Table 4.3. NRS were calculated by normalizing the dissimilarity values from Fig. 4.9 according to the reference values provided in the said figure. The two same reference textures (S7-S7, S13-S13) were averaged to obtain the lower bound, while the dissimilarity value of the extreme textures (S13-S7) was used as the upper bound. It can be seen that NRS for most pairs is around 90 % or higher, and the average for all the six pairs is at 94 %. Such a high

value of NRS indicates that the perceived realism of the authored textures strongly matched that of the original textures, and the participants did not face much difficulty in identifying the correct match for all the authored textures.

Results of evaluation experiment validate that the proposed method of synthesizing textures produces perceptually correct authored textures. Results also show that we can readily author any haptic texture with predefined affective properties. However, the range of the affective properties is limited to the convex hull of the authoring space. The current authoring space is established from 25 real life textures. Increasing the number and variety of textures could expand the authoring space and more diverse haptic textures could be authored.

It must also be noted that new textures can be authored with any combination of the affective values. In the evaluation experiment we selected these particular points so that authored textures could be compared to the original virtual textures, and authenticity of the algorithm could be evaluated. For this experiment, it was assumed that the haptic rendering algorithm provided perfect models of real life textured surfaces.

4.8   Chapter Summary

In this chapter, we provide a novel algorithm for haptic texture authoring. The affective properties of real life textures are manipulated to create virtual textures exhibiting predefined affective properties by using contact acceleration patterns. This algorithm finds great application in the realm of virtual reality, where on demand textures are need of the hour. More specifically, it can provide virtual textures as a combination of various real life textures.

Chapter 5

Conclusions and Future Directions

In this chapter, we conclude our contributions and provide some future direction for our research.

5.1 Conclusions

The main aim of the current thesis is to establish a Universal Haptic Texture Library in an effort to automate and streamline haptic content creation. The current thesis attempts to solve three open challenges in haptics technology. The first challenge is automation in haptic texture modeling, the second challenge is the provision of a universal haptic attribute space (HAS), and the third one is the ability to author virtual textures from real textures.

The automation of haptic texture modeling solves the problem of having to create models for every new texture surface. Traditionally, haptic models are either parameter or data-driven. The parametric models are manually tuned and require a haptic expert to create every single model. The data-driven models are created from interaction with surface and require a sophisticated sensorized tool for the interaction. Both these methods take a considerable amount of time and renders it next to impossible to generate haptic models on the go. The current thesis, therefore, provides an automatic haptic model assignment algorithm that can assign haptic textures (from the library) to new surfaces based on their images.

The HAS provides a standard model for describing textures in terms of their haptic attributes. The haptic world lacks a generic model that can represent, classify, or identify haptic textures based on a certain perceptual criterion. It is of utmost importance to establish a generalized system where haptic textures can be identified based on their perception. The HAS provides a platform where haptic textures are located based on their haptic attributes. New haptic textures can also be added readily to the HAS based on their image features. The multi-scale 1D-CNN enables the

population of the HAS with new textures.

The aforementioned techniques help to make virtual textures based on real textures and the automation of this process. In certain cases, there may arise a need to manipulate certain properties of real textures to create new virtual textures. The authoring environment introduced in this thesis helps us to create new virtual texture that can inherit properties of real textures. In essence, the authoring tool enables us to manipulate the haptic properties (perceptual attributes) of real textures to render new virtual textures.

5.2   Future Research Directions

A total of 100 different real life texture surfaces were used in the current thesis. Although, this a large number of surfaces having myriad surface textures, still there remains room for incorporating some totally different surfaces. For example, using oily or wet surfaces, organic surfaces, deformable surfaces etc. As a future direction, such surfaces can also be added to the library in addition to current ones.

In our current approach, all the machine learning algorithms are trained using image features. These image features are extracted using classical image feature extraction techniques except for the case of ResNet-50 (which is an object classification algorithm). In the future, it might prove beneficial to use state-of-the-art texture recognition algorithms [106–109] for training the subsequent machine learning algorithms for predicting the output.

A large number factors contribute into haptic perception of an object. The current research focused on haptic texture specifically, however one of the possible future directions could be to automate the modeling process for haptic properties other than texture. Haptic perception can include properties like shape or geometry, compliance, acceleration or velocity, force, etc.

Bibliography

[1] S. Lu, Y. Chen, and H. Culbertson, "Towards multisensory perception: Modeling and rendering sounds of tool-surface interactions," *IEEE transactions on haptics*, vol. 13, no. 1, pp. 94–101, 2020.

[2] G. Krolczyk, R. Maruda, J. Krolczyk, P. Nieslony, S. Wojciechowski, and S. Legutko, "Parametric and nonparametric description of the surface topography in the dry and mqcl cutting conditions," *Measurement*, vol. 121, pp. 225–239, 2018.

[3] P. de Groot, "Principles of interference microscopy for the measurement of surface topography," *Advances in Optics and Photonics*, vol. 7, no. 1, pp. 1–65, 2015.

[4] J. DiSciacca, C. Gomez, A. Thompson, S. Lawes, R. Leach, X. Colonna de Lega, and P. de Groot, "True-color 3d surface metrology for additive manufacturing using interference microscopy," 2017.

[5] J. Wang, Y. Cui, D. Liang, Y. Wang, and R. Ying, "Differential confocal measurement for surface topography with microstructures based on spiral scanning and wavelet filter," *Applied Optics*, vol. 59, no. 36, pp. 11 359–11 370, 2020.

[6] D. C. Ruspini, K. Kolarov, and O. Khatib, "The haptic display of complex graphical environments," in *Proceedings of the 24th annual conference on Computer graphics and interactive techniques*.   ACM Press/Addison-Wesley Publishing Co., 1997, pp. 345–352.

[7] H. Culbertson, J. Unwin, and K. J. Kuchenbecker, "Modeling and rendering realistic textures from unconstrained tool-surface interactions," *IEEE transactions on haptics*, vol. 7, no. 3, pp. 381–393, 2014.

[8] P. Fong, "Sensing, acquisition, and interactive playback of data-based models for elastic deformable objects," *The International Journal of Robotics Research*, vol. 28, no. 5, pp. 630–655, 2009.

[9] M. Mahvash and V. Hayward, "High-fidelity haptic synthesis of contact with deformable bodies," *Computer Graphics and Applications, IEEE*, vol. 24, no. 2, pp. 48–55, 2004.

[10] S. Andrews and J. Lang, "Haptic texturing based on real-world samples," in *Haptic, Audio and Visual Environments and Games, 2007. HAVE 2007. IEEE International Workshop on*. IEEE, 2007, pp. 142–147.

[11] S. Jeon and S. Choi, "Real stiffness augmentation for haptic augmented reality," *Presence: Teleoperators and Virtual Environments*, vol. 20, no. 4, pp. 337–370, 2011.

[12] T. Yamamoto, B. Vagvolgyi, K. Balaji, L. L. Whitcomb, and A. M. Okamura, "Tissue property estimation and graphical display for teleoperated robot-assisted surgery," in *Robotics and Automation, 2009. ICRA'09. IEEE International Conference on*. IEEE, 2009, pp. 4239–4245.

[13] A. M. Okamura, M. R. Cutkosky, and J. T. Dennerlein, "Reality-based models for vibration feedback in virtual environments," *Mechatronics, IEEE/ASME Transactions on*, vol. 6, no. 3, pp. 245–252, 2001.

[14] C. H. Ho, C. Basdogan, and M. A. Srinivasan, "Efficient point-based rendering techniques for haptic display of virtual objects," *Presence*, vol. 8, no. 5, pp. 477–491, 1999.

[15] M. A. Costa, M. R. Cutkosky, and S. Lau, "Roughness perception of haptically displayed fractal surfaces," in *proceedings of ASME Dynamic Systems and Control Division*, vol. 69, no. 2, 2000, pp. 1073–1079.

[16] J. P. Fritz and K. E. Barner, "Stochastic models for haptic texture," in *Telemanipulator and Telepresence Technologies III*, vol. 2901. International Society for Optics and Photonics, 1996, pp. 34–45.

[17] L. Kim, A. Kyrikou, G. S. Sukhatme, and M. Desbrun, "An implicit-based haptic rendering technique," in *Intelligent Robots and Systems, 2002. IEEE/RSJ International Conference on*, vol. 3. IEEE, 2002, pp. 2943–2948.

[18] A. Abdulali and S. Jeon, "Data-driven modeling of anisotropic haptic textures: Data segmentation and interpolation," in *International Conference on Human Haptic Sensing and Touch Enabled Computer Applications*. Springer, 2016, pp. 228–239.

[19] Y. Ujitoko and Y. Ban, "Vibrotactile signal generation from texture images or attributes using generative adversarial network," in *International Conference on Human Haptic Sensing and Touch Enabled Computer Applications*. Springer, 2018, pp. 25–36.

[20] S. J. Lederman and S. G. Abbott, "Texture perception: studies of intersensory organization using a discrepancy paradigm, and visual versus tactual psychophysics." *Journal of Experimental Psychology: Human perception and performance*, vol. 7, no. 4, p. 902, 1981.

[21] J. Eck, A. L. Kaas, and R. Goebel, "Crossmodal interactions of haptic and visual texture information in early sensory cortex," *Neuroimage*, vol. 75, pp. 123–135, 2013.

[22] M. O. Ernst and M. S. Banks, "Humans integrate visual and haptic information in a statistically optimal fashion," *Nature*, vol. 415, no. 6870, pp. 429–433, 2002.

[23] A. Abdulali and S. Jeon, "Data-driven rendering of anisotropic haptic textures," in *International AsiaHaptics conference*. Springer, 2016, pp. 401–407.

[24] A. Al Maimani and A. Roudaut, "Frozen suit: designing a changeable stiffness suit and its application to haptic games," in *Proceedings of the 2017 CHI Conference on Human Factors in Computing Systems*, 2017, pp. 2440–2448.

[25] O. Georgiou, C. Jeffrey, Z. Chen, B. X. Tong, S. H. Chan, B. Yang, A. Harwood, and T. Carter, "Touchless haptic feedback for vr rhythm games," in *2018 IEEE Conference on Virtual Reality and 3D User Interfaces (VR)*. IEEE, 2018, pp. 553–554.

[26] E. Gatti, D. Pittera, J. B. Moya, and M. Obrist, "Haptic rules! augmenting the gaming experience in traditional games: The case of foosball," in *2017 IEEE World Haptics Conference (WHC)*. IEEE, 2017, pp. 430–435.

[27] R. Gutschmidt, M. Schiewe, F. Zinke, and H. Jürgensen, "Haptic emulation of games: haptic sudoku for the blind," in *Proceedings of the 3rd International conference on Pervasive Technologies Related to Assistive environments*, 2010, pp. 1–8.

[28] X. Hou, O. Sourina, and S. Klimenko, "Haptic-based serious games," in *2014 International Conference on Cyberworlds*. IEEE, 2014, pp. 39–46.

[29] A. V. Citrin, D. E. Stem Jr, E. R. Spangenberg, and M. J. Clark, "Consumer need for tactile input: An internet retailing challenge," *Journal of Business research*, vol. 56, no. 11, pp. 915–922, 2003.

[30] J. D. Victor, S. M. Rizvi, and M. M. Conte, "Two representations of a high-dimensional perceptual space," *Vision research*, vol. 137, pp. 1–23, 2017.

[31] M. Yoshida, "Dimensions of tactual impressions (1)," *Japanese Psychological Research*, vol. 10, no. 3, pp. 123–137, 1968.

[32] M. Hollins, S. Bensmaïa, K. Karlof, and F. Young, "Individual differences in perceptual space for tactile textures: Evidence from multidimensional scaling," *Perception & Psychophysics*, vol. 62, no. 8, pp. 1534–1544, 2000.

[33] S. Okamoto, H. Nagano, and Y. Yamada, "Psychophysical dimensions of tactile perception of textures," *Haptics, IEEE Transactions on*, vol. 6, no. 1, pp. 81–93, 2013.

[34] D. Picard, C. Dacremont, D. Valentin, and A. Giboreau, "Perceptual dimensions of tactile textures," *Acta psychologica*, vol. 114, no. 2, pp. 165–184, 2003.

[35] H. Shirado and T. Maeno, "Modeling of human texture perception for tactile displays and sensors," in *First Joint Eurohaptics Conference and Symposium on Haptic Interfaces for Virtual Environment and Teleoperator Systems. World Haptics Conference*. IEEE, 2005, pp. 629–630.

[36] R. H. LaMotte, "Softness discrimination with a tool," *Journal of neurophysiology*, vol. 83, no. 4, pp. 1777–1786, 2000.

[37] M. Hollins, F. Lorenz, A. Seeger, and R. Taylor, "Factors contributing to the integration of textural qualities: Evidence from virtual surfaces," *Somatosensory & motor research*, vol. 22, no. 3, pp. 193–206, 2005.

[38] R. Klatzky, S. Lederman, C. Hamilton, and G. Ramsay, "Perceiving roughness via a rigid probe: Effects of exploration speed," in *Proceedings of the ASME Dynamic Systems and Control Division*, vol. 67, 1999, pp. 27–33.

[39] W. Hassan and S. Jeon, "Evaluating differences between bare-handed and tool-based interaction in perceptual space," in *2016 IEEE Haptics Symposium (HAPTICS)*. IEEE, 2016, pp. 185–191.

[40] M. A. Heller, "Visual and tactual texture perception: Intersensory cooperation," *Perception & psychophysics*, vol. 31, no. 4, pp. 339–344, 1982.

[41] Y. Vardar, C. Wallraven, and K. J. Kuchenbecker, "Fingertip interaction metrics correlate with visual and haptic perception of real surfaces," in *2019 IEEE World Haptics Conference (WHC)*. IEEE, 2019, pp. 395–400.

[42] E. Baumgartner, C. B. Wiebel, and K. R. Gegenfurtner, "Visual and haptic representations of material properties," *Multisensory research*, vol. 26, no. 5, pp. 429–455, 2013.

[43] S. K. Podrebarac, M. A. Goodale, and J. C. Snow, "Are visual texture-selective areas recruited during haptic texture discrimination?" *Neuroimage*, vol. 94, pp. 129–137, 2014.

[44] R. M. Haralick, K. Shanmugam *et al.*, "Textural features for image classification," *IEEE Transactions on systems, man, and cybernetics*, no. 6, pp. 610–621, 1973.

[45] L. Liu and P. Fieguth, "Texture classification from random features," *IEEE transactions on pattern analysis and machine intelligence*, vol. 34, no. 3, pp. 574–586, 2012.

[46] J. Kannala and E. Rahtu, "Bsif: Binarized statistical image features," in *Proceedings of the 21st international conference on pattern recognition (ICPR2012)*. IEEE, 2012, pp. 1363–1366.

[47] T. Ojala, M. Pietikainen, and T. Maenpaa, "Multiresolution gray-scale and rotation invariant texture classification with local binary patterns," *IEEE Transactions on pattern analysis and machine intelligence*, vol. 24, no. 7, pp. 971–987, 2002.

[48] N. Alpaslan and K. Hanbay, "Multi-resolution intrinsic texture geometry-based local binary pattern for texture classification," *IEEE Access*, vol. 8, pp. 54 415–54 430, 2020.

[49] ——, "Multi-scale shape index-based local binary patterns for texture classification," *IEEE Signal Processing Letters*, vol. 27, pp. 660–664, 2020.

[50] J. Li, A. Song, and X. Zhang, "Image-based haptic texture rendering," in *Proceedings of the 9th ACM SIGGRAPH Conference on Virtual-Reality Continuum and its Applications in Industry*, 2010, pp. 237–242.

[51] N. Heravi, W. Yuan, A. M. Okamura, and J. Bohg, "Learning an action-conditional model for haptic texture generation," in *2020 IEEE International Conference on Robotics and Automation (ICRA)*. IEEE, 2020, pp. 11 088–11 095.

[52] K. Takahashi and J. Tan, "Deep visuo-tactile learning: Estimation of tactile properties from images," in *2019 International Conference on Robotics and Automation (ICRA)*. IEEE, 2019, pp. 8951–8957.

[53] M. Strese, J.-Y. Lee, C. Schuwerk, Q. Han, H.-G. Kim, and E. Steinbach, "A haptic texture database for tool-mediated texture recognition and classification," in *2014 IEEE International Symposium on Haptic, Audio and Visual Environments and Games (HAVE) Proceedings*. IEEE, 2014, pp. 118–123.

[54] M. Strese, C. Schuwerk, A. Iepure, and E. Steinbach, "Multimodal feature-based surface material classification," *IEEE transactions on haptics*, vol. 10, no. 2, pp. 226–239, 2016.

[55] M. Strese, L. Brudermueller, J. Kirsch, and E. Steinbach, "Haptic material analysis and classification inspired by human exploratory procedures," *IEEE transactions on haptics*, vol. 13, no. 2, pp. 404–424, 2019.

[56] J. M. Romano and K. J. Kuchenbecker, "Methods for robotic tool-mediated haptic surface recognition," in *2014 IEEE Haptics Symposium (HAPTICS)*. IEEE, 2014, pp. 49–56.

[57] M. Kerzel, M. Ali, H. G. Ng, and S. Wermter, "Haptic material classification with a multi-channel neural network," in *2017 International Joint Conference on Neural Networks (IJCNN)*. IEEE, 2017, pp. 439–446.

[58] B. M. R. Lima, V. P. da Fonseca, T. E. A. de Oliveira, Q. Zhu, and E. M. Petriu, "Dynamic tactile exploration for texture classification using a miniaturized multi-modal tactile sensor and machine learning," in *2020 IEEE International Systems Conference (SysCon)*. IEEE, 2020, pp. 1–7.

[59] H. Vasudevan and M. Manivannan, "Recordable haptic textures," in *Haptic Audio Visual Environments and Their Applications, 2006. HAVE 2006. IEEE International Workshop on*. IEEE, 2006, pp. 130–133.

[60] S. S. Wall and W. S. Harwin, "Modelling of surface identifying characteristics using fourier series," 1999.

[61] K. E. MacLean, "The ¡®haptic camera¡¯: A technique for characterizing and playing back haptic properties of real environments," *Proc. of Haptic Interfaces for Virtual Environments and Teleoperator Systems (HAPTICS)*, pp. 459–467, 1996.

[62] L. Kim, G. S. Sukhatme, and M. Desbrun, "Haptic editing of decoration and material properties," in *Haptic Interfaces for Virtual Environment and Teleoperator Systems, 2003. HAPTICS 2003. Proceedings. 11th Symposium on*. IEEE, 2003, pp. 213–220.

[63] J. Pasquero, J. Luk, S. Little, and K. MacLean, "Perceptual analysis of haptic icons: an investigation into the validity of cluster sorted mds," in *Haptic Interfaces for Virtual Environment and Teleoperator Systems, 2006 14th Symposium on*. IEEE, 2006, pp. 437–444.

[64] M. Hollins, R. Faldowski, S. Rao, and F. Young, "Perceptual dimensions of tactile surface texture: A multidimensional scaling analysis," *Perception & psychophysics*, vol. 54, no. 6, pp. 697–705, 1993.

[65] J. B. Kruskal, "Multidimensional scaling by optimizing goodness of fit to a nonmetric hypothesis," *Psychometrika*, vol. 29, no. 1, pp. 1–27, 1964.

[66] F. Wickelmaier, "An introduction to mds," *Sound Quality Research Unit, Aalborg University, Denmark*, vol. 46, no. 5, pp. 1–26, 2003.

[67] M. M. Galloway, "Texture analysis using gray level run lengths," *Computer graphics and image processing*, vol. 4, no. 2, pp. 172–179, 1975.

[68] A. Chu, C. M. Sehgal, and J. F. Greenleaf, "Use of gray value distribution of run lengths for texture analysis," *Pattern Recognition Letters*, vol. 11, no. 6, pp. 415–419, 1990.

[69] B. V. Dasarathy and E. B. Holder, "Image characterizations based on joint gray level-run length distributions," *Pattern Recognition Letters*, vol. 12, no. 8, pp. 497–502, 1991.

[70] G. Thibault, B. Fertil, C. Navarro, S. Pereira, P. Cau, N. Levy, J. Sequeira, and J. Mari, "Texture indexes and gray level size zone matrix application to cell nuclei classification," 2009.

[71] D. A. Clausi, "An analysis of co-occurrence texture statistics as a function of grey level quantization," *Canadian Journal of remote sensing*, vol. 28, no. 1, pp. 45–62, 2002.

[72] M. Amadasun and R. King, "Textural features corresponding to textural properties," *Systems, Man and Cybernetics, IEEE Transactions on*, vol. 19, no. 5, pp. 1264–1274, 1989.

[73] R. Kohavi and G. H. John, "Wrappers for feature subset selection," *Artificial intelligence*, vol. 97, no. 1, pp. 273–324, 1997.

[74] B. Thompson and L. G. Daniel, "Factor an alytic evidence for the construct validity of scores: A historical overview and some guidelines," *Educational and psychological measurement*, vol. 56, no. 2, pp. 197–208, 1996.

[75] J. C. Hayton, D. G. Allen, and V. Scarpello, "Factor retention decisions in exploratory factor analysis: A tutorial on parallel analysis," *Organizational research methods*, vol. 7, no. 2, pp. 191–205, 2004.

[76] J. Weston and C. Watkins, "Multi-class support vector machines," Citeseer, Tech. Rep., 1998.

[77] D. Arthur and S. Vassilvitskii, "k-means++: The advantages of careful seeding," in *Proceedings of the eighteenth annual ACM-SIAM symposium on Discrete algorithms*. Society for Industrial and Applied Mathematics, 2007, pp. 1027–1035.

[78] S. Choi, L. Walker, H. Z. Tan, S. Crittenden, and R. Reifenberger, "Force constancy and its effect on haptic perception of virtual surfaces," *ACM Transactions on Applied Perception (TAP)*, vol. 2, no. 2, pp. 89–105, 2005.

[79] B. De Bruyn and G. A. Orban, "Human velocity and direction discrimination measured with random dot patterns," *Vision research*, vol. 28, no. 12, pp. 1323–1335, 1988.

[80] A. C. Grant, M. C. Thiagarajah, and K. Sathian, "Tactile perception in blind braille readers: a psychophysical study of acuity and hyperacuity using gratings and dot patterns," *Attention, Perception, & Psychophysics*, vol. 62, no. 2, pp. 301–312, 2000.

[81] M. A. Lawrence, R. Kitada, R. L. Klatzky, and S. J. Lederman, "Haptic roughness perception of linear gratings via bare finger or rigid probe," *Perception*, vol. 36, no. 4, pp. 547–557, 2007.

[82] M. A. Srinivasan and C. Basdogan, "Haptics in virtual environments: Taxonomy, research status, and challenges," *Computers & Graphics*, vol. 21, no. 4, pp. 393–404, 1997.

[83] W. M. B. Tiest and A. M. Kappers, "Analysis of haptic perception of materials by multidimensional scaling and physical measurements of roughness and compressibility," *Acta psychologica*, vol. 121, no. 1, pp. 1–20, 2006.

[84] F. Shao, X. Chen, C. Barnes, and B. Henson, "A novel tactile sensation measurement system for qualifying touch perception," *Proceedings of the Institution of Mechanical Engineers, Part H: Journal of Engineering in Medicine*, vol. 224, no. 1, pp. 97–105, 2010.

[85] S. Okamoto, H. Nagano, and Y. Yamada, "Psychophysical dimensions of tactile perception of textures," *IEEE Transactions on Haptics*, vol. 6, no. 1, pp. 81–93, 2012.

[86] S. Mun, H. Lee, and S. Choi, "Perceptual space of regular homogeneous haptic textures rendered using electrovibration," in *2019 IEEE World Haptics Conference (WHC)*.   IEEE, 2019, pp. 7–12.

[87] I. Hwang and S. Choi, "Perceptual space and adjective rating of sinusoidal vibrations perceived via mobile device," in *2010 IEEE Haptics Symposium*.   IEEE, 2010, pp. 1–8.

[88] Y. Yoo, I. Hwang, and S. Choi, "Consonance of vibrotactile chords," *IEEE transactions on haptics*, vol. 7, no. 1, pp. 3–13, 2013.

[89] Y. Yoo, J. Lee, J. Seo, E. Lee, J. Lee, Y. Bae, D. Jung, and S. Choi, "Large-scale survey on adjectival representation of vibrotactile stimuli," in *Proc. HAPTICS*, 2016, pp. 393–395.

[90] W. Hassan, A. Abdulali, M. Abdullah, S. C. Ahn, and S. Jeon, "Towards universal haptic library: Library-based haptic texture assignment using image texture and perceptual space," *IEEE transactions on haptics*, vol. 11, no. 2, pp. 291–303, 2017.

[91] K. He, X. Zhang, S. Ren, and J. Sun, "Deep residual learning for image recognition," in *Proceedings of the IEEE conference on computer vision and pattern recognition*, 2016, pp. 770–778.

[92] Y. Gao, L. A. Hendricks, K. J. Kuchenbecker, and T. Darrell, "Deep learning for tactile understanding from visual and haptic data," in *2016 IEEE International Conference on Robotics and Automation (ICRA)*.   IEEE, 2016, pp. 536–543.

[93] K. Priyadarshini, S. Chaudhuri, and S. Chaudhuri, "Perceptnet: Learning perceptual similarity of haptic textures in presence of unorderable triplets," in *2019 IEEE World Haptics Conference (WHC)*.   IEEE, 2019, pp. 163–168.

[94] G. T. Taye, H.-J. Hwang, and K. M. Lim, "Application of a convolutional neural network for predicting the occurrence of ventricular tachyarrhythmia using heart rate variability features," *Scientific reports*, vol. 10, no. 1, pp. 1–7, 2020.

[95] W. Hassan, A. Abdulali, and S. Jeon, "Perceptual thresholds for haptic texture discrimination," in *2017 14th International Conference on Ubiquitous Robots and Ambient Intelligence (URAI)*. IEEE, 2017, pp. 293–298.

[96] J. Dagman, M. Karlsson, and L. Wikström, "Investigating the haptic aspects of verbalised product experiences," *International Journal of Design*, vol. 4, no. 3, 2010.

[97] C. O'Sullivan and A. Chang, "An activity classification for vibrotactile phenomena," in *International Workshop on Haptic and Audio Interaction Design*. Springer, 2006, pp. 145–156.

[98] A. Costes, F. Danieau, F. Argelaguet, A. Lécuyer, and P. Guillotel, "Haptic material: A holistic approach for haptic texture mapping," in *International Conference on Human Haptic Sensing and Touch Enabled Computer Applications*. Springer, 2018, pp. 37–45.

[99] J. A. Fishel and G. E. Loeb, "Bayesian exploration for intelligent identification of textures," *Frontiers in neurorobotics*, vol. 6, p. 4, 2012.

[100] H.-G. Kim, N. Moreau, and T. Sikora, *MPEG-7 audio and beyond: Audio content indexing and retrieval*. John Wiley & Sons, 2006.

[101] M. Strese, C. Schuwerk, and E. Steinbach, "Surface classification using acceleration signals recorded during human freehand movement," in *World Haptics Conference (WHC), 2015 IEEE*. IEEE, 2015, pp. 214–219.

[102] S. W. Smith, "The scientist and engineer's guide to digital signal processing," California Technical Pub. San Diego, 1997.

[103] D. Guo, M. Perc, Y. Zhang, P. Xu, and D. Yao, "Frequency-difference-dependent stochastic resonance in neural systems," *Physical Review E*, vol. 96, no. 2, p. 022415, 2017.

[104] G. E. Roberts, *From music to mathematics: exploring the connections*.   JHU Press, 2016.

[105] D. R. Chialvo, O. Calvo, D. L. Gonzalez, O. Piro, and G. V. Savino, "Subharmonic stochastic synchronization and resonance in neuronal systems," *Physical Review E*, vol. 65, no. 5, p. 050902, 2002.

[106] W. Zhai, Y. Cao, Z.-J. Zha, H. Xie, and F. Wu, "Deep structure-revealed network for texture recognition," in *Proceedings of the IEEE/CVF Conference on Computer Vision and Pattern Recognition*, 2020, pp. 11 010–11 019.

[107] M. Rasouli, Y. Chen, A. Basu, S. L. Kukreja, and N. V. Thakor, "An extreme learning machine-based neuromorphic tactile sensing system for texture recognition," *IEEE transactions on biomedical circuits and systems*, vol. 12, no. 2, pp. 313–325, 2018.

[108] S. Luo, W. Yuan, E. Adelson, A. G. Cohn, and R. Fuentes, "Vitac: Feature sharing between vision and tactile sensing for cloth texture recognition," in *2018 IEEE International Conference on Robotics and Automation (ICRA)*.   IEEE, 2018, pp. 2722–2727.

[109] R. M. Anwer, F. S. Khan, J. van de Weijer, M. Molinier, and J. Laaksonen, "Binary patterns encoded convolutional neural networks for texture recognition and remote sensing scene classification," *ISPRS journal of photogrammetry and remote sensing*, vol. 138, pp. 74–85, 2018.

Appendix A

List of Publications

International Journal Papers:

[1] **Waseem Hassan,** Hwangil Kim, Aishwari Talhan, and Seokhee Jeon. "A Pneumatically-Actuated Mouse for Delivering Multimodal Haptic Feedback." Applied Sciences 10, no. 16 (2020): 5611. **[IF 2.679]**

[2] **Waseem Hassan,** Arsen Abdulali, and Seokhee Jeon. "Authoring new haptic textures based on interpolation of real textures in affective space." IEEE Transactions on Industrial Electronics 67, no. 1 (2019): 667-676. **[IF 8.235]**

[3] **Waseem Hassan,** Arsen Abdulali, Muhammad Abdullah, Sang Chul Ahn, and Seokhee Jeon. "Towards universal haptic library: Library-based haptic texture assignment using image texture and perceptual space." IEEE Transactions on Haptics 11, no. 2 (2017): 291-303. **[IF 2.487]**

[4] Raza, Ahsan, **Waseem Hassan**, Tatyana Ogay, Inwook Hwang, and Seokhee Jeon. "Perceptually correct haptic rendering in mid-air using ultrasound phased array." IEEE Transactions on Industrial Electronics 67, no. 1 (2019): 736-745. **[IF 8.235]**

[5] **Waseem Hassan,** Raza, A., Abdullah, M., Shadman, H.Md., Jeon, S., "HapWheel: Bringing in-Car Controls to Driver's Fingertips by Embedding Ubiquitous Haptic Displays into a Steering Wheel." IEEE Transactions on Intelligent Transportation Systems **[Under Revision] [IF 6.492]**

[6] **Waseem Hassan**, Joolee, J.B., and, Jeon, S. "Towards universal haptic attribute space: Predicting haptic attributes of texture from image features." IEEE Transactions on Haptics, **[Sub-**

mission Ready] [IF 2.487]

[7] Joolekha Bibi Joolee, Mohammad Shadman Hashem, **Waseem Hassan**, and Seokhee Jeon, "Deep Encoder-Decoder Network Based Data-driven Approach for Realistic Impact Feedback on Head During Earthquake.", IEEE Transactions on Haptics. **[Under Revision] [IF 2.487]**

[8] Aishwari Talhan, Hwangil Kim, **Waseem Hassan,** Seokhee Jeon, "Multi-Mode Soft Haptic Thimble for Haptic Augmented Reality Based Application of Texture Overlaying" IEEE Transactions on Haptics. **[Under Revision] [IF 2.487]**

Patent:

[1] **Waseem Hassan,** Raza, A., Abdullah, M., Shadman, H.Md., Jeon, S., "Apparatus for controlling electronic function module in the vehicle using steering wheel with dual ubiquitous haptic sensor(듀얼 유비쿼터스 햅틱 센서가 적용된 스티어링 휠을 이용한 차량 내 전장 제어 장치)." South Korean patent 1022757610000, registered July 5, 2021.

International Conference Papers:

[1] **Waseem Hassan,** Arsen Abdulali, and Seokhee Jeon. "Haptic Texture Authoring: A Demonstration." In International AsiaHaptics conference, pp. 18-20. Springer, Singapore, 2018.

[2] **Waseem Hassan,** Arsen Abdulali, and Seokhee Jeon. "Perceptual thresholds for haptic texture discrimination." In 2017 14th International Conference on Ubiquitous Robots and Ambient Intelligence (URAI), pp. 293-298. IEEE, 2017. **[Outstanding paper award]**

[3] Seo, Sang-Woo, SeungJoon Kwon, **Waseem Hassan**, Aishwari Talhan, and Seokhee Jeon. "Interactive virtual-reality fire extinguisher with haptic feedback." In 25th ACM Symposium on Virtual Reality Software and Technology, pp. 1-2. 2019.

[4] Abdulali, Arsen, **Waseem Hassan,** Baek Seung Jin, and Seokhee Jeon. "Hands-On Demonstration of Heterogeneous Haptic Texturing of Mesh Models Based on Image Textures." In International AsiaHaptics conference, pp. 61-65. Springer, Singapore, 2018.

[5] Raza, Ahsan, Muhammad Abdullah, **Waseem Hassan,** Arsen Abdulali, Aishwari Talhan, and Seokhee Jeon. "Painting Skill Transfer Through Haptic Channel." In International Asia-Haptics conference, pp. 66-68. Springer, Singapore, 2018.

[6] Rakhmatov, Ruslan, Arsen Abdulali, **Waseem Hassan**, Minji Kim, and Seokhee Jeon. "Virtual reality bicycle with data-driven vibrotactile responses from road surface textures." In 2018 IEEE Games, Entertainment, Media Conference (GEM), pp. 1-9. IEEE, 2018.

[7] Abdullah, Muhammad, **Waseem Hassan,** Ahsan Raza, and Seokhee Jeon. "Haptic Logos: Insight into the feasibility of digital haptic branding." In International conference on human haptic sensing and touch enabled computer applications, pp. 696-708. Springer, Cham, 2018.

[8] Abdullah, Muhammad, Minji Kim, **Waseem Hassan,** Yoshihiro Kuroda, and Seokhee Jeon. "HapticDrone: An encountered-type kinesthetic haptic interface with controllable force feedback: Example of stiffness and weight rendering." In 2018 IEEE Haptics Symposium (HAPTICS), pp. 334-339. IEEE, 2018.

[9] Abdullah, Muhammad, Minji Kim, **Waseem Hassan,** Yoshihiro Kuroda, and Seokhee Jeon. "HapticDrone: An encountered-type kinesthetic haptic interface with controllable force feedback: Initial example for 1d haptic feedback." In Adjunct Publication of the 30th Annual ACM Symposium on User Interface Software and Technology, pp. 115-117. 2017.

[10] Abdulali, Arsen, **Waseem Hassan,** and Seokhee Jeon. "Sample selection of multi-trial data for data-driven haptic texture modeling." In 2017 IEEE World Haptics Conference (WHC), pp. 66-71. IEEE, 2017.

International Conference: Non-refereed Papers/ Posters/Demonstrations:

[1] **Waseem Hassan**, Raza, A., Abdullah, M., Jeon, S., "Friction Wheel: Bringing in-Car Controls to Driver's Fingertips by Embedding Dual Ubiquitous Haptic Friction Displays into a

Steering Wheel." Student innovation challenge, World Haptics conference 2019. **[Best Student Innovation Challenge Award]**

[2] **Waseem Hassan,** and Seokhee Jeon, "Heterogeneous Haptic Texture Assignment to Mesh Models Based on Image." Demonstration, SIGGRAPH 2019.

[3] **Waseem Hassan,** Aishwari Talhan, Tatyana Ogay, Hwangil K im, and Seokhee Jeon, "Tactile and Kinesthetic Feedback for Safety Experience/Training Simulators: A Case Study of Fire Extinguisher.", Demonstration, SIGGRAPH 2019.

[4] **Waseem Hassan,** Arsen Abdulali, and Seokhee Jeon, "Authoring New Haptic Textures Based on Interpolation of Real Textures in Affective Space: A Demo", Demonstration, Haptics Symposium 2018